

DECEMBER 2019

Ph.D. in Mechanical Engineering

MEHMET ERKAN KÜTÜK

**REPUBLIC OF TURKEY
GAZİANTEP UNIVERSITY
GRADUATE SCHOOL OF NATURAL & APPLIED SCIENCES**

**TRAJECTORY PLANNING AND IMPLEMENTATION FOR
ROBOT-ASSISTED REHABILITATION**

**Ph.D. THESIS
IN
MECHANICAL ENGINEERING**

**BY
MEHMET ERKAN KÜTÜK
DECEMBER 2019**

**TRAJECTORY PLANNING AND IMPLEMENTATION FOR
ROBOT-ASSISTED REHABILITATION**

Ph.D. Thesis

in

Mechanical Engineering

Gaziantep University

Supervisor

Prof. Dr. L. Canan DÜLGER

Co-Supervisor

Asst. Prof. Dr. M. Taylan DAŞ

by

Mehmet Erkan KÜTÜK

December 2019



©2019[Mehmet Erkan KÜTÜK]

REPUBLIC OF TURKEY
GAZIANTEP UNIVERSITY
GRADUATE SCHOOL OF NATURAL & APPLIED SCIENCES
MECHANICAL ENGINEERING

Name of the Thesis : Trajectory Planning and Implementation for Robot-Assisted
Rehabilitation

Name of the Student : Mehmet Erkan KÜTÜK

Exam Date : 30.12.2019

Approval of the Graduate School of Natural and Applied Sciences

Prof. Dr. A. Necmeddin YAZICI
Director

I certify that this thesis satisfies all the requirements as a thesis for the degree of
Doctor of Philosophy.

Prof. Dr. Melda ÇARPINLIOĞLU
Head of Department

This is to certify that we have read this thesis and that in our consensus opinion it is
fully adequate, in scope and quality, as a thesis for the degree of Doctor of
Philosophy.

Asst. Prof. Dr. M. Taylan DAŞ
Co-Supervisor

Prof. Dr. L. Canan DÜLGER
Supervisor

Examining Committee Members:

Signature

Prof. Dr. Şeniz ERTUĞRUL

.....

Prof. Dr. Sedat BAYSEÇ

.....

Prof. Dr. Sadettin KAPUCU

.....

Prof. Dr. L. Canan DÜLGER

.....

Assoc. Prof. Dr. Oğuz YAKUT

.....

I hereby declare that all information in this document has been obtained and presented in accordance with academic rules and ethical conduct. I also declare that, as required by these rules and conduct, I have fully cited and referenced all material and results that are not original to this work.

Mehmet Erkan KÜTÜK

ABSTRACT

TRAJECTORY PLANNING AND IMPLEMENTATION FOR ROBOT- ASSISTED REHABILITATION

KÜTÜK, Mehmet Erkan

Ph.D. in Mechanical Engineering

Supervisor: Prof. Dr. L. Canan DÜLGER

Co-Supervisor: Asst. Prof. Dr. M. Taylan DAŞ

December 2019

121 pages

This study presents a methodology that describes how to adapt a serial manipulator to rehabilitation with a passive exoskeleton having no actuators. The system combines the end-effector- and exoskeleton-based systems. Thus, the passive exoskeleton designed for the wrist and forearm is attached to the end-effector of the manipulator, which provides motion for the rehabilitation process. Denso robot is used to control the motion of the exoskeleton during the rehabilitation process. The desired moving capabilities of the exoskeleton are Flexion–Extension (FE) and Adduction–Abduction (AA) motions for the wrist and Pronation–Supination (PS) motions for the forearm. Kinematic feedback of the experiments is performed by using a wireless motion tracker assembled on the exoskeleton. The results proved that motion transmission from robot to exoskeleton is satisfactorily achieved. The forward and inverse kinematic analyses of 6 Degrees of Freedom (DOF) serial robot manipulator (Denso VP- 6242G) with the closed-form solution are performed in this thesis. Off-line models are offered. Robotic Toolbox combined with GUI Development Environment in Matlab® is used for the forward kinematics solution. A Matlab® Simulink model with Simmechanics® blocks is used in the inverse kinematic analysis. Visualization is enriched by 3D Solidworks® models of the robot parts.

Key Words: Robotic rehabilitation, Wrist and forearm rehabilitation, Exoskeletons,
Denso VP6242G

ÖZET

ROBOT DESTEKLİ REHABİLİTASYON İÇİN YÖRÜNGE PLANLANMASI VE UYGULANMASI

KÜTÜK, Mehmet Erkan
Doktora Tezi, Makine Mühendisliği
Danışman: Prof. Dr. L. Canan DÜLGER
İkinci Danışman: Dr. Öğr. Üyesi M. Taylan DAŞ
Aralık 2019
121 Sayfa

Bu çalışma bir seri manipülatörün eyleyicisi olmayan pasif bir dış iskelet ile rehabilitasyona nasıl uyarlanabileceğini açıklayan bir metodoloji sunmaktadır. Sistem, uç işlevci ve dış iskelet tabanlı sistemlerin birleşimidir. El bileği ve ön kol için tasarlanan pasif dış iskelet rehabilitasyon amaçlı hareket sağlayan manipülatörün uç işlevcisine tutturulmuştur. Denso robot rehabilitasyon sürecinde dış iskeletin hareketini kontrol etmek için kullanılmıştır. Dış iskeletin istenen hareket kabiliyetleri, bilek için Fleksiyon-Ekstensiyon (FE), Addüksiyon-Abdüksiyon (AA) hareketleri ve ön kol için Pronasyon-Supinasyon (PS) hareketleridir. Deneyle kinematik geri beslemesi dış iskelet üzerine monte edilmiş bir kablosuz hareket izleyici kullanılarak gerçekleştirilmiştir. Sonuçlarda robottan dış iskelete hareket iletiminin tatmin edici bir şekilde sağlandığı kanıtlanmıştır. Bu tezde, 6 Serbestlik Dereceli (DOF) seri robot manipülatörün (Denso VP-6242G) kapalı form çözüm ile ileri ve ters kinematik analizi yapılmıştır. Çevrimdışı modeller sunulmaktadır. İleri kinematik çözümü için Matlab®'daki GUI Geliştirme Ortamı ile birleştirilen Robotik Araç Kutusu kullanılmıştır. Ters kinematik analizinde ise Simmechanics® bloklar içeren Matlab® Simulink modeli kullanılmaktadır. Robot parçalarının 3D Solidworks® modelleri ile görsellik zenginleştirilmiştir.

Anahtar Kelimeler: Robotik Rehabilitasyon, Bilek ve Ön Kol Rehabilitasyonu, Dış İskeletler, Denso VP6242G



“Dedicated to Berrak”

ACKNOWLEDGEMENTS

I would like to thank my supervisors, Prof. Dr. L. Canan DÜLGER and Asst. Prof. Dr. M. Taylan DAŞ for their guidance and support throughout the study. I am thankful for their encouragement and motivation.

My sincere thanks go to Prof. Dr. Sadettin KAPUCU, Assoc. Prof. Dr. Pınar BOYRAZ BAYKAS and Assoc. Prof. Dr. Oğuz YAKUT for their suggestions and comments in progress reports.

I would like to express my love and gratitude to my parents, my wife and my daughter for their interest, patience and support. Always best wishes.

This work is supported by Gaziantep University/Scientific Research Projects Governing Unit (BAPYB) through project MF.DT.17.13 and has Ethics Committee Approval (Protocol No: 317).

TABLE OF CONTENTS

	Page
ABSTRACT	v
ÖZET	vi
ACKNOWLEDGEMENTS	viii
TABLE OF CONTENTS	ix
LIST OF TABLES	xi
LIST OF FIGURES	xii
LIST OF ABBREVIATIONS	xvi
CHAPTER I: INTRODUCTION	1
1.1. Medical Background	1
1.2. Robotic Rehabilitation.....	2
1.3. Aim of the Thesis	4
1.4. Thesis Outline.....	5
CHAPTER II: LITERATURE SURVEY	6
2.1. Robotic Devices for Upper Limb Rehabilitation	6
2.1.1. Application Field	6
2.1.2. Type of Assistance.....	7
2.1.3. Mechanical Design	8
2.1.4. Control Signals & Strategy.....	9
2.1.5. Review	10
2.2. Remarks on Literature Survey.....	27
CHAPTER III: DENSO VP6242G ROBOTIC SYSTEM, SOFTWARE AND KINEMATIC ISSUES	28
3.1. Introduction	28
3.2. Denso Robotic Arm.....	29
3.3. Robot Arm Kinematics Preliminaries	30
3.3.1. Forward Kinematics Analysis.....	31
3.3.2. Inverse Kinematics Analysis	36
3.3.3. Manipulator Jacobian.....	43

3.4. QUARC Control Software	46
3.4.1. Denso_Control Release	48
3.4.2. Inverse Position Kinematics & Forward Position Kinematics	50
3.5. Off-line Programming of Denso Robot.....	52
3.5.1. Off-line Studies for the Forward Kinematics	56
3.5.2. Off-line Studies for the Inverse Kinematics	59
CHAPTER IV: DESIGN OF A ROBOT-ASSISTED EXOSKELETON FOR WRIST AND FOREARM REHABILITATION.....	67
4.1. Wrist and Forearm Motions	67
4.2. Exoskeleton Design.....	68
4.3. Mtw Awinda (XSENS)	71
4.4. Exoskeleton with Denso Robot.....	75
4.4.1. Solution Method I.....	78
4.4.2. Solution Method II.....	81
4.5. Trajectory Planning & Experimental Measurement.....	85
4.6. FEM Analysis of the Exoskeleton.....	94
CHAPTER V: CONCLUSIONS.....	97
5.1. Conclusions of Kinematic Analysis and Off-line Programming.....	97
5.2. Conclusions of Robot-Assisted Exoskeleton for Rehabilitation	98
5.3. Recommendations for the Further Study.....	99
REFERENCES.....	101
CIRRICULUM VITAE (CV).....	117

LIST OF TABLES

	Page
Table 2.1 Upper limb robotic devices	22
Table 3.1 Encoder and motor properties of Denso robot	29
Table 3.2 DH parameters of Denso robotic arm.....	34
Table 4.1 Positions of the wrist joint, xyz_0 (m)	83
Table 4.2 ADL Torques.....	94

LIST OF FIGURES

		Page
Figure 1.1	Stroke.....	1
Figure 1.2	Manual therapy.....	3
Figure 2.1	End-effector- and exoskeleton-based devices	8
Figure 2.2	MIT-MANUS	10
Figure 2.3	ARM-Guide.....	11
Figure 2.4	Gentle/S.....	11
Figure 2.5	Bi-Manu-Track.....	12
Figure 2.6	REHAROB.....	12
Figure 2.7	Pneu-WREX.....	13
Figure 2.8	MIME.....	13
Figure 2.9	RUPERT.....	14
Figure 2.10	ARMin.....	14
Figure 2.11	IPAM.....	15
Figure 2.12	NeReBot.....	15
Figure 2.13	MEDARM.....	16
Figure 2.14	ReachMAN.....	17
Figure 2.15	ARAMIS.....	17
Figure 2.16	ACT-4D.....	18
Figure 2.17	UL-EXO7.....	18
Figure 2.18	RehabRoby.....	19
Figure 2.19	ETS-MARSE.....	19
Figure 2.20	Harmony.....	20
Figure 2.21	PHYSIOTHERABOT/WF.....	21
Figure 3.1	Axes and workspace of Denso robot.....	30
Figure 3.2	Denso (RRRRRR) arm & Stanford (RRRPRR) arm.....	31
Figure 3.3	A DH representation of a general purpose joint-link combination ...	32
Figure 3.4	Denso robot.....	33
Figure 3.5	Representation of an object in space.....	35

Figure 3.6	'Read' block and 'Write' block.....	47
Figure 3.7	Main model of Denso robot.....	48
Figure 3.8	Jacobian subsystem of Denso robot	49
Figure 3.9	Details of singularity handler	49
Figure 3.10	IPK and FPK of Denso	51
Figure 3.11	Examples obtained by Robotic Toolbox	55
Figure 3.12	Examples obtained by GUIDE	56
Figure 3.13	fig. file of GUI.....	56
Figure 3.14	Designed GUI example	57
Figure 3.15	Designed GUI example II.....	58
Figure 3.16	Simulink model for inverse kinematics analysis	60
Figure 3.17	Denso robot in home position.....	61
Figure 3.18	The configuration of the Denso robot with pure orientation changes	62
Figure 3.19	The configuration of the Denso robot with pure position changes	62
Figure 3.20	The configuration of the Denso robot with position and orientation changes	63
Figure 3.21	The orientation with prescribed timing	64
Figure 3.22	Angular displacements of the links for the orientation changes.....	64
Figure 3.23	Geometrical shapes to be traced by the end-effector.....	65
Figure 3.24	Angular displacements of the links - circular trajectory	65
Figure 3.25	Angular displacements of the links - quadratic trajectory.....	65
Figure 3.26	Robot in motion - circular trajectory	66
Figure 3.27	Robot in motion – quadratic trajectory.....	66
Figure 4.1	Degrees of Freedom of the wrist and forearm.....	67
Figure 4.2	Designed exoskeleton.....	68
Figure 4.3	Mechanical limits of exoskeleton parts	69
Figure 4.4	Virtual FE motions with exoskeleton	70
Figure 4.5	Virtual AA motions with exoskeleton.....	70
Figure 4.6	Virtual PS motions with exoskeleton	70
Figure 4.7	Manufactured exoskeleton.....	71

Figure 4.8	The motion tracker and USB dongle	72
Figure 4.9	The Xsens MT Manager software	72
Figure 4.10	Manual FE motions with exoskeleton	73
Figure 4.11	Experimental results of FE measured by the wireless sensor.....	73
Figure 4.12	Manual AA motions with exoskeleton.....	74
Figure 4.13	The experimental results of AA measured by the wireless sensor....	74
Figure 4.14	Manual PS motions with exoskeleton	74
Figure 4.15	Experimental results of PS measured by the wireless sensor.....	74
Figure 4.16	Exoskeleton driven by Denso robot	75
Figure 4.17	FE motion with Denso robot	76
Figure 4.18	AA motion with Denso robot	76
Figure 4.19	PS motion with Denso robot.....	76
Figure 4.20	Limit condition of the fifth axis.....	77
Figure 4.21	New home position and system with the designed apparatus	78
Figure 4.22	Details of the designed apparatus	79
Figure 4.23	Coordinate frames of new end-effector and human wrist	79
Figure 4.24	AA motion with apparatus.....	80
Figure 4.25	PS motion with apparatus	80
Figure 4.26	Configurations of exoskeleton & Denso robot.....	81
Figure 4.27	FE&PS configuration and rotatable system	82
Figure 4.28	AA configuration and rotatable system.....	82
Figure 4.29	Two positions of the part carrying the exoskeleton.....	83
Figure 4.30	Human wrist positions.....	84
Figure 4.31	Overall system with base for forearm	85
Figure 4.32	The trajectories with different velocity levels for PS, FE and AA motions	86
Figure 4.33	The trajectories and Simmechanics® blocks of the exoskeleton	88
Figure 4.34	Graphical display of the exoskeleton	89
Figure 4.35	PS measurement with IMU	90
Figure 4.36	AA measurement with IMU	91

Figure 4.37	FE measurement with IMU	92
Figure 4.38	The angular displacements of the robot links.....	93
Figure 4.39	FEM analysis of the exoskeleton.....	95
Figure 4.40	FEM analysis of the exoskeleton without robot.....	96



LIST OF ABBREVIATIONS

FE	Flexion-Extension
AA	Adduction-Abduction
PS	Pronation-Supination
ADL	Activities of Daily Livings
CTC	Computed Torque Control
PCM	Pulse Code Modulation
SMC	Sliding Mode Control
FFC	Force Forward Control
RC	Robust Control
FC	Force Control
SME	Sliding Mode Control with Exponential Reaching
IC	Impedance Control
AC	Admittance Control
EMG	Electromyography
PID	Proportional-Derivative-Integral Control
exo	Exoskeleton Type Robot
ee	End-effector Type Robot
e	Electric Actuation
p	Pneumatic Actuation
h	Hydraulic Actuation
u	Unilateral
b	Bilateral
ub	Unilateral-Bilateral
r	Rehabilitation
pa	Power Assistance
rp	Rehabilitation-Power Assistance
g	Grounded
ug	Ungrounded

CHAPTER I

INTRODUCTION

1.1 Medical Background

Cerebral Vascular Accident (CVA) is also named stroke. An interruption in supplying blood to the brain or other regions of the central nervous system cause stroke. This phenomenon results in some parts of the brain not to take enough oxygenated blood and leading to neural death in that area. Stroke can form in two ways; the first one covers the big amount of cases. It is due to disturbance in blood supply. Necrosis of brain tissue and impairment of the affected area are the results of oxygen shortage. The second one is due to the accumulation of blood in the brain or skull. Blood vessels are harmed because of high blood pressure causing rupture. Stroke is a significant reason for adult disability, paralysis, contracture and movement disorders for example (Donnan et al., 2008) and may be fatal.

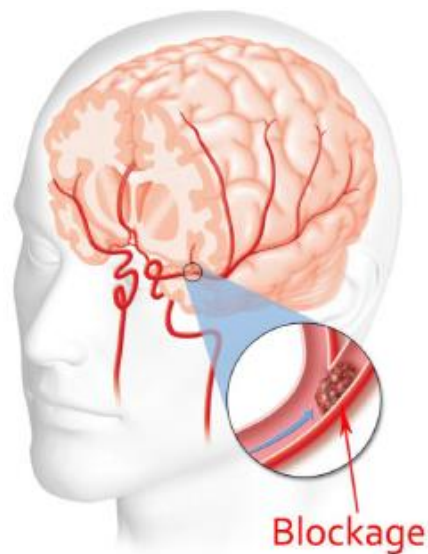


Figure 1.1 Stroke.

Paralysis is a common result of stroke. It causes function loss in the muscles. It may affect either the whole body or one side of the body (hemiparesis). Memory problems may come up after stroke in addition to the loss of physical strength. Motor impairments after stroke require rehabilitation. However, rehabilitation requirement is not only formed after stroke but also it is necessary to gain motor functions lost after cerebral palsy, multiple sclerosis (MS) and spinal cord injuries, etc. (Mehta and Bain, 2004). The exercises, especially repetitive motions have a great healing effect on the motor capabilities of human beings.

Contracture is a limitation of movement in the joints for various reasons like prolonged immobilization, edema, spasticity and fracture caused by trauma or disease. It occurs as a result of fibrotic changes resulting from joint movement restriction and shortening of the connective tissue.

Movement disorders reduce or restrict the quality of life of human beings significantly. In particular, the problems in the upper extremity directly affect the independencies of the patients. The impairment yields several impacts on domestic and social life. The disease not only brings pain to patients and but also brings huge economic losses. The extension of the rehabilitation process creates negative impacts on the psychological situations of the patients. There are many physiotherapy methods like orthosis, electrotherapy, exercise treatments and manual therapy in order to recover the functionality of the upper extremities.

1.2 Robotic Rehabilitation

Rehabilitation is an action to decrease permanent disabilities. It brings a handicapped person to a better situation in terms of medical, psychological, social and vocational (Akdemir and Akkuş, 2006). Rehabilitation robotics is an area of research devoted to understand and augment rehabilitation through the implementation of robotic devices.

Neurological lesions result in impairments of muscle strength and movement coordination. Task-oriented repetitive movements are used to improve those impairments. In recent years, robotic devices have been started to be used in the rehabilitation field with the developments of efficient computers, computational

approaches and sophisticated electromechanical elements. The applications, which are a combination of robots and medical technology, attract attention all over the world. Robotic devices are capable of measuring displacements, velocities, forces, and other derived parameters. Hence, they may be successfully operated for both training and evaluation in rehabilitation. Changes of biomechanical parameters can be neutrally quantified. Thus, recovery of the subjects during the rehabilitation period can be monitored accurately. High-dosage and high-intensity training in rehabilitation are possible with robot technology. This feature makes robotic therapy a promising novel technology used in rehabilitation.



Figure 1.2 Manual therapy.

Traditional therapy shown in Figure 1.2 not only requires a great effort but also requires the manual assistance of physiotherapists. The one-to-one contact of the therapists with their patients leaves the therapists exhausted. Additionally, they spend significant time. Robotic devices can imitate the manual assistance of the therapists. They can perform mechanical manipulations that are impossible for the therapists. Because the neuromuscular system of the therapists has limited speed, strength and repeatability. Besides, robots can operate both active and passive exercises. The purpose of the rehabilitation robotics is not to deactivate the therapists. The therapist is very important for successful therapy because the patients should feel confident. Patients should not be afraid of robots in any way. Otherwise, the continuity of therapy cannot be ensured. Thus, integrating robotic therapy into the existing practice will alleviate the labor-intensive part of physical rehabilitation. It will increase the effectiveness of therapists (Lum et al., 2002). The studies in the literature confirm that robotic rehabilitation is advantageous in regaining motor functions lost in contrast to traditional treatment (Lum et al., 2002; Dobkin, 2004; Bayona et al., 2005; Masiero et al., 2006; Prange et al., 2006; Kwakkel et al., 2007).

1.3 Aim of the Thesis

Rehabilitation robotics is an interdisciplinary field that has been highly sought by researchers in the last two decades. In particular, the application of research in the field of robotics to rehabilitation has made this subject attractive to engineers. There is lack of the number of therapists per person both in our country and in the world, therefore the prolongation of the rehabilitation periods and the increase in costs have revealed the necessity of improvements to this subject.

There is a 6 DOF serial robot in Mechatronic Lab, Gaziantep University. It is firstly aimed to make orientation studies with the robot in order to use it for rehabilitation purposes. The intension is to enrich the analytical studies with the off-line programming method. After acquiring the ability to use the robot efficiently, it is aimed to make the serial robot suitable for wrist and forearm rehabilitation, which is a frequently used area in daily life. Subjects with contracture problems are considered as the target group in this thesis.

As a result of the literature studies, it was observed that the mechanical designs of the robots used in rehabilitation are end-effector-based and exoskeletons. Both systems have advantages and disadvantages. However, there is no study in the literature using these two different techniques together. By hybridizing these two different structures, their advantages are utilized and their disadvantages are tried to be omitted.

The design and manufacture of a passive (without actuator) exoskeleton to be compatible with human anatomy is desired. The serial robot is considered a Continuous Passive Motion (CPM) provider. The other purpose of the study is to plan and perform trajectories with different magnitudes and velocities. The magnitudes and velocities of the trajectories are defined according to the movement limits of the related limbs and level of illnesses, respectively. The expectation is that this study will be a design guide leading to future studies in this field.

1.4 Thesis Outline

The chapters of the thesis are organized as;

Chapter 1 starts with an introduction to the medical background of rehabilitation. Then, the importance and necessities of robotic rehabilitation are given. The aims of the thesis are mentioned. Chapter 1 ends with the structure of the thesis.

Chapter 2 contains a detailed literature survey. The terms that are mostly used are described. Besides the major works given with explanations, a tabulated form of the studies is presented in order of years. The remarks of the literature survey are offered at the end.

Chapter 3 includes the kinematic analysis of Denso robot. Forward, inverse kinematics and manipulator Jacobian equations are derived. The software of the robot is presented. Off-line programming examples enriched with GUI are given. Orientation studies are performed to form a background of adapting Denso robot to rehabilitation.

Chapter 4 provides the wrist and forearm exoskeleton design and manufacture. Mounting the exoskeleton to the robot is explained in detail. The proposed method in performing the related therapeutic exercises is given. Trajectory planning issues are also explored. Acquiring the orientation changes of exoskeleton by a wireless motion tracker is included.

Chapter 5 sums up the achievements and contributions of the thesis. Discussions on the present study and recommendations for the future works are finally given.

CHAPTER II

LITERATURE SURVEY

Robotic devices for upper limb rehabilitation have been searched in this chapter. The major works published in upper extremity rehabilitation have been included especially for wrist and forearm with a tabulated form of the studies.

2.1 Robotic Devices for Upper Limb Rehabilitation

The terminology and definitions concerning robot-mediated rehabilitation systems are given in this section. The application field, type of assistance, mechanical design and control strategies are the basic issues taken into consideration. Systematic technical reviews, meta-analyses, influence of training intensity and impact of particular upper limb rehabilitation techniques have already been included (Barreca et al., 2003; Platz, 2003; Prange et al., 2006; Riener, 2007; Mehrholz et al., 2008; Zhang et al., 2018; Duret et al., 2019).

2.1.1 Application Field

Robotic devices can be categorized into two main groups according to application field: the first one is taken as a supporter to perform some activities of daily living (ADL) like *power assistance* and tremor suppression and the second one is taken to provide *physical training (therapy)* (Maciejasz et al., 2014). The devices taking place in the first group should make better the user's life. Otherwise, dissatisfaction occurs (Hasegava et al., 2008; Rocon et al., 2007). Some properties that they must have are safety, easy handling, being inexpensive and portability of course. The second group of devices, physical therapy devices, used for rehabilitation is much more than the group of devices developed for supporting ADL. They may be placed in the institutes

or home conditions. However, most of them are available in the therapeutic institutes due to the necessity of expert assistance and offering high prices for personal use.

2.1.2 Type of Assistance

Types of motion assistance used in rehabilitation devices can be grouped as active and passive.

- ✓ Active Device; if the patient is too weak to perform the tasks defined, active assistance of movement is required. They are able to move limbs and need active actuators, which may increase the weight. They can be applied to subjects who cannot completely move their limbs.
- ✓ Passive Device; sometimes active assistance is not necessary to resist movements of patients to increase their effort. The patient may be expected to trace the desired trajectory. Passive devices can be equipped with a brake (resisting force). They may also have mechanical linkages moving when it is pushed. They consume less energy, cheaper and lighter than the active devices having actuators. They cannot move the limbs; however, they create resistance (Kikuchi et al., 2007; Oda et al., 2009).

Exercises can also be grouped into two parts;

- ✓ Active Exercise; an exercise is called as active when subjects put an effort to move their limbs. Device assistance may be supplied. Any devices listed above can be used in such type of exercise.
- ✓ Passive Exercise; an exercise is called as passive when the subjects stay passive and not put an effort when the limb is moved by a device. This type of exercise requires an active device.

Being active and passive in device and exercise may be confusing. An exercise with an active device may be qualified as passive if an exertion from the patient is not required.

2.1.3 Mechanical Design

Two categories can be considered in the mechanical structure of rehabilitation robots; *end-effector-* and *exoskeleton-based* shown in Figure 2.1 (a, b), respectively. The movement transfer type from the device to the patient limb is the main difference between these two groups.

End-effector type robots cover a big workspace without having the capability to apply torques to specific joints of the arm. Having a simpler control structure than exoskeletons is an advantage of end-effector type devices. There is a point of contact between the most distal part of the robot and the patient limb. The segments of the upper extremity can be regarded as a mechanically induced chain. Therefore, motion in the end-effector of the robot will automatically move other (proximal) segments of the patient. They may cause redundant configurations of the patient upper extremity and injury risk. MIT-MANUS (Krebs et al., 1998) and MIME (Lum et al., 2002) are included in the first part. The end-effector systems may be serial (Krebs et al., 1998, Schoone et al., 2007) and parallel (Takaiwa and Noritsugu, 2005; Spencer et al., 2008) manipulator type.

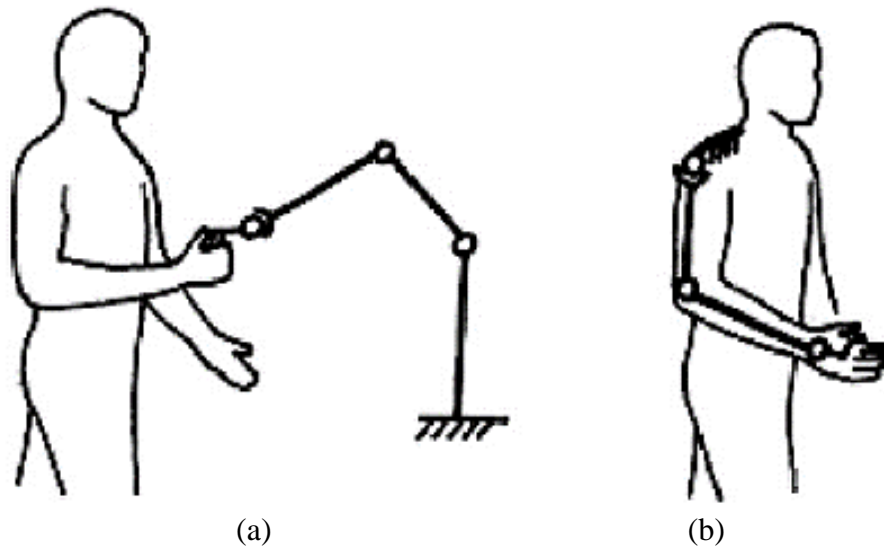


Figure 2.1 End-effector- and exoskeleton-based devices (Lo and Xie, 2012).

Exoskeletons are the external structural mechanisms with joints and links that can collaborate with the human body. They have a mechanical structure mirroring the skeletal structure of the patient's limb. As a result, movement in the particular joint of the device directly causes a movement of the specific joint of the limb. They

encapsulate the limb in a mechanism. Exoskeletons must be able to carry out movements within the natural limitations of human beings for an ergonomic design.

The application of the exoskeleton-based approach allows for independent control of the specific motion of the patient's limb in many joints. Fixing the particular links of the exoskeleton to the segments of the patient limb is necessary to reduce the risk of injury. In addition, the rotation centre position of the human body joints may alter particularly during the motion. Special mechanisms may be required to provide patient safety and comfort (Kiguchi et al., 2003). Therefore, the mechanical and control algorithm of the exoskeletons is remarkably more complex than the end-effector-based devices. A 5 DOF MAHI (Gupta and O'Malley, 2006), 6 DOF ARMin (Nef et al., 2007) and 7 DOF CADEN-7 (Perry et al., 2007) are counted as some examples of exoskeletons used in the upper extremity rehabilitation.

2.1.4 Control Signals & Strategy

There are various signals used as control input of the devices. *Kinematic*, *dynamic* and *trigger* signals can be regarded as the most used ones. Kinematic signals are involved in positions, orientations, velocities and accelerations of the specific segments or joints of the device or of the limb. Dynamic signals are involved in the force or torque acquired from the subjects, links of the exoskeleton or end-effector of end-effector-based device. Trigger signals having a threshold value initiate the specific action. They act like a switch or a button. Electromyography (EMG) is used in some systems as an input signal. EMG controlled systems for different joints can be given as; (Kiguchi et al., 2003) for shoulder, (Song et al., 2007) for wrist and (Gopura and Kiguchi, 2008) for wrist and forearm rehabilitation.

Different control strategies have been offered in the literature. Position control, force control, sliding mode control (SMC), computed torque control (CTC), impedance and admittance control are some types used. They may be combined to generate High-level control strategies to induce motor plasticity (Marchal-Crespo and Reinkensmeyer, 2009; Maciejasz et al., 2014; Proietti et al., 2016).

2.1.5 Review

Many robots are developed for physical therapy and rehabilitation of upper limbs in the literature. The major works published are explained in details.

Krebs et al. (1998, 2004) designed a robot called MIT - MANUS (Massachusetts Institute of Technology - MANUS) shown in Figure 2.2. The robot, which is one of the best known of the upper limb robotic rehabilitation studies, has two types of modules. Elbow and forearm exercises are carried out with the planar module consisting of five bar mechanisms that allow movement in two dimensions. Wrist exercises are performed with 3 DOF modules connected to the planar module end. Active, passive and resistant exercises can be performed by using impedance control method and game-based tasks. It is commercially available under the name of InMotion-ARM.

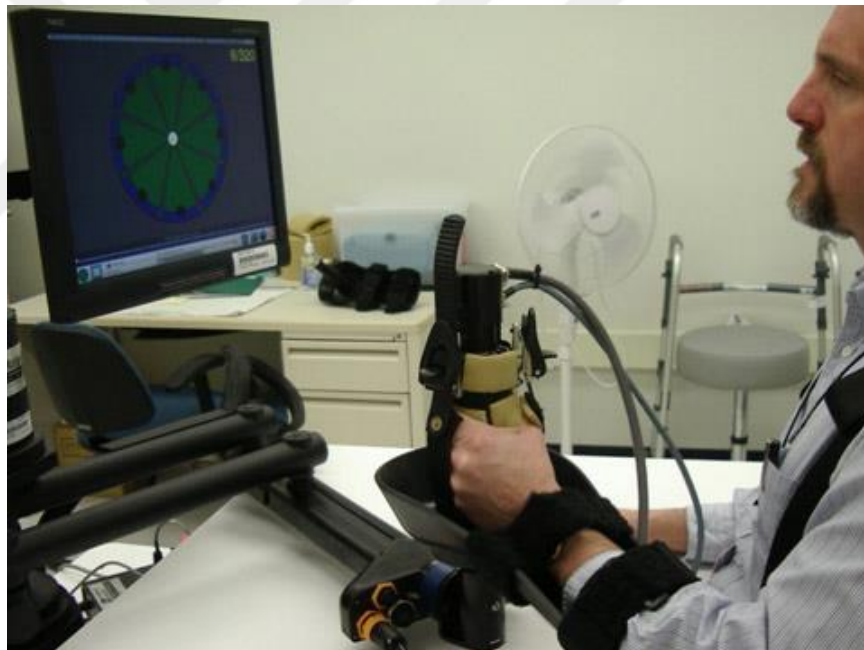


Figure 2.2 MIT-MANUS (Krebs et al., 2004).

Reinkensmeyer et al. (2001) developed a robot called ARM - Guide (Assisted Rehabilitation and Measurement) for 1 active and 2 passive DOF in the shoulder and elbow rehabilitation. The robot in Figure 2.3 can perform gravity compensation, passive, active-assisted and resistant exercises. Reaching the target object can also be performed with the sliding mechanism on it.

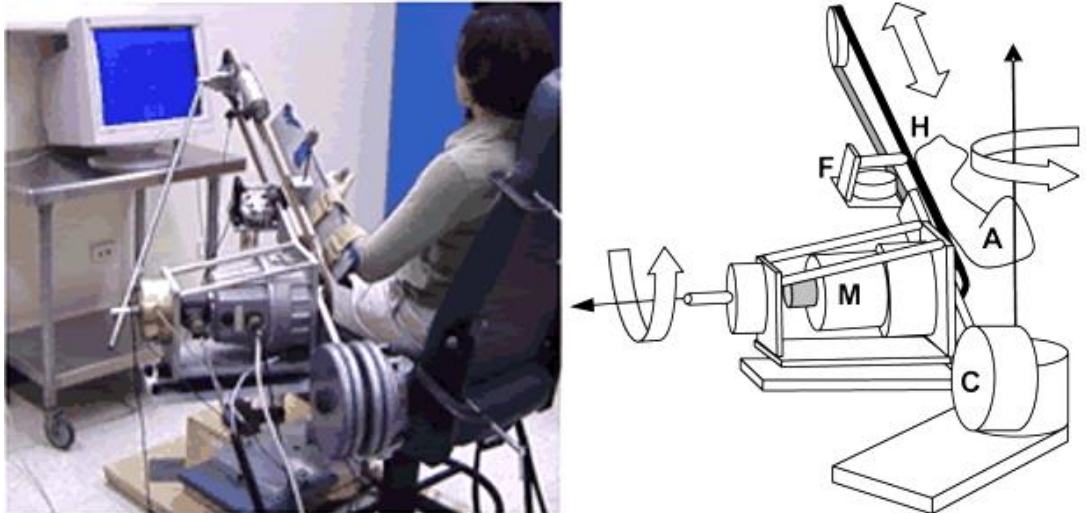


Figure 2.3 ARM-Guide (Reinkensmeyer et al., 2001).

Loureiro et al. (2003) developed a system called Gentle/S which can fulfil passive, active-assisted and resistant exercises for shoulder, elbow, wrist and forearm rehabilitation (Figure 2.4). Haptic Master robot with 3 DOF is used in the system. The movement of the patient is provided with visual and tactile feedback by creating 3-dimensional visual environments. The minimum jerk approach is used in motion and trajectory planning.



Figure 2.4 Gentle/S (Loureiro et al., 2003).

Hesse et al. (2003) devised a system consisting of 1 DOF robot manipulators called Bi-Manu-Track given in Figure 2.5. Passive, active-assisted and resistant exercises for wrist and forearm rehabilitation are performed. The system has three operating modes. The first one is passive exercises where the speed and the range of motion can be adjusted. In the second, the paretic limb is moved by the intact limb via the robot manipulators. In the third mode, as in the second mode, the paretic limb is

moved with the aid of the intact limb. However, additional resistance to the paretic limb movement is applied here.

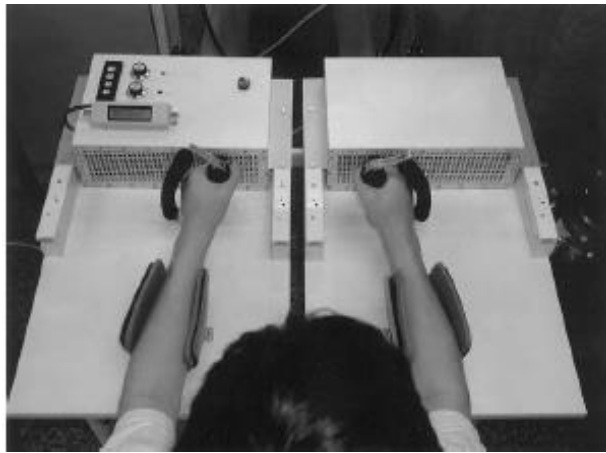


Figure 2.5 Bi-Manu-Track (Hesse et al., 2003).

Toth et al. (2005) devised a system called REHAROB capable of performing passive exercises for forearm, elbow and shoulder rehabilitation. The system shown in Figure 2.6 uses two 6 DOF industrial robotic arms (ABB IRB 140 and ABB IRB 1400H). Treatment applications such as passive exercises and opening of joints with contracture can be performed in the system where the force control method is used.



Figure 2.6 REHAROB (Toth et al., 2005).

Sanchez et al. (2005) designed a pneumatically driven robot called Pneu-WREX that can be used for shoulder and elbow rehabilitation. It is shown in Figure 2.7.

Nonlinear force control and passive counterbalance methods were used in the control of the robot. It has passive exercise and gravity compensation features.

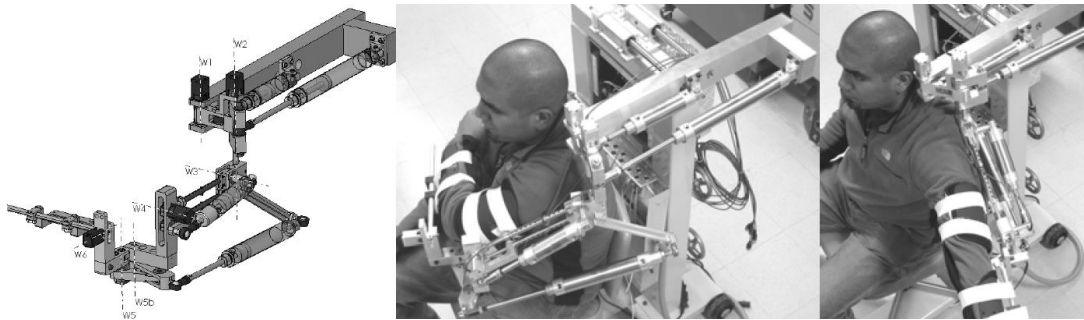


Figure 2.7 Pneu-WREX.

Lum et al. (2006) developed a 3 DOF system called MIME (Mirror Image Movement Enabler) given in Figure 2.8 for shoulder and elbow rehabilitation. PUMA 560 robot was used in the system. Trajectory tracking and control of one limb (mirror rehabilitation method) can be performed. The system using PID and force-torque control methods can perform passive, active-assisted and resistant exercises.



Figure 2.8 MIME (Lum et al., 2006).

Sugar et al. (2007) performed a 4 DOF exoskeletal robot called RUPERT given in Figure 2.9 for the rehabilitation of the shoulder, elbow and wrist. The system can carry out passive and active-assisted exercises.



Figure 2.9 RUPERT (Sugar et al., 2007).

Nef et al. (2007) designed the exoskeletal robot called ARMin for shoulder and elbow rehabilitation. It is given in Figure 2.10. This system has 4 active and 2 passive DOF providing passive and active-assisted exercises. Gravity compensation has the ability to perform target mass applications and give audible, visual and tactile feedback. PD and impedance control methods were used herein.

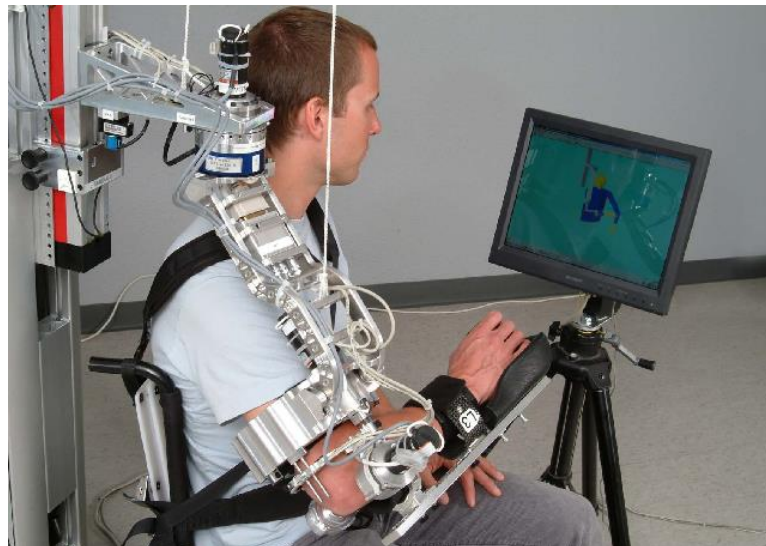


Figure 2.10 ARMin (Nef et al., 2007).

Jackson et al. (2007) developed a 5 DOF exoskeletal robot named iPAM (Intelligent Pneumatic Arm Movement) for the shoulder, elbow and forearm rehabilitation. Passive and active-assisted exercises can be operated. It is depicted in Figure 2.11.



Figure 2.11 iPAM (Jackson et al., 2007).

Rosati et al. (2007) developed a 3 DOF robot for shoulder and elbow rehabilitation, NeReBot (Neurorehabilitation Robot) shown in Figure 2.12. It is a wire-based system providing passive gravity support. Passive and active-assisted exercise movements are carried out by means of three motor controlled lengths. In the mechanical design of the system, the ease of transportation in the hospital environment has been prioritized. PD position control method was used in the robot.



Figure 2.12 NeReBot (Rosati et al., 2007).

Ball et al. (2007) and Ball (2008) performed a 5 DOF exoskeletal robot called MEDARM for the shoulder and elbow rehabilitation of paralyzed patients. Motion transfer is realized with wire and straps as shown in Figure 2.13. Passive and active-assisted exercises can be performed.



Figure 2.13 MEDARM (Ball et al., 2007).

Deneve et al. (2008) developed a 3 DOF robot used in shoulder and elbow rehabilitation. Position, force, impedance and force / impedance control methods are implemented in the system. It is required to switch to a different controller according to the type of exercise.

Oblak et al. (2009) offered a 2 DOF robotic system using the impedance control method. It is called UHD (Universal Haptic Device) for upper arm, wrist and forearm rehabilitation. The system has two mechanically adjustable modes: arm and wrist. In arm mode, reach and grip type exercises are performed for shoulder and elbow rehabilitation. In wrist mode, the exercises are performed for forearm and wrist rehabilitation.

Yeong et al. (2009, 2010) developed a 3 DOF wrist and forearm rehabilitation robot called ReachMAN (reach and manipulation) shown in Figure 2.14. In the control of the robot, admittance and impedance control methods were used. There are hold-drop, eating-drinking exercise modes.

Wang and Li (2010) designed a 3 DOF planar robot for wrist, forearm and shoulder rehabilitation in a simulation environment. Hybrid impedance control method is applied.

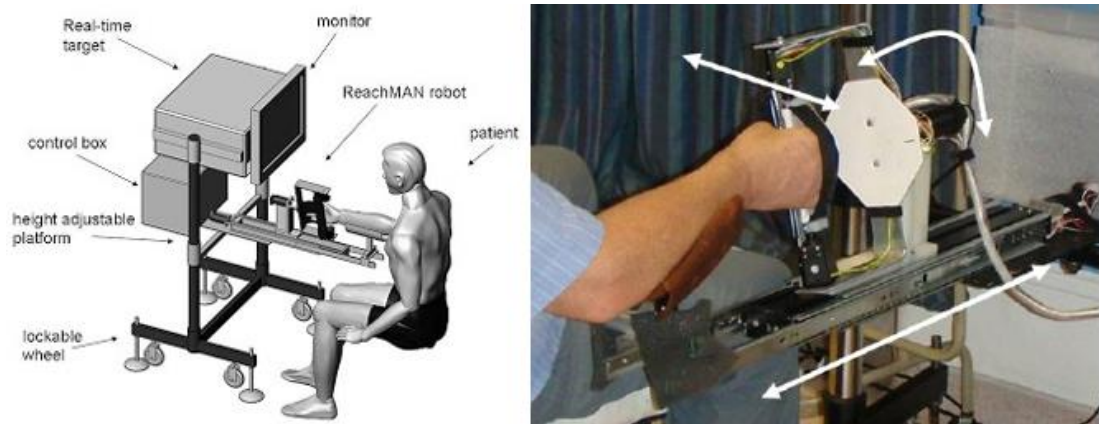


Figure 2.14 ReachMAN (Yeong et al., 2009).

Colizzi et al. (2010) designed ARAMIS (Automatic Recovery Arm Motility Integrated System) consisting of two 6 DOF exoskeleton robots depicted in Figure 2.15. Asynchronous (passive exercises independent of the physiotherapist), synchronous (passive exercises performed depending on the movements of the physiotherapist) and virtual reality (tasks such as reaching and holding) can be performed for the shoulder, elbow and forearm.



Figure 2.15 ARAMIS (Colizzi et al., 2010).

Stienen et al. (2011) developed a 4 DOF robotic system called ACT-4D for wrist and elbow rehabilitation. The system given in Figure 2.16 is a modified version of the ACT3D (Sukal et al., 2005) system. Unlike ACT3D, the elbow rotation mechanism has been added. The system has two modes; compliant and stiff. The compliant mode is the mode where the mass and friction values are set at the lowest level, allowing the patient to perform the movements easily. The stiff mode is the mode where the

passive exercises can be performed by adjusting the position and speed values. The admittance control method was used in the system.



Figure 2.16 ACT-4D (Stienen et al., 2011).

Mao and Agrawal (2012) generated a 5 DOF exoskeleton robot called CAREX (Cable-Driven Arm Exoskeleton) for the shoulder, elbow and forearm rehabilitation. All motors are located at the top and the joints are driven by cables in the system. Two types of control approaches, force control and cable tension control, are used in the system.

Kim et al. (2013) developed a system called UL-EXO7. It uses two 7 DOF manipulators to rehabilitate the shoulder, elbow and forearm as shown in Figure 2.17. The system can operate passive and active-assisted exercises to the different limbs at the same time. Gravity and friction compensation and position and force control methods are used in the system.



Figure 2.17 UL-EXO7 (Kim et al., 2013).

Barkana and Ozkul (2013) & Ozkul and Barkana (2013) developed a 6 DOF exoskeletal robot system named RehabRoby shown in Figure 2.18. The robot, which can be adjusted to different limb sizes, can perform AA and FE for the shoulder, FE for the elbow, PS for the forearm, and FE for the wrist. The admittance control technique was used in the control of the system.

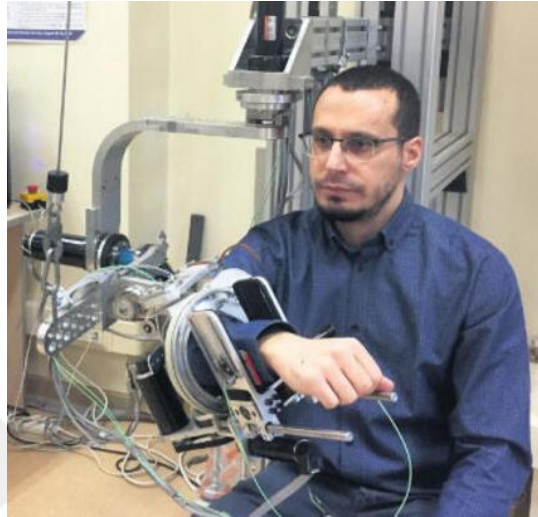


Figure 2.18 RehabRoby (Barkana and Ozkul, 2013).

Sivan et al. (2014) developed a low-cost home-based robotic system called hCAAR (Home-Based Computer-Assisted Arm Rehabilitation) for upper limb rehabilitation. They examined the safety, ease of use and effect of the robotic system on the treatment of the disease.

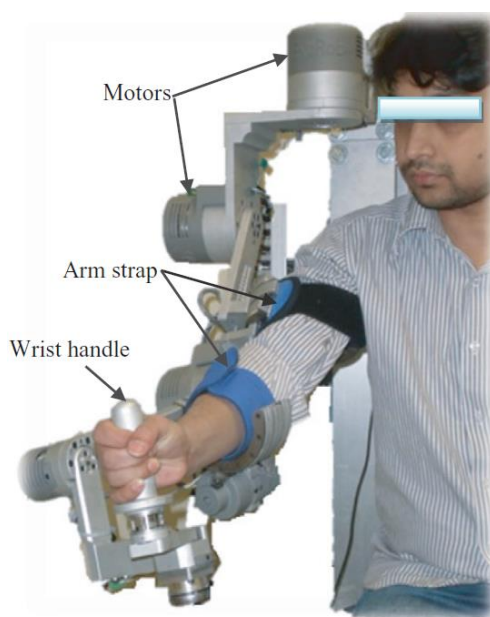


Figure 2.19 ETS-MARSE (Rahman et al., 2015).

Rahman et al. (2015) presented a 7 DOF exoskeleton robot for shoulder, elbow, forearm and wrist rehabilitation. It is called ETS - MARSE (Motion Assistive Robotic Exoskeleton for Superior Extremity) given in Figure 2.19. The system has also been developed to help users doing their daily activities.

Khor et al. (2017) developed a single DOF robot that is portable and mechanically adjustable for different types of motion. It allows the movements of shoulder, elbow, forearm and wrist rehabilitation to be performed in different holding positions. The robot, which can perform passive and active-assisted exercises, is intended for paralyzed patients.

Kim et al. (2017) developed a 5+5 DOF exoskeletal robot for the right and left arms to rehabilitate the shoulder, elbow and forearm. It is called Harmony shown in Figure 2.20. The impedance control technique was applied to control the robot.



Figure 2.20 Harmony (Kim et al., 2017).

Higuma et al. (2018) performed a wrist exoskeletal mechanism capable of wrist FE and AA movements. The unique side of this mechanism is that it can accurately model 2 DOF of the wrist and use 2 leaf springs and linear motors to perform the movements. The range of motion of the joint was measured with the camera and the joint force was measured with the force sensor. A performance analysis of the mechanism was carried out.

Akdogan et al. (2018) developed a 3 DOF robot called PHYSIOTHERABOT © / WF for the rehabilitation of the wrist and forearm. The robot shown in Figure 2.21 can perform passive and resistant therapeutic exercises by using the hybrid

impedance control method. The robot was tested with healthy and sick subjects and an improvement was seen in the patients.



Figure 2.21 PHYSIOTHERABOT/WF (Akdoğan et al., 2018).

A comprehensive tabulated form of the studies is given in Table 2.1. Almost all studies are related to the wrist and forearm region. System name and reference, DOF, scope of movement, main control type, operation mode and type of the system are given as column names in Table 2.1. Some abbreviations are used herein;

FE, AA and PS in the *movement scope* column stand for Flexion-Extension, Abduction-Adduction and Pronation-Supination, respectively.

CTC, PCM, SMC, FFC, RC, FC, SME, IC, AC, EMG, PD and PID in *main control type* column stand for computed torque control, pulse code modulation, sliding mode control, force forward control, robust control, force control, sliding mode control with exponential reaching, impedance control, admittance control, electromyography, proportional-derivative control and proportional-integral-derivative control, respectively.

exo, ee, e, p, h, u, b, ub, r, pa, rp, g and ug in *type* column stand for exoskeleton type robot, end-effector type robot, electric actuation, pneumatic actuation, hydraulic actuation, unilateral, bilateral, unilateral-bilateral, rehabilitation, power assistance, rehabilitation-power assistance, grounded and ungrounded, respectively.

Table 2.1 Upper limb robotic devices.

System Name, Reference	DOF	Movement Scope	Main Control Type	Operation Mode	Type
MIME (Lum et al., 2002, 2006)	6	Shoulder, Elbow	PID, FC	Active-Passive Assist, Resist	ee, r, e, ub, g
Bi_Manu-Track (Hesse et al., 2003)	1	Forearm (PS) Wrist (FE)	IC	Active-Passive Assist, Resist	ee, r, e, ub, g
ASSIST (Sasaki et al., 2004)	1	Wrist (FE)	EMG	Active Assist	exo, pa, p, u, ug
(Takaiwa et al., 2005)	3	Forearm (PS) Wrist (FE, AA)	IC	Active Assist	ee, r, p, u, g
REHAROB (Toth et al., 2005)	12	Shoulder Elbow	--	Passive Assist	ee, r, e,u, g
MAHI (Gupta and O'Malley, 2006)	5	Elbow (FE) Forearm (PS) Wrist (AA, FE)	IC, AC	Active-Passive Assist	exo, r, e, u, ug
(Kung et al., 2007)	1	Forearm (PS)	FC	Active-Passive Assist	exo, r, e, u, g
RUPERT (Sugar et al., 2007)	4	Shoulder (FE) Wrist (FE) Forearm (PS)	FFC	Active-Passive Assist	exo, r,p,u,ug

			Elbow (FE)			
(Colombo et al., 2007)	1		Wrist (FE)	AC	Active Assist	ee, r, e, u, g
(Song et al., 2007)	1		Wrist (FE)	PID, EMG	Active Assist	exo, r, e, u, g
WOTAS (Rocon et al., 2007)	3		Elbow (FE) Wrist (FE) Forearm (PS)	IC	Resist	exo, r, e, u, ug
CADEN-7 (Perry et al., 2007)	7		Elbow (FE) Wrist (FE, AA) Shoulder (AA, FE) Forearm (PS)	PID, EMG	Active-Passive Assist	exo, rp, e, b, g
InMotion WRIST (Krebs et al., 2007)	3		Forearm (PS) Wrist (FE, AA)	IC	Active-Passive Assist, Resist	ee, r, e, u, g
Gentle/S (Amirabdollahian et al., 2007, Coote et al., 2008)	6		Shoulder Elbow Forearm	--	Active-Passive Assist, Resist	ee, r, e, u, g
CRAMER (Spencer et al., 2008)	3		Forearm (PS) Wrist (FE, AA)	PCM	Active Assist	exo, r,p, u, g
(Hu et al., 2009)	1		Wrist (FE)	EMG	Active Assist	ee, r,e,u,g
L-EXOS (Frisoli et al., 2009)	5		Elbow (FE) Forearm (PS)	IC	Active-Passive Assist	exo, r, e, u, g

			Shoulder (AA, FE)			
ARMin-III (Nef et al., 2009)	6	Shoulder (AA, FE) Forearm (PS) Elbow (FE) Wrist (FE)	PD, CTC, IC	Active-Passive Assist	exo, r, e, u, g	
ExoRob (Rahman et al., 2010)	4	Wrist (FE, AA) Forearm (PS) Elbow (FE)	PID, CTC, SMC	Passive Assist	exo, r, e, u, g	
MARSE-7 (Rahman et al., 2010, 2013)	7	Elbow (FE) Wrist (FE, AA) Shoulder (AA, FE) Forearm (PS)	PID, EMG, CTC, SMC, SME	Active-Passive Assist	exo, r, e, u, g	
MARSE-5, (Rahman et al., 2012)	5	Elbow (FE) Forearm (PS) Shoulder (AA, FE)	SMC	Active-Passive Assist	exo, r, e, u, g	
MAHI Exo II (Fitle et al., 2015)	4	Elbow (FE) Forearm (PS) Wrist (FE, AA)	IC, AC	Active-Passive Assist	exo, r, e, u, ug	
(Chen et al., 2015)	6	Elbow (FE) Wrist (FE, AA) Shoulder (AA,	--	Passive Assist	exo, r, e, u, g	



6-REXOS (Malin, 2015)	4	FE) Forearm (PS) Elbow (FE) Wrist (FE, AA) Forearm (PS)	--	Passive Assist	exo, r, e, u, g
(John et al., 2016)	5	Elbow (FE) Forearm (PS) Shoulder (AA, FE)	---	Passive Assist	exo, r, e, u, ug
(Garrido et al., 2016)	7	Elbow (FE) Wrist (FE, AA) Shoulder (AA, FE) Forearm (PS)	AC	Active-Passive Assist	exo, r, e, u, g
Rehab-Arm (Liu et al., 2016)	7	Elbow (FE) Wrist (FE, AA) Shoulder (AA, FE) Forearm (PS)	PID	Active Assist	ee, r, h, u, g
(Mushage et al., 2017)	5	Elbow (FE) Wrist (FE) Shoulder (AA, FE)	SMC	Active-Passive Assist	exo, r, u, ug



(Kang and Wang, 2017)	5	Elbow (FE) Wrist (FE) Shoulder (AA) Forearm (PS)	RC	Passive Assist	exo, r, e, ub, ug
CABexo (Xiao et al., 2017)	6	Elbow (FE) Wrist (FE, AA) Shoulder (AA, FE) Forearm (PS)	--	Passive Assist	exo, r, e, u, g
CAREX-7 (Cui et al., 2017)	7	Elbow (FE) Wrist (FE, AA) Shoulder (AA, FE) Forearm (PS)	PID, CTC	Active-Passive Assist	exo, r, e, u, g
(Kim and Kim, 2017)	7	Elbow (FE) Wrist (FE, AA) Shoulder (AA, FE) Forearm (PS)	--	Active-Passive Assist	exo, pa, e, u, g

2.2 Remarks on Literature Survey

The previous studies illustrated that the implementation of robot technology to physical therapy and rehabilitation is a novelty. It is foreseen that the studies on this subject will continue increasingly. Because innovations in the field of robotics and control theory are very appropriate to be used in the implementations of medical rehabilitation.

The studies are composed of end-effector- and exoskeleton-based devices. However, most of the studies are involved in exoskeletons. Each of the end-effector type and exoskeleton studies has advantages and disadvantages. No study has been found on the combination of these two techniques and what kind of results may emerge. Focusing on these issues, the combination of passive exoskeleton systems designed for different regions with serial robots as the main motion provider can yield interesting results. In the literature studies, it has been observed that exoskeletal systems capable of operating more than one region have a highly complex mechanical structure. This makes their designs quite difficult. The use of motors for each axis also makes them costly. End-effector type devices have deficiencies in proper and controllable therapy for the desired muscle group.

The ideas and applications to be presented to solve these problems will be advantageous in contributing to the literature.

CHAPTER III

DENSO VP6242G ROBOTIC SYSTEM, SOFTWARE AND KINEMATIC ISSUES

3.1 Introduction

The structure of the robotic systems is formed by the movement of multi-degree of freedom kinematic chains. Robot kinematics implements geometry to that movement. The expression of geometry means that modelling the robot links as rigid bodies and assuming their joints to ensure pure rotation or translation. Robot kinematics examines the relationship between the dimensions and connecting types of kinematic chains and the position, velocity and acceleration of each link in the robotic system. The movement is then planned and controlled to compute the actuator forces and torques.

Kinematics is related to the motion of bodies without regarding forces and torques. Robot kinematics specifies the analytical survey of the motion of a robot manipulator. Forming the appropriate kinematics models is very vital for examining the behaviour of the industrial manipulators. Two main types of spaces, Cartesian and Quaternion, are used to model the kinematics of manipulators. The transformation between two Cartesian coordinate systems can be disintegrated into a translation and a rotation. Gibbs vector, Euler angles, Cayley-Klein parameters, orthonormal matrices etc. are the main methods in representing the rotation. Homogenous transformations based on 4×4 real matrices (orthonormal matrices) have been mostly used in robotics (Funda et al., 1990).

The Jacobian or Jacobian matrix is one of the most significant quantities in the analysis and control of the robot motion. Jacobian matrix is derived for velocity relationship. It establishes a connection with the linear & angular velocities of any point of the manipulator to the joint velocities. It emerges every particular part of robotic manipulation. Planning and execution of smooth trajectories, determination of singular

configurations, derivation of the dynamic equations of motion and in the transformations of forces and torques from end-effector to joints of the manipulator are the subjects that Jacobian can be used (Niku, 2001).

3.2 Denso Robotic Arm

Denso VP6242G is a 6 Degree-of-Freedom (DOF) serial manipulator. The robotic arm has six electric motors. The payload is 2 kg and the maximum compound speed at the centre of the end-effector is 3.9 m/s. Figure 3.1(a) illustrates links of Denso robot and configuration of joints. The allowable moments of inertias for 4th and 5th joints are equal and 0.3 kgm² each while it is 0.007 kgm² for 6th joint. The repeatability in x, y and z directions is ± 0.02 mm. Denso robot weighs approximately 14 kg. There are two options in mounting; to the floor and to the ceiling. The total arm length is 420 mm.

The actuators are AC servo motors having brakes for all axes. The absolute encoders are used as position detectors. The encoders and motors properties are presented in Table 3.1 listing the resolutions of encoders, the motor's torque constants and the angular limits of the joints.

Table 3.1 Encoder and motor properties of Denso robot.

Joint i	Encoder (Count/degree)	Torque Constant (N.m/Amp)	Joint Limits (degrees)	Motor Gear Ratio
1	43690	0.38	-160, 160	120:1
2	58254	0.38	-120, 120	160:1
3	43690	0.22	20,160	120:1
4	36408	0.21	-160, 160	100:1
5	36408	0.21	- 120, 120	100:1
6	36408	0.21	-360, 360	100:1

Cao et al. (2011) defines the workspace of the robot manipulator as the set of points that the end-effector of the robot can reach. Therefore, the workspace of a manipulator is the total volume hatched by the end-effector while the manipulator performs all possible motions. The workspace is important in designing trajectories for robot applications. The workspace is constrained in two ways; the geometry of the

manipulator and mechanical constraints of the joints. Detail drawing of the workspace of Denso robot is given in Figure 3.1 (b).

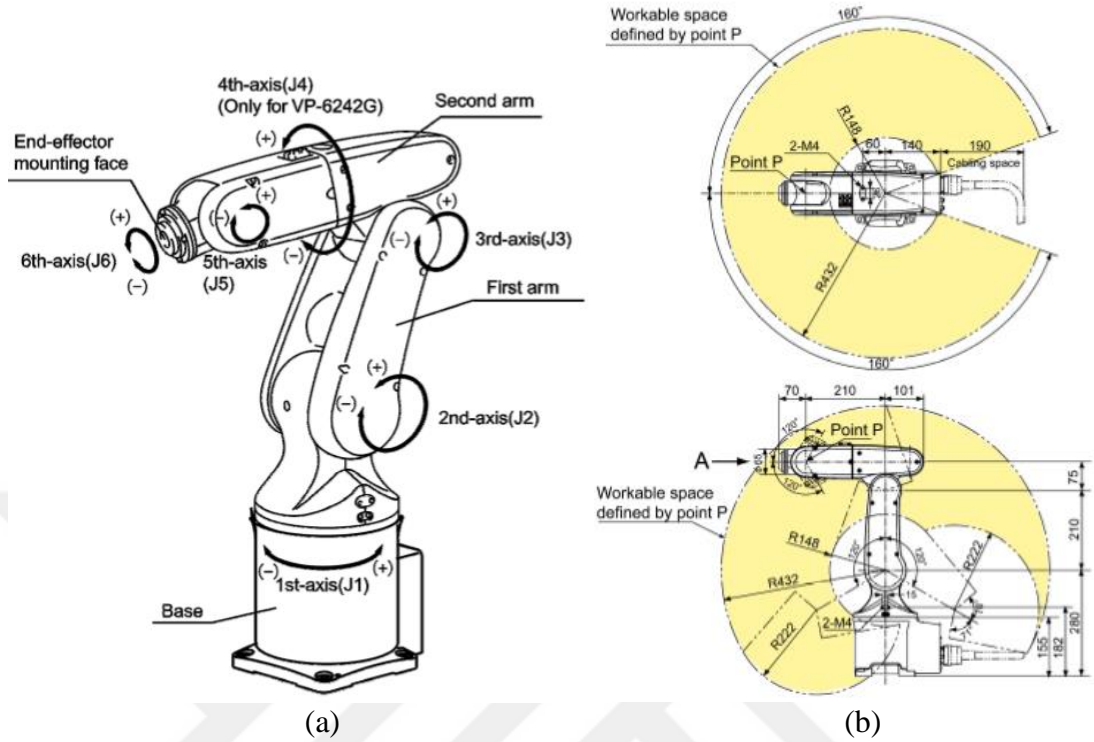


Figure 3.1 Axes and workspace of Denso robot (Denso, 2018; Quanser, 2018).

The system consists of six amplifiers operating about each motor equipped with built-in feed-forward and PID controllers. 1 kHz is the processing rate of each controller. Ethernet-based computer communications are used to control the system. Quarc blockset supplies the gains in the built-in controller. It is possible to access the current values of the amplifiers in real time. Quarc interface offers to tune the gains of the built-in controller. A new controller can also be designed in MATLAB/Simulink with the aid of fully open-architecture operation. The communication between Denso robot and MATLAB/Simulink is via TCP/IP.

3.3 Robot Arm Kinematics Preliminaries

A serial link manipulator contains a chain of mechanical links and joints. Each joint moves its outward adjacent link with respect to its inward adjacent link. One end of the chain is the base. The other end that is free to move in space holds the tool or end-effector. DOF of the joints may be either translational or rotational. The joints of robots that are frequently used in industry are revolute type like Denso robot given in Figure

3.2 (a). However, there are also robots with a prismatic joint such as the Stanford robot presented in Figure 3.2 (b). Strings like “RRRRRR” for the Denso and “RRPRRR” for the Stanford can define the joint structure of a robot. ‘R’ and ‘P’ stand for the type of joint, either Revolute or Prismatic.

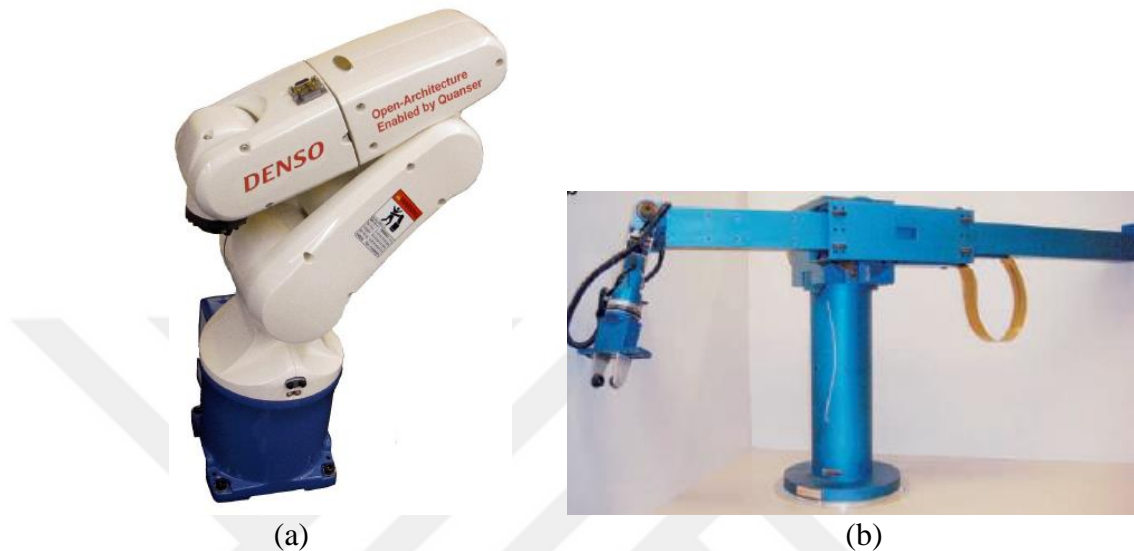


Figure 3.2 Denso (RRRRRR) arm & Stanford (RRRPRR) arm.

The robot kinematics can be categorized into two main parts; forward and inverse kinematics. Forward kinematics problem is not difficult to perform. There is no complexity in deriving the equations in contrast to the inverse kinematics. Especially nonlinear equations make the inverse kinematics problem complex. They may also be coupled and not have unique solutions (Craig, 2005).

3.3.1 Forward Kinematics Analysis

The forward kinematics problem is related between the individual joints of the robot manipulator and the position and orientation of the tool or end-effector. The joint variables are the angles between the links for revolute or prismatic joints and the link extensions (Niku, 2001).

A systematic way of describing the geometry of a serial chain of links and joints was proposed by Denavit and Hartenberg and is known today as Denavit-Hartenberg (DH) notation (Denavit and Hartenberg, 1955). Figure 3.3 illustrates the notation.

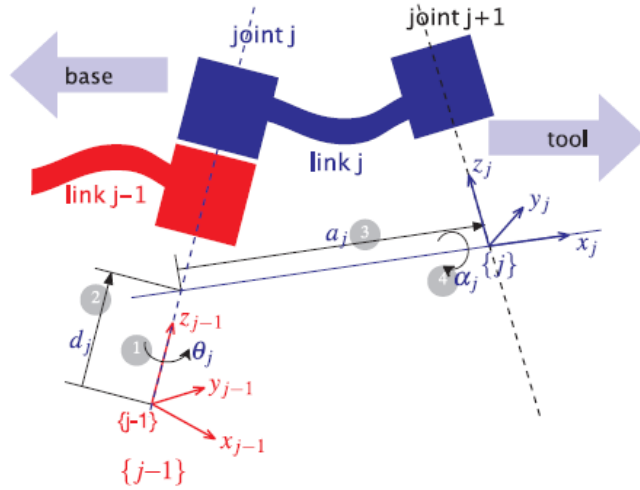


Figure 3.3 A DH representation of a general purpose joint-link combination (Corke, 2011).

The matrix A representing four movements is found by post-multiplying the four matrices representing four movements to reach frame $\{j-1\}$ to frame $\{j\}$ in Figure 3.3. They are rotation about z -axis an angle of θ_j , translation along the z -axis a distance of d_j , translation along the x -axis a distance of a_j and then rotation about x -axis an angle of α_j . These multiplication order and definitions of rotation and translation matrices are given in Eq. (3.1).

$${}^{j-1}A_j(\theta_j, d_j, a_j, \alpha_j) = T_{R_z}(\theta_j)T_z(d_j)T_x(a_j)T_{R_x}(\alpha_j) \quad \text{where}$$

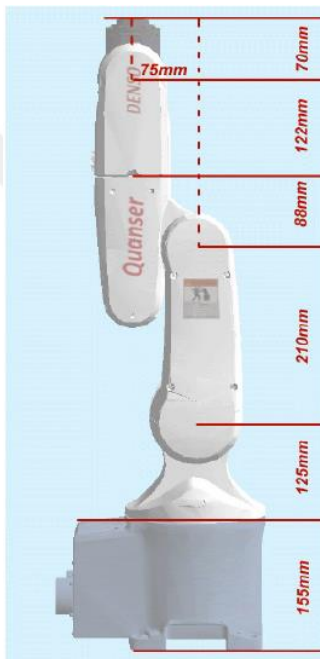
$$T_{R_z}(\theta_j) = \begin{bmatrix} C\theta_j & -S\theta_j & 0 & 0 \\ S\theta_j & C\theta_j & 0 & 0 \\ 0 & 0 & 1 & 0 \\ 0 & 0 & 0 & 1 \end{bmatrix} \quad T_z(d_j) = \begin{bmatrix} 1 & 0 & 0 & 0 \\ 0 & 1 & 0 & 0 \\ 0 & 0 & 1 & d_j \\ 0 & 0 & 0 & 1 \end{bmatrix}$$

$$T_x(a_j) = \begin{bmatrix} 1 & 0 & 0 & a_j \\ 0 & 1 & 0 & 0 \\ 0 & 0 & 1 & 0 \\ 0 & 0 & 0 & 1 \end{bmatrix} \quad T_{R_x}(\alpha_j) = \begin{bmatrix} 1 & 0 & 0 & 0 \\ 0 & -C\alpha_j & -S\alpha_j & 0 \\ 0 & S\alpha_j & C\alpha_j & 0 \\ 0 & 0 & 0 & 1 \end{bmatrix} \quad (3.1)$$

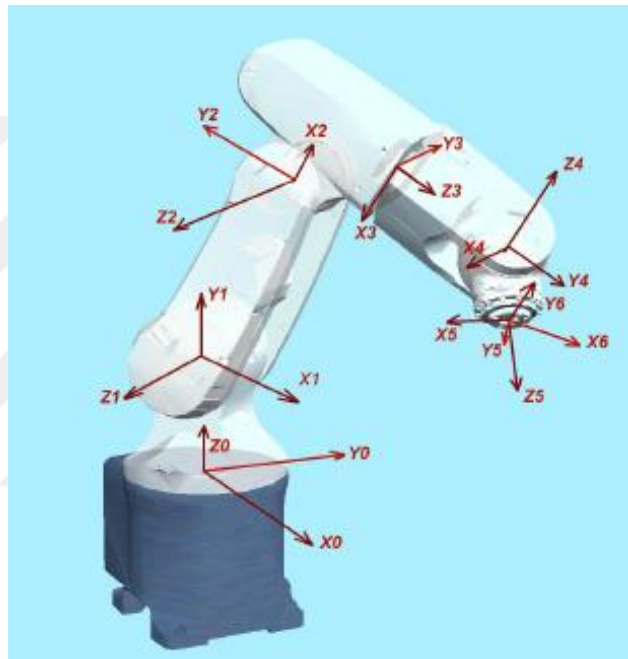
Transformation between two joints in a generic form (Corke, 2011) is given in Eq. (3.2).

$${}^{j-1}A_j = \begin{bmatrix} \cos \theta_j & -\sin \theta_j \cos \alpha_j & \sin \theta_j \sin \alpha_j & a_j \cos \theta_j \\ \sin \theta_j & \cos \theta_j \cos \alpha_j & -\cos \theta_j \sin \alpha_j & a_j \sin \theta_j \\ 0 & \sin \alpha_j & \cos \alpha_j & d_j \\ 0 & 0 & 0 & 1 \end{bmatrix} \quad (3.2)$$

The link lengths of Denso robot are given in Figure 3.4(a). The world frame and joint frames used in the calculations and home position of Denso robot are shown in Figure 3.4(b) and Figure 3.4(c), respectively.



(a)



(b)



(c)

Figure 3.4 Denso robot (Quanser, 2018).

Table 3.2 shows DH parameters of the Denso robotic arm necessary to derive the kinematics of the robot. Gripper is not included in the analysis.

Table 3.2 DH parameters of the Denso robotic arm

Joint i	θ_i	d_i	a_i	α_i
1	q_1	d_1	0	$\pi/2$
2	q_2	0	a_2	0
3	q_3	0	$-a_3$	$-\pi/2$
4	q_4	d_4	0	$\pi/2$
5	q_5	0	0	$-\pi/2$
6	q_6	d_6	0	0

where $d_1 = 0.125\text{m}$, $a_2 = 0.21\text{m}$, $a_3 = 0.075\text{m}$, $d_4 = 0.21\text{m}$ and $d_6 = 0.07\text{m}$.

The transformation matrix for each joint can be obtained by using Eq. (3.2). The parameters given in Table 3.2 are substituted into Eq. (3.2) to find each of them. Six transformation matrices are presented in Eq. (3.3).

$$\begin{aligned}
 A_1 &= \begin{bmatrix} C_1 & 0 & S_1 & 0 \\ S_1 & 0 & -C_1 & 0 \\ 0 & 1 & 0 & d_1 \\ 0 & 0 & 0 & 1 \end{bmatrix} & A_2 &= \begin{bmatrix} C_2 & -S_2 & 0 & a_2 C_2 \\ S_2 & C_2 & 0 & a_2 S_2 \\ 0 & 0 & 1 & 0 \\ 0 & 0 & 0 & 1 \end{bmatrix} & A_3 &= \begin{bmatrix} C_3 & 0 & -S_3 & a_3 C_3 \\ S_3 & 0 & C_3 & a_3 S_3 \\ 0 & -1 & 0 & 0 \\ 0 & 0 & 0 & 1 \end{bmatrix} \\
 A_4 &= \begin{bmatrix} C_4 & 0 & S_4 & 0 \\ S_4 & 0 & -C_4 & 0 \\ 0 & 1 & 0 & d_4 \\ 0 & 0 & 0 & 1 \end{bmatrix} & A_5 &= \begin{bmatrix} C_5 & 0 & -S_5 & 0 \\ S_5 & 0 & C_5 & 0 \\ 0 & -1 & 0 & 0 \\ 0 & 0 & 0 & 1 \end{bmatrix} & A_6 &= \begin{bmatrix} C_6 & -S_6 & 0 & 0 \\ S_6 & C_6 & 0 & 0 \\ 0 & 0 & 1 & d_6 \\ 0 & 0 & 0 & 1 \end{bmatrix}
 \end{aligned} \tag{3.3}$$

where $\text{Cos}(\pm \theta_n)$ and $\text{Sin}(\pm \theta_n)$ are abbreviated to $C_{\pm n}$ and $S_{\pm n}$, S_{nm} and C_{nm} stand for $\text{Sin}(\theta_n + \theta_m)$ and $\text{Cos}(\theta_n + \theta_m)$, respectively.

The total transformation between the base of the robot and the end-effector is;

$${}^R T_H = A_1 A_2 A_3 A_4 A_5 A_6 \tag{3.4}$$

An object can be represented in space by attaching a frame on it. Because the object is permanently attached to this frame, its position and orientation are always known (Niku, 2001). Consequently, the frame can be described in space, the position and orientation relative to the fixed frame will be known as given in Figure 3.5.

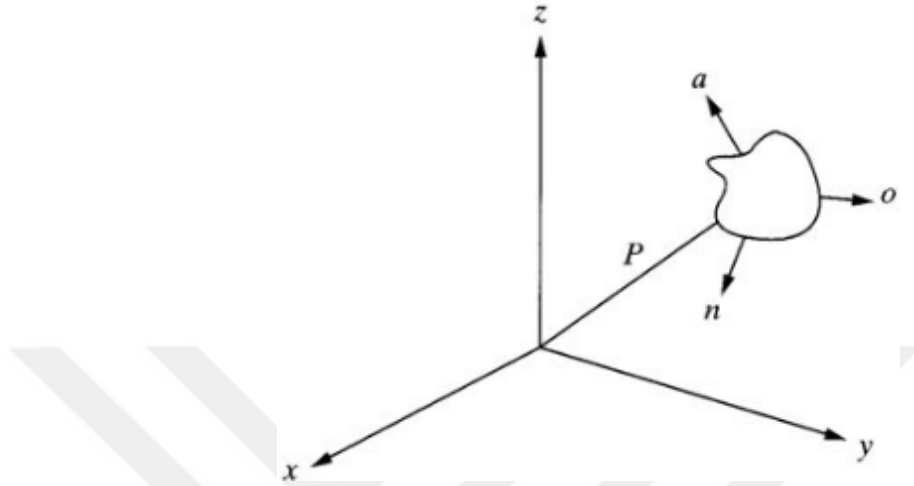


Figure 3.5 Representation of an object in space (Niku, 2001).

where n (normal), o (orientation), a (approach) elements are for orientation and P (position) elements are position elements relative to the reference frame. It can be represented in a matrix form as shown in Eq. (3.5).

$$F_{object} = \begin{bmatrix} n_x & o_x & a_x & P_x \\ n_y & o_y & a_y & P_y \\ n_z & o_z & a_z & P_z \\ 0 & 0 & 0 & 1 \end{bmatrix} \quad (3.5)$$

Transformation matrices for six axes given in Eq. (3.3) are post-multiplied in an order which is given in Eq. (3.4). Then it is equated to Eq. (3.5). This equality is shown in Eq. (3.6).

$$\begin{bmatrix} n_x & o_x & a_x & P_x \\ n_y & o_y & a_y & P_y \\ n_z & o_z & a_z & P_z \\ 0 & 0 & 0 & 1 \end{bmatrix} = A_1 A_2 A_3 A_4 A_5 A_6 \quad (3.6)$$

The elements of the matrix shown in left hand side of Eq. (3.6) are presented in Eqs. (3.7-3.10).

$$\begin{aligned}
n_x &= -S_6(C_4S_1 + S_4(C_1C_2C_3 - C_1S_2S_3)) - C_6(C_5(S_1S_4 - C_4(C_1C_2C_3 - C_1S_2S_3)) + S_5(C_1C_2S_3 + C_1C_3S_2)) \\
n_y &= S_6(C_1C_4 + S_4(S_1S_2S_3 - C_2C_3S_1)) + C_6(C_5(C_1S_4 - C_4(S_1S_2S_3 - C_2C_3S_1)) - S_5(C_2S_1S_3 + C_3S_1S_2)) \\
n_z &= C_6(S_5(C_2C_3 - S_2S_3) + C_4C_5(C_2S_3 + C_3S_2)) - S_4S_6(C_2S_3 + C_3S_2)
\end{aligned} \tag{3.7}$$

$$\begin{aligned}
o_x &= S_6(C_5(S_1S_4 - C_4(C_1C_2C_3 - C_1S_2S_3)) + S_5(C_1C_2S_3 + C_1C_3S_2)) - C_6(C_4S_1 + S_4(C_1C_2C_3 - C_1S_2S_3)) \\
o_y &= C_6(C_1C_4 + S_4(S_1S_2S_3 - C_2C_3S_1)) - S_6(C_5(C_1S_4 - C_4(S_1S_2S_3 - C_2C_3S_1)) - S_5(C_2S_1S_3 + C_3S_1S_2)) \\
o_z &= -S_6(S_5(C_2C_3 - S_2S_3) + C_4C_5(C_2S_3 + C_3S_2)) - C_6S_4(C_2S_3 + C_3S_2)
\end{aligned} \tag{3.8}$$

$$\begin{aligned}
a_x &= S_5(S_1S_4 - C_4(C_1C_2C_3 - C_1S_2S_3)) - C_5(C_1C_2S_3 + C_1C_3S_2) \\
a_y &= -S_5(C_1S_4 - C_4(S_1S_2S_3 - C_2C_3S_1)) - C_5(C_2S_1S_3 + C_3S_1S_2) \\
a_z &= C_5(C_2C_3 - S_2S_3) - C_4S_5(C_2S_3 + C_3S_2)
\end{aligned} \tag{3.9}$$

$$\begin{aligned}
P_x &= d_6(S_5(S_1S_4 - C_4(C_1C_2C_3 - C_1S_2S_3)) - C_5(C_1C_2S_3 + C_1C_3S_2)) - d_4(C_1C_2S_3 + C_1C_3S_2) + a_2C_1C_2 + a_3C_1C_2C_3 - a_3C_1S_2S_3 \\
P_y &= a_2C_2S_1 - d_6(S_5(C_1S_4 - C_4(S_1S_2S_3 - C_2C_3S_1)) + C_5(C_2S_1S_3 + C_3S_1S_2)) - d_4(C_2S_1S_3 + C_3S_1S_2) + a_3C_2C_3S_1 - a_3S_1S_2S_3 \\
P_z &= d_1 + d_4(C_2C_3 - S_2S_3) + d_6(C_5(C_2C_3 - S_2S_3) - C_4S_5(C_2S_3 + C_3S_2)) + a_2S_2 + a_3C_2S_3 + a_3C_3S_2
\end{aligned} \tag{3.10}$$

3.3.2 Inverse Kinematics Analysis

What it is interested to solve in this section is to show the procedure of the inverse kinematics solution. Inverse kinematics analysis is necessary for the manipulator control. Computing the inverse kinematics solution is comprehensive and generally requires a very long time in the real-time control of manipulators. A manipulator

performs the tasks in the Cartesian space, while actuators work in the joint space. Cartesian space includes an orientation matrix and a position vector. However, joint space only uses joint angles. Therefore, a conversion from the orientation and position of the robot end-effector to joint angles is necessary to perform. It is named the inverse kinematics solution. There are three approaches; analytical, numerical and semi-analytical (Kucuk and Bingul, 2004). The analytical approach is used herein. Liu et al. (2015) applied geometric approach for inverse kinematics analysis of a 6 DOF robot. Qiao et al. (2010) used double quaternions to get a solution for the inverse kinematics problem. Nubiola and Bonev (2014) offered a simple and efficient way to solve the inverse kinematics problem for 6R robots. It is noticed that Artificial Intelligence (AI) methods are frequently used in inverse kinematics problem (Köker, 2013; Duka, 2014; Almusawi et al., 2016) in recent years.

The equation representing the orientation and position of the robot was given in Eq. (3.6), let recall it.

$${}^R T_H = \begin{bmatrix} n_x & o_x & a_x & P_x \\ n_y & o_y & a_y & P_y \\ n_z & o_z & a_z & P_z \\ 0 & 0 & 0 & 1 \end{bmatrix} = A_1 A_2 A_3 A_4 A_5 A_6 \quad (3.11)$$

(Known Part) (Part including
unknown angular
displacements)

To find the inverse kinematics solution for the first joint (θ_1) as a function of the known elements, the inverse transformation matrix of the sixth link is postmultiplied as follows in Eq. (3.12).

$$A_1 A_2 A_3 A_4 A_5 A_6 A_6^{-1} = \begin{bmatrix} n_x & o_x & a_x & P_x \\ n_y & o_y & a_y & P_y \\ n_z & o_z & a_z & P_z \\ 0 & 0 & 0 & 1 \end{bmatrix} x A_6^{-1} \quad (3.12)$$

where $A_6A_6^{-1} = I$. I is the identity matrix. The above equation is resulted in Eq. (3.13).

$$A_1A_2A_3A_4A_5 = \begin{bmatrix} n_x & o_x & a_x & P_x \\ n_y & o_y & a_y & P_y \\ n_z & o_z & a_z & P_z \\ 0 & 0 & 0 & 1 \end{bmatrix} {}_x A_6^{-1} \quad (3.13)$$

Transformation matrix of each joint was given in Eq. (3.3). The required multiplication in Eq. (3.13) is carried out and yielding as Eq. (3.14).

$$\begin{bmatrix} " & " & " & C_1 \\ " & " & " & S_1 \\ " & " & " & " \\ 0 & 0 & 0 & 1 \end{bmatrix} = \begin{bmatrix} n_x C_6 - o_x S_6 & o_x C_6 + n_x S_6 & a_x & P_x - a_x d_6 \\ n_y C_6 - o_y S_6 & o_y C_6 + n_y S_6 & a_y & P_y - a_y d_6 \\ n_z C_6 - o_z S_6 & o_z C_6 + n_z S_6 & a_z & P_z - a_z d_6 \\ 0 & 0 & 0 & 1 \end{bmatrix} \quad (3.14)$$

It is noticed that the elements located in the first row & fourth column (abbreviated to (1, 4)) and second row & fourth column (abbreviated to (2, 4)) can be used in defining θ_1 (these abbreviations are also used in the remaining part of the inverse kinematics analysis). All elements in the left hand side of the Eq. (3.14) are known. However, all of them are not used in the calculation of θ_1 and they cover a big volume. Here ‘”’ symbol is used instead of writing them. It will be valid for the remaining parts of the chapter.

From (1, 4) and (2, 4) elements, θ_1 is found as illustrated in Eq. (3.15)

$$\theta_1 = A \tan 2(P_y - a_y d_6, P_x - a_x d_6) \quad (3.15)$$

The inverse transformation matrix of the first link is premultiplied by Eq. (3.13) to find the inverse kinematics solution for the third joint (θ_3) as a function of the known elements. It is given in Eq. (3.16).

$$A_1^{-1}A_1A_2A_3A_4A_5 = A_1^{-1} {}_x \begin{bmatrix} n_x & o_x & a_x & P_x \\ n_y & o_y & a_y & P_y \\ n_z & o_z & a_z & P_z \\ 0 & 0 & 0 & 1 \end{bmatrix} {}_x A_6^{-1} \quad (3.16)$$

where $A_1 A_1^{-1} = I$. I is the identity matrix. The above equation is resulted in Eq. (3.17).

$$A_2 A_3 A_4 A_5 = A_1^{-1} x \begin{bmatrix} n_x & o_x & a_x & P_x \\ n_y & o_y & a_y & P_y \\ n_z & o_z & a_z & P_z \\ 0 & 0 & 0 & 1 \end{bmatrix} x A_6^{-1} \quad (3.17)$$

The required multiplication in Eq. (3.17) is carried out as Eq. (3.18).

$$\begin{bmatrix} " & " & " & a_3 C_{23} - d_4 S_{23} + a_2 C_2 \\ " & " & " & d_4 C_{23} + a_3 S_{23} + a_2 S_2 \\ " & " & " & " \\ 0 & 0 & 0 & 1 \end{bmatrix} = \begin{bmatrix} " & " & " & C_1(P_x - a_x d_6) + S_1(P_y - l_5 a_y) \\ " & " & " & P_z - d_1 - l_5 a_z \\ " & " & " & " \\ 0 & 0 & 0 & 1 \end{bmatrix} \quad (3.18)$$

From (1, 4) and (2, 4) elements of the equation,

$$\begin{aligned} a_3 C_{23} - d_4 S_{23} + a_2 C_2 &= C_1(P_x - a_x d_6) + S_1(P_y - l_5 a_y) \\ d_4 C_{23} + a_3 S_{23} + a_2 S_2 &= P_z - d_1 - l_5 a_z \end{aligned} \quad (3.19)$$

Right hand side of the Eq. (3.19) is known. They are recalled as;

$$\begin{aligned} A &= C_1(P_x - a_x d_6) + S_1(P_y - l_5 a_y) \\ B &= P_z - d_1 - l_5 a_z \end{aligned} \quad (3.20)$$

Eq. (3.19) can be rewritten as below.

$$\begin{aligned} a_3 C_{23} - d_4 S_{23} + a_2 C_2 &= A \\ d_4 C_{23} + a_3 S_{23} + a_2 S_2 &= B \end{aligned} \quad (3.21)$$

After taking the squares of these expressions, they are added to each other and it yields as;

$$a_2^2 + a_3^2 + d_4^2 + 2a_2 a_3 \underbrace{(C_2 C_{23} + S_2 S_{23})}_{\text{Cos}(-\theta_3)} + 2a_2 d_4 \underbrace{(S_2 C_{23} - C_2 S_{23})}_{\text{Sin}(-\theta_3)} = A^2 + B^2 \quad (3.22)$$

The known parts are taken to the right hand side as shown in Eq. (3.23),

$$2a_2 a_3 C_{-3} + 2a_2 d_4 S_{-3} = A^2 + B^2 - a_2^2 - a_3^2 - d_4^2 \quad (3.23)$$

Eq. (3.23) is simplified and rewritten as Eq. (3.24),

$$XC_{-3} + YS_{-3} = Z \quad (3.24)$$

where

$$X = 2a_2a_3$$

$$Y = 2a_2d_4$$

$$Z = A^2 + B^2 - a_2^2 - a_3^2 - d_4^2$$

(X, Y and Z are known values.)

Then, θ_3 is found as given in Eq. (3.25).

$$\theta_3 = -(A \tan 2(Y, X) \mp A \tan 2(\sqrt{Y^2 + X^2 - Z^2}, Z)) \quad (3.25)$$

The inverse transformation matrix of the second link is premultiplied by Eq. (3.17) to find the inverse kinematics solution for the second joint (θ_2) as a function of the known elements. It is given in Eq. (3.26).

$$A_2^{-1}A_2A_3A_4A_5 = A_2^{-1}A_1^{-1}x \begin{bmatrix} n_x & o_x & a_x & P_x \\ n_y & o_y & a_y & P_y \\ n_z & o_z & a_z & P_z \\ 0 & 0 & 0 & 1 \end{bmatrix} xA_6^{-1} \quad (3.26)$$

where $A_2A_2^{-1} = I$. I is the identity matrix. In this case, the above equation is resulted in Eq. (3.27).

$$A_3A_4A_5 = A_2^{-1}A_1^{-1}x \begin{bmatrix} n_x & o_x & a_x & P_x \\ n_y & o_y & a_y & P_y \\ n_z & o_z & a_z & P_z \\ 0 & 0 & 0 & 1 \end{bmatrix} xA_6^{-1} \quad (3.27)$$

The required multiplication in Eq. (3.27) is carried out and it yields as Eq. (3.28).

$$\begin{bmatrix} " & " & " & a_3C_3 - d_4S_3 \\ " & " & " & d_4C_3 + a_3S_3 \\ " & " & " & " \\ 0 & 0 & 0 & 1 \end{bmatrix} = \begin{bmatrix} " & " & " & C_2(C_1(P_x - a_x d_6) + S_1(P_y - a_y - d_6)) - a_2 - S_2(d_1 - P_z + a_z d_6) \\ " & " & " & -S_2(C_1(P_x - a_x d_6) + S_1(P_y - a_y d_6)) - C_2(d_1 - P_z + a_z d_6) \\ " & " & " & " \\ 0 & 0 & 0 & 1 \end{bmatrix} \quad (3.28)$$

From (1, 4) elements of the equation above,

$$a_3C_3 - d_4S_3 = C_2(C_1(P_x - a_x d_6) + S_1(P_y - a_y - d_6)) - a_2 - S_2(d_1 - P_z + a_z d_6) \quad (3.29)$$

Eq. (3.29) can be rewritten as,

$$C_2K_1 + S_2(K_2) = D \quad (3.30)$$

where

$$K_1 = (C_1(P_x - a_x d_6) + S_1(P_y - a_y - d_6))$$

$$K_2 = -(d_1 - P_z + a_z d_6) \quad (K_1, K_2 \text{ and } D \text{ are known values})$$

$$D = a_3C_3 - d_4S_3 + a_2$$

Then, θ_2 is found as given in Eq. (3.31).

$$\theta_2 = A \tan 2(K_2, K_1) \mp A \tan 2(\sqrt{K_2^2 + K_1^2 - D^2}, D) \quad (3.31)$$

The inverse transformation matrix of the first, second and third joint is premultiplied by Eq. (3.11). The inverse kinematics solution for the fifth joint (θ_5) is found as a function of the known elements. It is given in Eq. (3.32).

$$(A_1A_2A_3)^{-1}A_1A_2A_3A_4A_5A_6 = (A_1A_2A_3)^{-1}x \begin{bmatrix} n_x & o_x & a_x & P_x \\ n_y & o_y & a_y & P_y \\ n_z & o_z & a_z & P_z \\ 0 & 0 & 0 & 1 \end{bmatrix} \quad (3.32)$$

where $(A_1A_2A_3)^{-1}A_1A_2A_3 = I$. I is the identity matrix. In this case, the above equation is resulted in Eq. (3.33).

$$A_4A_5A_6 = (A_1A_2A_3)^{-1}x \begin{bmatrix} n_x & o_x & a_x & P_x \\ n_y & o_y & a_y & P_y \\ n_z & o_z & a_z & P_z \\ 0 & 0 & 0 & 1 \end{bmatrix} \quad (3.33)$$

The required multiplication in Eq. (3.33) is carried out and it yields as Eq. (3.34).

$$\begin{bmatrix} " & " & " & " \\ " & " & " & " \\ " & " & C_5 & " \\ 0 & 0 & 0 & 1 \end{bmatrix} = \begin{bmatrix} " & " & " & " \\ " & " & " & " \\ " & " & " & a_z C_{23} - a_x S_{23} C_1 - a_y S_{23} S_1 \\ 0 & 0 & 0 & 1 \end{bmatrix} \quad (3.34)$$

From (3, 3) elements of the equation above,

$$C_5 = \underbrace{a_z C_{23} - a_x S_{23} C_1 - a_y S_{23} S_1}_{\Omega} \quad (3.35)$$

Then, θ_5 is found as given in Eq. (3.36).

$$\theta_5 = A \tan 2(\mp \sqrt{1 - \Omega^2}, \Omega) \quad (3.36)$$

The inverse transformation matrix of the first, second and third joint is premultiplied by Eq. (3.11) to find the inverse kinematics solution for the fourth joint (θ_4) as a function of the known elements. The multiplied matrix used in the previous step is also used in the determination of θ_4 angle. It is given in Eq. (3.37).

(1, 3) and (2, 3) elements of the equation are preferred as given Eq. (3.37),

$$\begin{bmatrix} " & " & -C_4 S_5 & " \\ " & " & -S_4 S_5 & " \\ " & " & " & " \\ 0 & 0 & 0 & 1 \end{bmatrix} = \begin{bmatrix} " & " & a_z S_{23} + a_x C_{23} C_1 + a_y C_{23} S_1 & " \\ " & " & a_y C_1 - a_x S_1 & " \\ " & " & " & " \\ 0 & 0 & 0 & 1 \end{bmatrix} \quad (3.37)$$

Then, θ_4 is found as given in Eq. (3.38).

$$\theta_4 = A \tan 2(a_y C_1 - a_x S_1, a_z S_{23} + a_x C_{23} C_1 + a_y C_{23} S_1) \quad (3.38)$$

The inverse transformation matrix of first, second and third joint is premultiplied by Eq. (3.11) to find the inverse kinematics solution for the sixth joint (θ_6) as a function of the known elements. Multiplied matrix used in the previous two steps (θ_4 and θ_5) is also used in determination of θ_6 angle.

(3, 1) and (3, 2) elements are preferred in Eq. (3.39),

$$\begin{bmatrix} " & " & " & " \\ " & " & " & " \\ C_6 S_5 & -S_5 S_6 & " & " \\ 0 & 0 & 0 & 1 \end{bmatrix} = \begin{bmatrix} " & " & " & " \\ " & " & " & " \\ n_z C_{23} - n_x S_{23} C_1 - n_y S_{23} S_1 & o_z C_{23} - o_x S_{23} C_1 - o_y S_{23} S_1 & " & " \\ 0 & 0 & 0 & 1 \end{bmatrix} \quad (3.39)$$

Then, θ_6 is found as given in Eq. (3.40).

$$\theta_6 = A \tan 2(- (o_z C_{23} - o_x S_{23} C_1 - o_y S_{23} S_1), (n_z C_{23} - n_x S_{23} C_1 - n_y S_{23} S_1)) \quad (3.40)$$

The solution of the inverse problem is not always unique in contrast to the forward kinematics problem. The same end-effector pose can be reached by various configurations (Manocha and Canny, 1994). Previous positions of the motors are fed to the program in each step. The difference between the calculated position and the previous position is obtained. The solution having the minimum difference is selected. By this way, the robot will not try to jump far positions, it will go to reach the nearest solution. Each solution obtained by inverse kinematics analysis should be checked to determine whether they bring the end-effector to the desired position.

3.3.3 Manipulator Jacobian

The Jacobian is a depiction of the geometry of mechanism elements in time. It is used to convert differential motions or velocities of joints to differential motions or velocities of points of interest. Jacobian is time-related (Niku, 2001) as given in Eq. (3.41). The following expression can be written for Denso robot to relate joint differential motions of a robot to the differential motion of its end-effector frame.

$$\begin{bmatrix} \partial x \\ \partial y \\ \partial z \\ \partial \theta_x \\ \partial \theta_y \\ \partial \theta_z \end{bmatrix} = \begin{bmatrix} Robot \\ Jacobian \end{bmatrix} \begin{bmatrix} d\theta_1 \\ d\theta_2 \\ d\theta_3 \\ d\theta_4 \\ d\theta_5 \\ d\theta_6 \end{bmatrix} \quad \text{or} \quad [D] = [J][D_\theta] \quad (3.41)$$

Open form of Jacobian matrix for RRRRRR robot,

$$[J] = \begin{bmatrix} \frac{\partial x}{\partial \theta_1} & \frac{\partial x}{\partial \theta_2} & \frac{\partial x}{\partial \theta_3} & \frac{\partial x}{\partial \theta_4} & \frac{\partial x}{\partial \theta_5} & \frac{\partial x}{\partial \theta_6} \\ \frac{\partial y}{\partial \theta_1} & \frac{\partial y}{\partial \theta_2} & \frac{\partial y}{\partial \theta_3} & \frac{\partial y}{\partial \theta_4} & \frac{\partial y}{\partial \theta_5} & \frac{\partial y}{\partial \theta_6} \\ \frac{\partial z}{\partial \theta_1} & \frac{\partial z}{\partial \theta_2} & \frac{\partial z}{\partial \theta_3} & \frac{\partial z}{\partial \theta_4} & \frac{\partial z}{\partial \theta_5} & \frac{\partial z}{\partial \theta_6} \\ \frac{\partial \theta_x}{\partial \theta_1} & \frac{\partial \theta_x}{\partial \theta_2} & \frac{\partial \theta_x}{\partial \theta_3} & \frac{\partial \theta_x}{\partial \theta_4} & \frac{\partial \theta_x}{\partial \theta_5} & \frac{\partial \theta_x}{\partial \theta_6} \\ \frac{\partial \theta_y}{\partial \theta_1} & \frac{\partial \theta_y}{\partial \theta_2} & \frac{\partial \theta_y}{\partial \theta_3} & \frac{\partial \theta_y}{\partial \theta_4} & \frac{\partial \theta_y}{\partial \theta_5} & \frac{\partial \theta_y}{\partial \theta_6} \\ \frac{\partial \theta_z}{\partial \theta_1} & \frac{\partial \theta_z}{\partial \theta_2} & \frac{\partial \theta_z}{\partial \theta_3} & \frac{\partial \theta_z}{\partial \theta_4} & \frac{\partial \theta_z}{\partial \theta_5} & \frac{\partial \theta_z}{\partial \theta_6} \end{bmatrix} \quad (3.42)$$

where ∂x , ∂y and ∂z symbolize the differential motions of the end-effector along x, y and z axes, respectively. Similarly $\partial \theta_x$, $\partial \theta_y$ and $\partial \theta_z$ are for the differential rotations of the end-effector around x, y and z axes, respectively. When these two matrices are divided by dt, they will represent velocities.

The 6x6 Jacobian matrix of the robot can be obtained by using the following equation (Spong et.al, 2004);

$$J = \begin{bmatrix} z_0^x (p - p_0) & z_1^x (p - p_1) & z_2^x (p - p_2) & z_3^x (p - p_3) & z_4^x (p - p_4) & z_5^x (p - p_5) \\ z_0 & z_1 & z_2 & z_3 & z_4 & z_5 \end{bmatrix} \quad (3.43)$$

where $z_0 = [0 \ 0 \ 1]^T$, $p_0 = [0 \ 0 \ 0]^T$, $z_i = T_i(1:3,3)$ and $p_i = T_i(1:3,4)$ for $i=1, \dots, 6$

where

$$T_i = A_1 \times \dots \times A_i \text{ and } p = T_H(1:3,4).$$

Jacobian elements are found by applying mathematical operations given in Eq. (3.43). They are shown in Eqs. (3.44-3.49).

$$\begin{aligned}
J_{1,1} &= d_4(C_2S_1S_3 + C_3S_1S_2) + d_6(S_5(C_1S_4 - C_4(S_1S_2S_3 - C_2C_3S_1)) + C_5(C_2S_1S_3 + C_3S_1S_2)) - \\
&\quad a_2C_2S_1 - a_3C_2C_3S_1 + a_3S_1S_2S_3 \\
J_{2,1} &= d_6(S_5(S_1S_4 - C_4(C_1C_2C_3 - C_1S_2S_3)) - C_5(C_1C_2S_3 + C_1C_3S_2)) - d_4(C_1C_2S_3 + C_1C_3S_2) + \\
&\quad a_2C_1C_2 + a_3C_1C_2C_3 - a_3C_1S_2S_3 \\
J_{3,1} &= 0 \\
J_{4,1} &= 0 \\
J_{5,1} &= 0 \\
J_{6,1} &= 1
\end{aligned} \tag{3.44}$$

$$\begin{aligned}
J_{1,2} &= -C_1(d_4(C_2C_3 - S_2S_3) + d_6(C_5(C_2C_3 - S_2S_3) - C_4S_5(C_2S_3 + C_3S_2)) + a_2S_2 + a_3C_2S_3 + \\
&\quad a_3C_3S_2) \\
J_{2,2} &= -S_1(d_4(C_2C_3 - S_2S_3) + d_6(C_5(C_2C_3 - S_2S_3) - C_4S_5(C_2S_3 + C_3S_2)) + a_2S_2 + a_3C_2S_3 + \\
&\quad a_3C_3S_2) \\
J_{3,2} &= C_1(d_6(S_5(S_1S_4 - C_4C_1C_{23}) - C_5C_1S_{23}) - d_4C_1S_{23} + a_2C_1C_2 + a_3C_1C_{23}) - S_1(d_4(S_1S_{23} + d_6(S_5(C_1S_4 + \\
&\quad C_4S_1C_{23})) + C_5S_1S_{23}) - a_2C_2S_1 - a_3(C_2C_3S_1 - S_1S_2S_3)) \\
J_{4,2} &= S_1 \\
J_{5,2} &= -C_1 \\
J_{6,2} &= 0
\end{aligned} \tag{3.45}$$

$$\begin{aligned}
J_{1,3} &= -C_1(d_4(C_2C_3 - S_2S_3) + d_6(C_5(C_2C_3 - S_2S_3) - C_4S_5(C_2S_3 + C_3S_2)) + a_3C_2S_3 + a_3C_3S_2) \\
J_{2,3} &= -S_1(d_4(C_2C_3 - S_2S_3) + d_6(C_5(C_2C_3 - S_2S_3) - C_4S_5(C_2S_3 + C_3S_2)) + a_3C_2S_3 + a_3C_3S_2) \\
J_{3,3} &= C_1(d_6(S_5(S_1S_4 - C_4C_1C_{23}) - C_5C_1S_{23}) - d_4C_1S_{23} + a_3C_1C_{23}) - S_1(d_4(S_1S_{23} + d_6(S_5(C_1S_4 + C_4S_1C_{23})) \\
&\quad + C_5S_1S_{23}) - a_3(C_2C_3S_1 - S_1S_2S_3)) \\
J_{4,3} &= S_1 \\
J_{5,3} &= -C_1 \\
J_{6,3} &= 0
\end{aligned} \tag{3.46}$$

$$\begin{aligned}
J_{1,4} &= d_4(S_1S_{23}) + d_6(S_5(C_1S_4 + C_4(S_1C_{23})) + C_5(S_1S_{23}))(C_{23}) - (d_4(C_{23}) + d_6(C_5(C_{23}) - \\
&\quad C_4S_5(S_{23}))(S_1S_{23})) \\
J_{2,4} &= (d_6(S_5(S_1S_4 - C_4C_1C_{23}) - C_5C_1S_{23}) - d_4C_1S_{23} + a_3C_1C_{23}) - (d_4C_1S_{23})(C_{23}) + \\
&\quad (C_1S_{23})(d_4(C_{23}) + d_6(C_5(C_{23}) - C_4S_5(S_{23}))) \\
J_{3,4} &= (C_1S_{23})(d_4(S_1S_{23}) + d_6(S_5(C_1S_4 + C_4(S_1C_{23})) + C_5(S_1S_{23}))) + (d_6(S_5(S_1S_4 - C_4(C_1C_{23}))) - \\
&\quad C_5(C_1S_{23})) - d_4(C_1S_{23})(S_1S_{23}) \\
J_{4,4} &= -C_1C_2S_3 - C_1C_3S_2
\end{aligned}$$

$$\begin{aligned}
J_{5,4} &= -C_2 S_1 S_3 - C_3 S_1 S_2 \\
J_{6,4} &= C_2 C_3 - S_2 S_3
\end{aligned} \tag{3.47}$$

$$\begin{aligned}
J_{1,5} &= d_6 S_4 (S_5 (C_1 S_4 + C_4 (S_1 C_{23})) + C_5 (S_1 S_{23})) (S_{23}) - d_6 (C_1 C_4 - S_4 (S_1 C_{23})) (C_5 (C_{23}) - \\
&\quad C_4 S_5 (S_{23})) \\
J_{2,5} &= d_6 S_4 (S_5 (S_1 S_4 - C_4 (C_1 C_2 C_3 - C_1 S_2 S_3)) - C_5 (C_1 C_2 S_3 + C_1 C_3 S_2)) (C_2 S_3 + C_3 S_2) - d_6 (C_5 (C_2 C_3 - S_2 S_3) - \\
&\quad C_4 S_5 (C_2 S_3 + C_3 S_2)) (C_4 S_1 + S_4 (C_1 C_2 C_3 - C_1 S_2 S_3)) \\
J_{3,5} &= d_6 (C_1 C_4 - S_4 (S_1 C_{23})) (S_5 (S_1 S_4 - C_4 (C_1 C_{23})) - C_5 (C_1 S_{23})) - d_6 (S_5 (C_1 S_4 + C_4 (S_1 C_{23})) + \\
&\quad C_5 (S_1 S_{23})) (C_4 S_1 S_4 (C_1 C_{23})) \\
J_{4,5} &= C_4 S_1 + S_4 (C_1 C_2 C_3 - C_1 S_2 S_3) \\
J_{5,5} &= -C_1 C_4 - S_4 (S_1 S_2 S_3 - C_2 C_3 S_1) \\
J_{6,6} &= S_4 (C_2 S_3 + C_3 S_2)
\end{aligned} \tag{3.48}$$

$$\begin{aligned}
J_{1,6} &= 0 \\
J_{2,6} &= 0 \\
J_{3,6} &= 0 \\
J_{4,6} &= S_5 (S_1 S_4 - C_4 (C_1 C_2 C_3 - C_1 S_2 S_3)) - C_5 (C_1 C_2 S_3 + C_1 C_3 S_2) \\
J_{5,6} &= -S_5 (C_1 S_4 - C_4 (S_1 S_2 S_3 - S_1 C_2 C_3)) - C_5 (C_2 S_1 S_3 + C_3 S_1 S_2) \\
J_{6,6} &= C_5 (C_2 C_3 - S_2 S_3) - C_4 S_5 (C_2 S_3 + C_3 S_2)
\end{aligned} \tag{3.49}$$

Additionally, the Jacobian matrix is being used in inverse kinematics analysis as an iterative technique (Duleba and Opalka, 2013). It is used in the singularity analysis of robot manipulators. The singularity problem occurs when the inverse Jacobian becomes singular (determinant = 0) (Chiaverini and Egeland, 1990).

3.4 QUARC Control Software

QUARC is an open-architecture control module. This module includes six amplifiers and FF (feed-forward) + PID (proportional, integral, derivative) controllers. The controllers operate at 1 kHz for each motor. It is possible to change the controller gains. It is also possible to bypass PID controllers and manage the amplifier currents by using FF torque (Quanser, 2018).

The QUARC has a Simulink Library. It is a collection of custom blocks created for the 6 DOF Denso robot. Real-time code is generated by the QUARC. The ‘Denso

Read' block is used to read the joint encoder positions, effort (joint control currents), defined status codes, and error signals. 'denso' is a reference to the Denso robot. It is required to pass to the 'denso' input port of the 'Write' block. In case of a failure to connect this signal to the 'Denso Write' block will result in an error. 'position' is a 6-vector including encoder positions. Conversion factors given in Table 3.1 are used to convert them into joint angles. 'effort' is a 6-vector showing the control currents of the joints. 'status' and 'errors' are 6-vector containing the per-axis state and error codes, respectively. When the state vector value is 8, 'open architecture mode' is ready to take commands from other subsystems. When it is 7, the robot is not ready to take the commands. However, the encoder data received from the robot is started and the current positions of the joints are detected.

The 'Denso Write' block is used to transmit the joint position and the joint velocity commands. PID and feedforward gains of the joints are also transferred. According to the block control mode, the robot commands are either desired joint encoder positions or a desired change in joint encoder positions. This block sends commands to the Denso robot every 1ms. Figure 3.6 shows 'Denso Read' block and 'Denso Write' block.

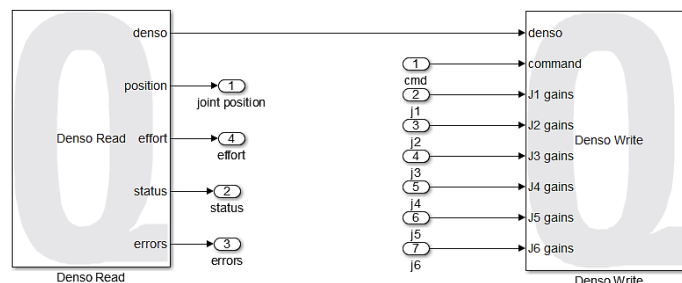


Figure 3.6 'Read' block and 'Write' block.

The command is a 6-vector including the joint encoder position commands or delta position commands if the Velocity mode is active. The J (1:6) gains are a 4-vector showing the controller gains [P I D F] for joints, where P is the proportional gain, I is the integral gain, D is the derivative gain, and F is a feedforward input. Communication between the Denso robot and the QUARC external Simulation mode is provided through a real-time point-to-point network link. Ethernet protocol is used in transmitting the exchanged data.

3.4.1 Denso_Control Release

This model contains the controllers and kinematics for the Denso robot and tool actuator. It can be used to control the robot in both joint level and workspace level. It is given in Figure 3.7.

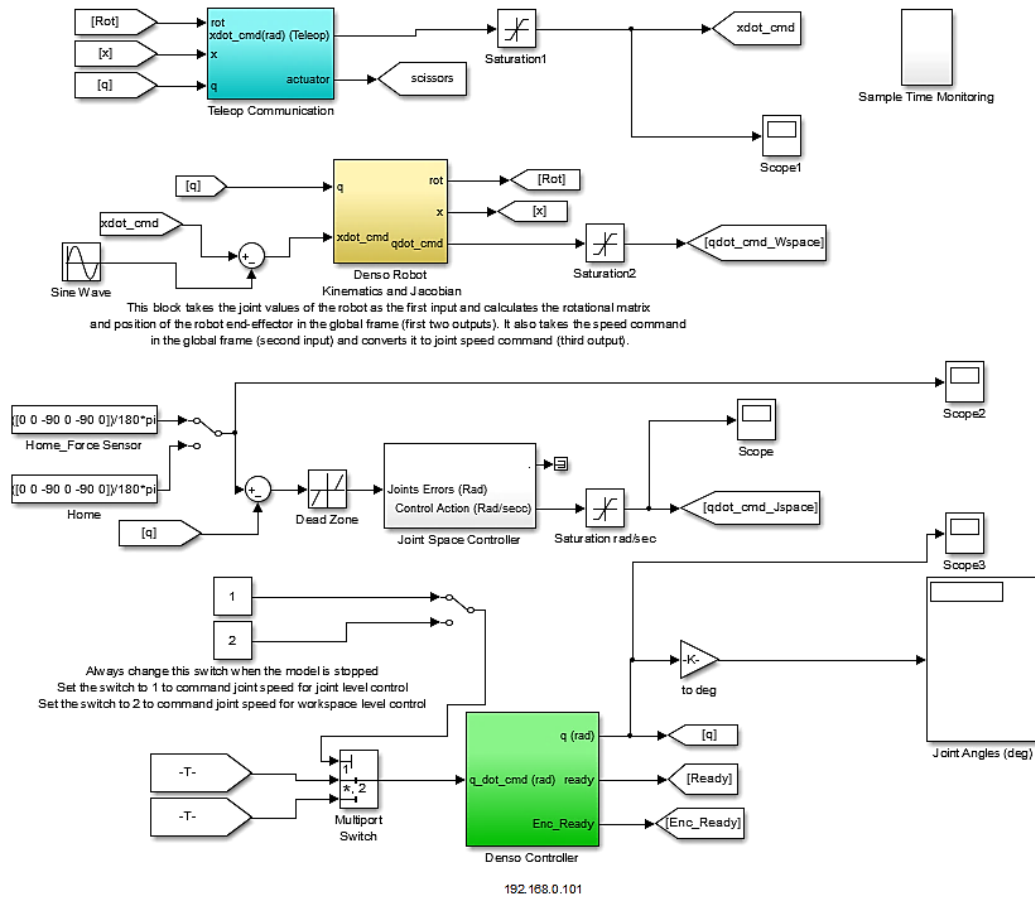


Figure 3.7 Main model of Denso robot.

The green block in Figure 3.7 contains the Denso robot controller and Read/Write blocks. The input to this subsystem is \dot{q}_{cmd} that is a 6-element vector with the Denso's desired joint values in rads. The first output of the block is the measured joint values of the robot. The second and the third outputs of the block are generated based on the Denso state value.

The yellow subsystem in Figure 3.7 contains the Denso robot kinematics and the Jacobian subsystem. Figure 3.8 displays the blocks used inside the subsystem. The orange block called Jacobian manipulator derives the kinematics and Jacobian of the Denso arm. Eq. (3.43) is embedded in it. The inverse of Jacobian matrix is also

calculated herein. If the condition number is lower than the condition number threshold, inverse operation is being applied to the Jacobian matrix. Otherwise, pseudo-inverse operation is being applied to the Jacobian matrix due to loss of rank (Sponge et al., 2004).

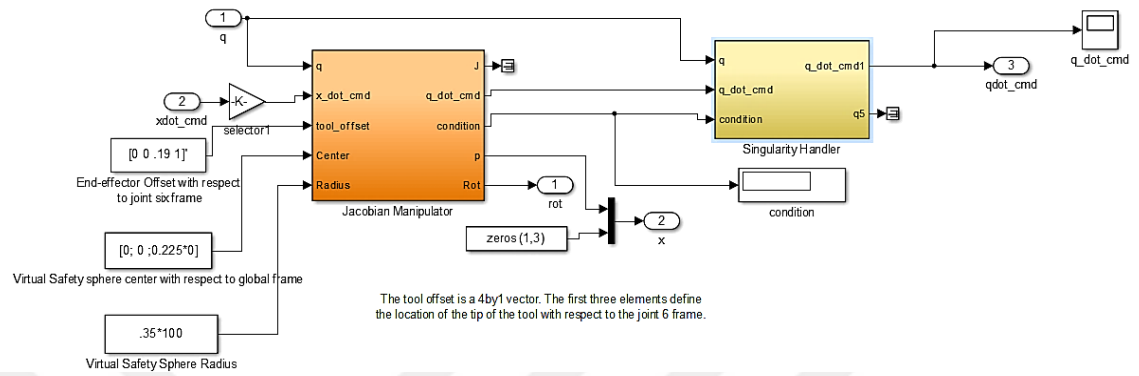


Figure 3.8 Jacobian subsystem of Denso robot.

The yellow subsystem in Figure 3.8 is used to handle singularity issues. The details of ‘Singularity Handler’ are given in Figure 3.9.

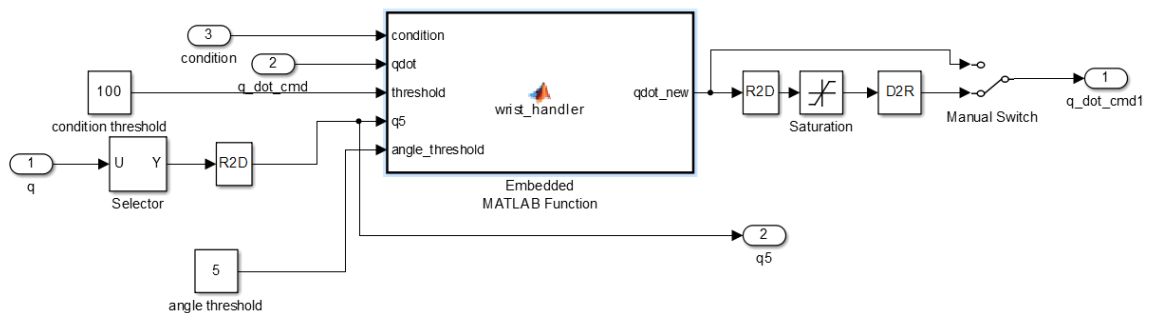


Figure 3.9 Details of singularity handler.

The embedded function states that if the condition number is greater than the condition threshold and the absolute value of the angular displacement of the fifth axis is lower than the angle threshold, joint velocity of the fourth axis is taken stationary and joint velocity of the sixth axis is obtained by addition of joint velocities of the fourth and sixth axes.

The condition number of a matrix is used for estimating the error in the solution of a linear system. Considering in expression of the Jacobian matrix, the condition number

is an error-amplifying factor of actuators. It affects the accuracy of the Cartesian velocity of the end-effector (Küçük and Bingül, 2006).

The condition number for the Jacobian matrix is shown in Eq. (3.50).

$$\kappa = \|J\| \|J^{-1}\| \quad (3.50)$$

where $\| \cdot \|$ is the Euclidian norm of the matrix, which can be defined as

$$\|J\| = \sqrt{\text{tr}(JNJ^T)}$$

where tr symbolize trace and N is a matrix calculated by $(1/n)[I]$.

The dimension of the square matrix is n and I is the identity matrix. The matrix J is well-conditioned when the condition number approaches to 1. It shows that the configuration is far from the singularity. The matrix is called as ill-conditioned when the condition number approaches infinity. It is aimed to be kept as close to unity as possible. It varies from one to infinity.

$(1/\kappa)$ is defined as the local conditioning index (LCI) to assess the control accuracy, dexterity of the mechanism. (Angeles and Lopez-Cajun, 1988). LCI is desired to be as big as possible.

3.4.2 Inverse Position Kinematics (IPK) & Forward Position Kinematics (FPK)

This model can be used in order to control the robot in the Cartesian space. It is possible to command the robot to go to a specific pose within the workspace of the robot by using this model. Linear motions in x, y and z-axis and orientation changes in roll, pitch and yaw angles are the input of this model. The model is illustrated in Figure 3.10. The steps should be followed for this model.

1. The switch must be set to 'Home'. If the robot is not at home, stop the model and restart it.
2. Make sure that the constant 'xyz_0' is equal to P_0_EE value (output of the 'Denso VP 6242G FPK' block) when the robot is at homed at $t=0$, and 'xyz_command'=[0 0 0].

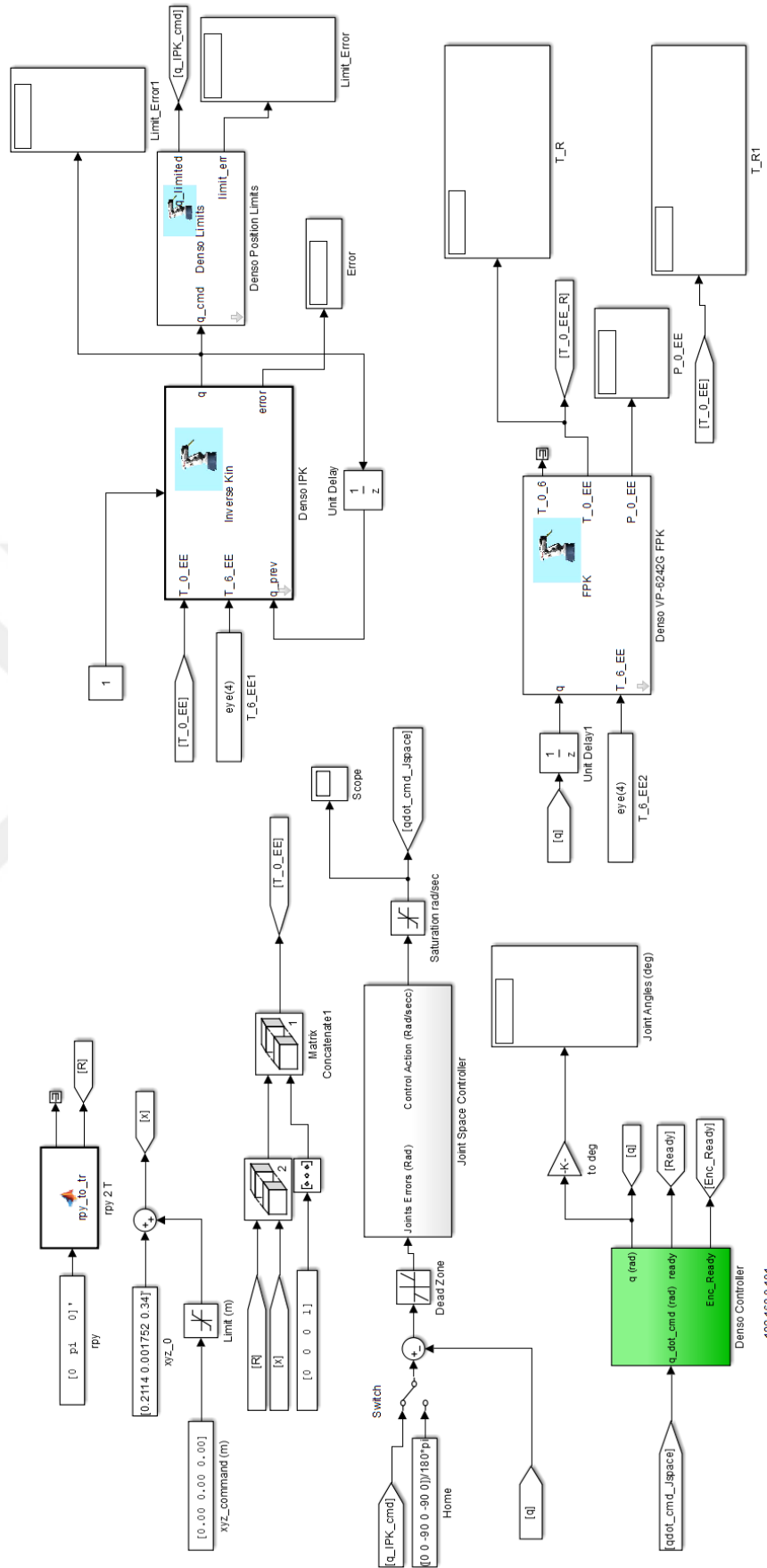


Figure 3.10 IPK and FPK of Denso.

3. Switch to q_IPK_cmd input mode.
4. Build the model and start it.
5. It is important to give commands in small increments from the current pose by changing the 'xyz_command' parameter in the model.

The location of the tip of the system is defined for xyz_0. Rotation [R] and translation [x] matrices are concatenated and the overall transformation matrix from base to end-effector $[T_{0_EE}]$ is obtained. A transformation matrix $[T_{6_EE}]$ is also defined between the end-effector (if available) and the sixth axis of the Denso robot. The multiplication of $[T_{0_6}]$ and $[T_{6_EE}]$ yields $[T_{0_EE}]$ as given in Eq. (3.51). If there is no end-effector, $[T_{0_EE}]$ and $[T_{0_6}]$ are equal to each other and $[T_{6_EE}]$ is an identity matrix. If there is an end-effector, $[T_{6_EE}]$ is defined. The multiplication of $[T_{0_EE}]$ and inverse of $[T_{6_EE}]$ matrices gives the transformation matrix of the Denso robot, $[T_{0_6}]$ as shown in Eq. (3.52). Then, the expressions mentioned in Section 3.3.2 are applied and the angular displacements of the robot links are found.

$$[T_{0_6}] \times [T_{6_EE}] = [T_{0_EE}] \quad (3.51)$$

$$[T_{0_6}] = [T_{0_EE}] \times [T_{6_EE}]^{-1} \quad (3.52)$$

The Denso VP 6242G_FPK block is to calculate forward kinematics analysis of the robot. The calculations in Section 3.3.1 are embedded inside the Denso VP 6242G_FPK mask. All kinematic parameters including DH and link lengths of the robot are included.

3.5 Off-line Programming of Denso Robot

Robot programming is an important assignment in robotics by combining theory and implementation. It can be grouped into two branches: on-line and off-line. On-line programming is used by the researchers when the system is appropriate to the programming interface. The others select off-line programming to see and evaluate the results without manipulating the robot. Off-line programming is the case where the robot and other equipment do not have power and run. Everything is being operated

on a computer. Type of robot to be used and the arrangement of equipment is determined according to the simulation results (Küçük and Bingül, 2005, 2009).

Off-line programming is not an automatic operation. Robot codes are edited manually by computer software. Real robotic scenarios are then simulated before real applications. The task sequence can be planned and programmed. This is the main advantage of off-line programming. Some considerable advantages of off-line programming are as follows:

- i. The robot in action is not stopped or disturbed for programming. Programming is carried out before installation. While re-programming for a new duty, the robot is stayed in production (Mitsi et al., 2004). Thus, programming and robot production can be handled in parallel.
- ii. Work safety is increased. The user does not stand in the robot workspace during programming.
- iii. Simulation tools are used to test the programs to expect real robot behaviour.

On the other hand, some disadvantages can be specified as:

- i. Software and training of the workers require relatively high investment.
- ii. Verification of the programs is carried out by testing them in real applications. Calibration errors may cause robot crashes (Neto and Mendes, 2013).

Up to now, robot software tools having specific abilities and properties have been developed. Robotica encapsulating over 30 functions was presented for kinematics and dynamics of robots. Robot animation was also possible (Nethery and Sponge, 1994). The Robotics Toolbox for Matlab (Corke, 1996) supplied many useful subroutines designed for robotics education. Kinematics, dynamics and trajectory generation were simply included. Although the user can form a serial-link manipulator, a limited number of robot examples like the PUMA and Stanford arm were also available. The Rapid Analysis Manipulator Program (RAMP) was designed for modelling and analysis of serial robots having revolute joints (Hill and Tesar, 1996). A commercial software package named Robot Computer Aided Analysis and Design (RCAAD) was offered by Das et al. (1999) and used to analyse and optimize robot arms for planetary rovers and landers. Solid and wire type visualization is available. A toolbox used only for the dynamics of a redundant manipulator was offered by Zlajpah (2000). A

simulation program named SimBot was offered to teach and develop autonomous robots (Turnell et al., 2001). Scenarios including multiple autonomous robots were focused on this program. A Windows-based GUI robot package (Robotect) was developed to model and analyse manipulators (Nayar, 2002). RoboSim based on COMMON LISP was developed to model, visualize and analyse the performance of a serial manipulator on a low cost PC platform (Bingül et al., 2002). KUKA's simulation tools were presented by Vollmann (2002). They are based on visual components. An educational tool for 6-DOF industrial robots was developed by Çakır and Bütün, (2002). Quaternion algebra was used for serial robots having only revolute joints with limited GUI options. Some important properties of robot programs were tabulated and their advantages and disadvantages were mentioned by Küçük and Bingül (2009). ROBOLAB is a program that can carry out a comprehensive analysis of 6 DOF robots having revolute and prismatic joints. It has a library including 16 robots with wire type visualization. Chinello et al. (2011) presented a study on the forward and inverse kinematics, cartesian control and trajectory planning of KUKA Robot. ReDySim (Shah et al., 2012) is a recursive algorithm developed for solving forward and inverse dynamics. Only computer coding is allowed, so there are no options of GUI. Solid model visualization is not available. Off-line robot programming via a CAD package was submitted by Neto and Mendes (2013). Serial n-axis manipulators (SnAM) (Gonzales et al., 2013) is generated on Visual Studio C++ based ADEFID (Advanced Engineering software for Industrial Development. The capability of SnAM is restricted with the kinematic analysis of systems having revolute joints. Gil et al. (2015) developed ARTE for simulation and visualization of up to 7 DOF robot manipulators. Kinematic and dynamic analysis can be carried out. Solid visualization is available. Build-A-Robot (Flanders and Kavanagh, 2015) is focused on GUI enriched forward kinematics of up to 7 DOF industrial robots. 3D solid model of the robots is seen in a window enhanced with virtual reality. Tao and Minghong (2017) modelled a welding robot with the Robotic Toolbox. The toolbox by Arnay et al. (2017) was generated in Unity3D and Python. The kinematic analysis of any serial-link manipulators having prismatic and revolute joints is practicable in this toolbox. Ozakyol et al. (2019) developed a toolbox for analysis, kinematic and dynamic design of high DOF serial manipulators. It can be applied to any robot with solid model visualization.

Robotics Toolbox contains a lot of functions that are demanded in robotics and address fields such as kinematics, dynamics, and trajectory generation. The Toolbox is convenient for simulation besides analysing results from experiments with real robots. It is also an effective tool for education. The Toolbox is organized on a very common method of representing the kinematics and dynamics of serial-link manipulators. It is described by the matrices. These include, in basic case, the Denavit and Hartenberg parameters of the robot (Denavit and Hartenberg, 1955). The user can configure any serial-link manipulator. A number of examples are provided for well-known robots such as the Puma 560 and the Stanford arm (Corke, 2011). Constantin et al. used Robotic Toolbox in forward kinematics analysis of an industrial robot (Constantin et al., 2015). Some examples designed by robotics toolbox is given in Figure 3.11 (Corke, 2011).

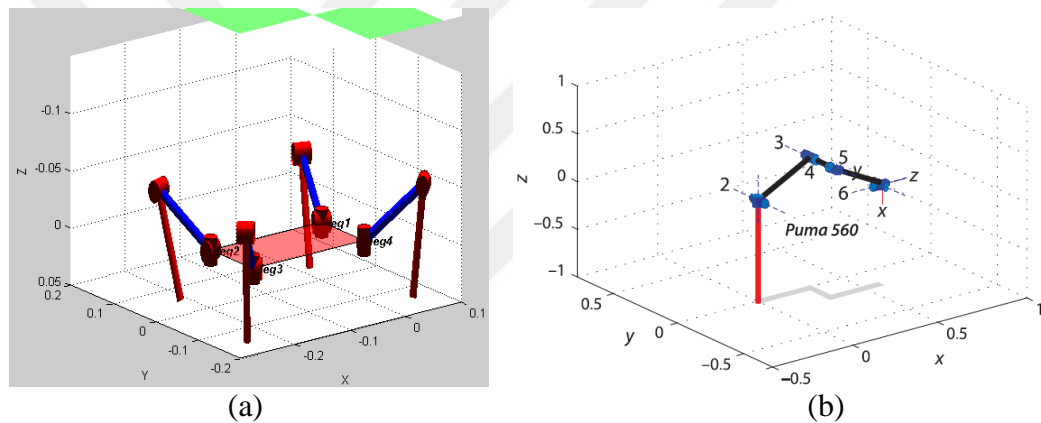


Figure 3.11 Examples obtained by Robotic Toolbox.

GUIDE, the MATLAB® Graphical User Interface Development Environment offers tools set to develop graphical user interfaces (GUIs). It extremely makes the process of designing and building GUIs easy. GUIDE tools can be employed to

- set the GUI in an easy way by clicking and dragging components into the layout area. Panels, buttons, text fields, sliders, menus are the components.
- generate an M-file automatically to control how the GUI performs. The M-file starts the GUI and includes a framework for all the GUI callbacks. Callbacks are the commands carried out when a GUI component is clicked. It is possible to add code to the callbacks to accomplish the functions desired (GUIDE Creating Graphical User Interfaces, 2018). Some GUI examples are given in Figure 3.12.

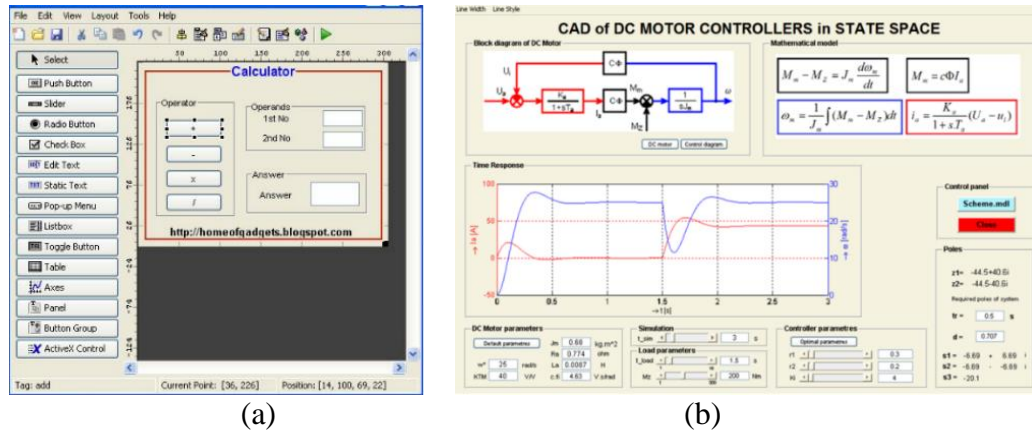


Figure 3.12 Examples obtained by GUIDE.

3.5.1 Off-line Studies for the Forward Kinematics

A GUI study enriched with Robotic Toolbox in Matlab® has been prepared for Denso robot including forward kinematics and manipulator Jacobian. The sketch of the GUI is given in Figure 3.13. As seen in the left hand side of the sketch, push buttons, sliders, axes etc. can be added on it. Additions are being visible on the m. file simultaneously as a function. Two different configurations can be seen in Figure 3.14 (a, b). Robotics Toolbox is embedded in GUI.

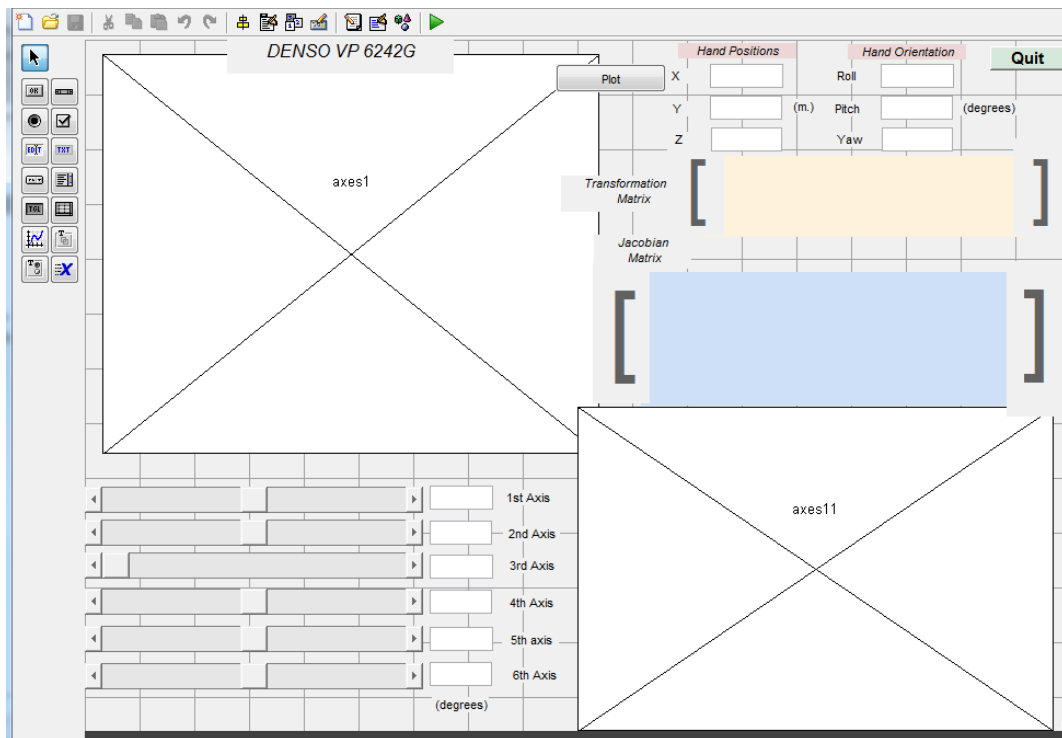
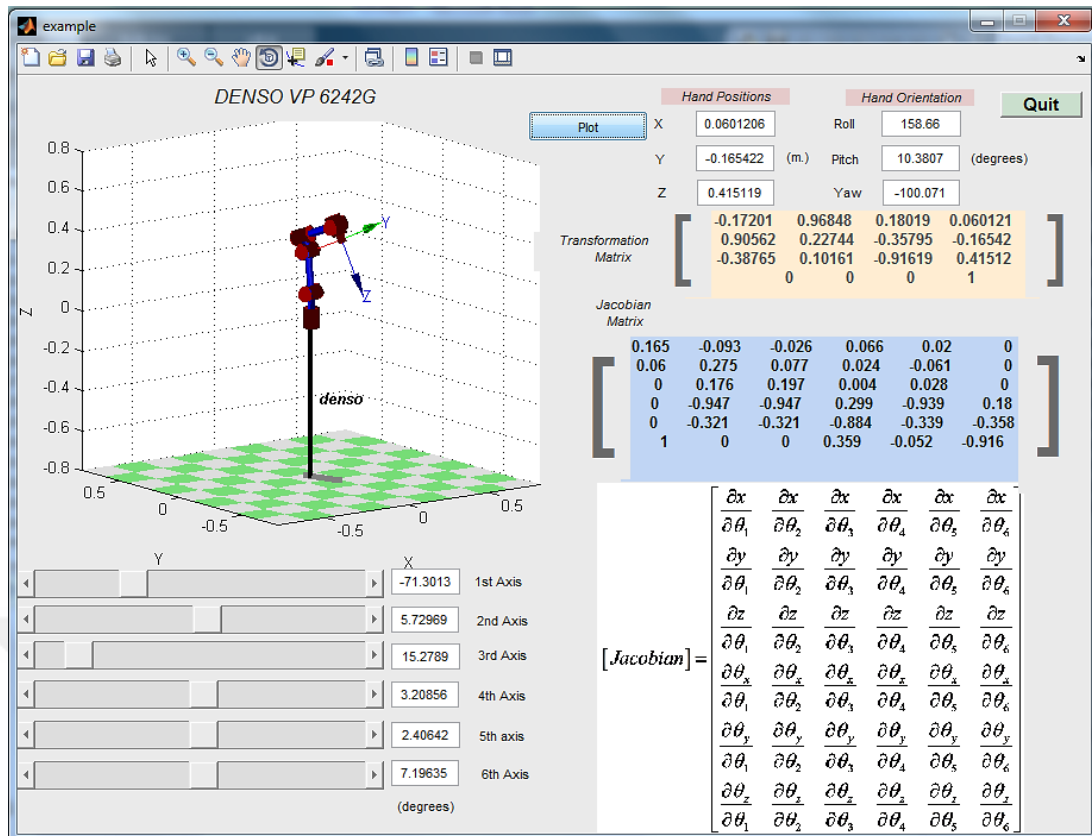
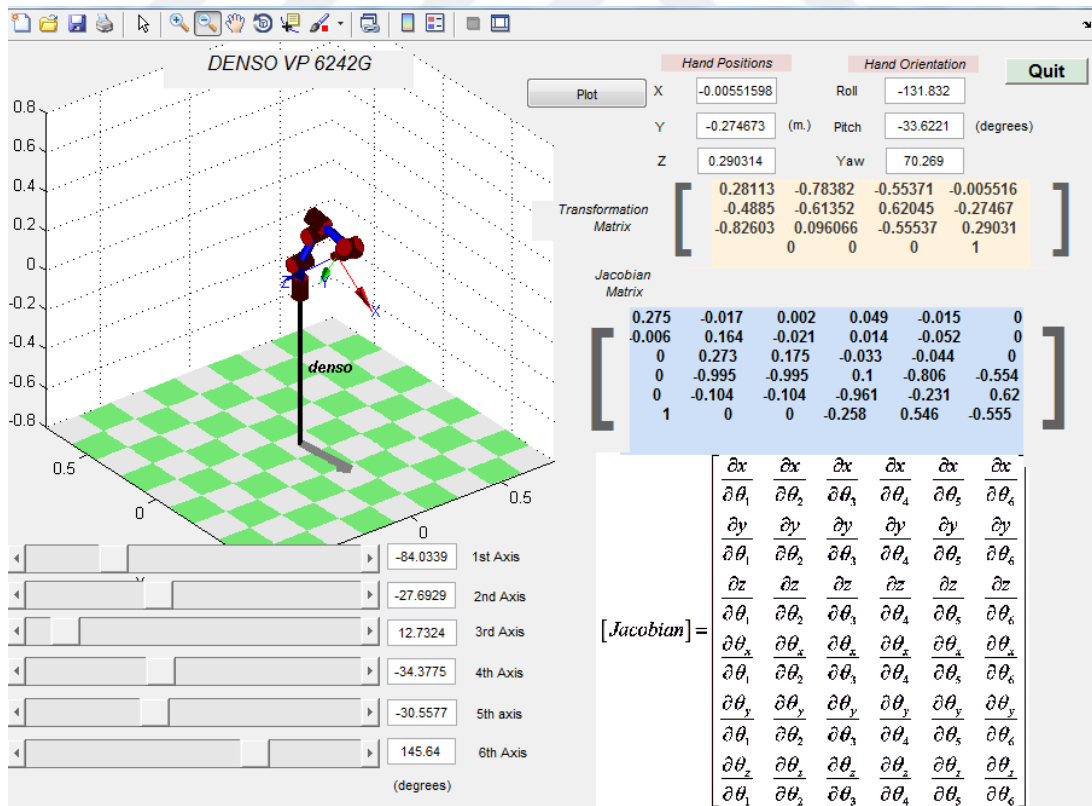


Figure 3.13 fig. file of GUI.

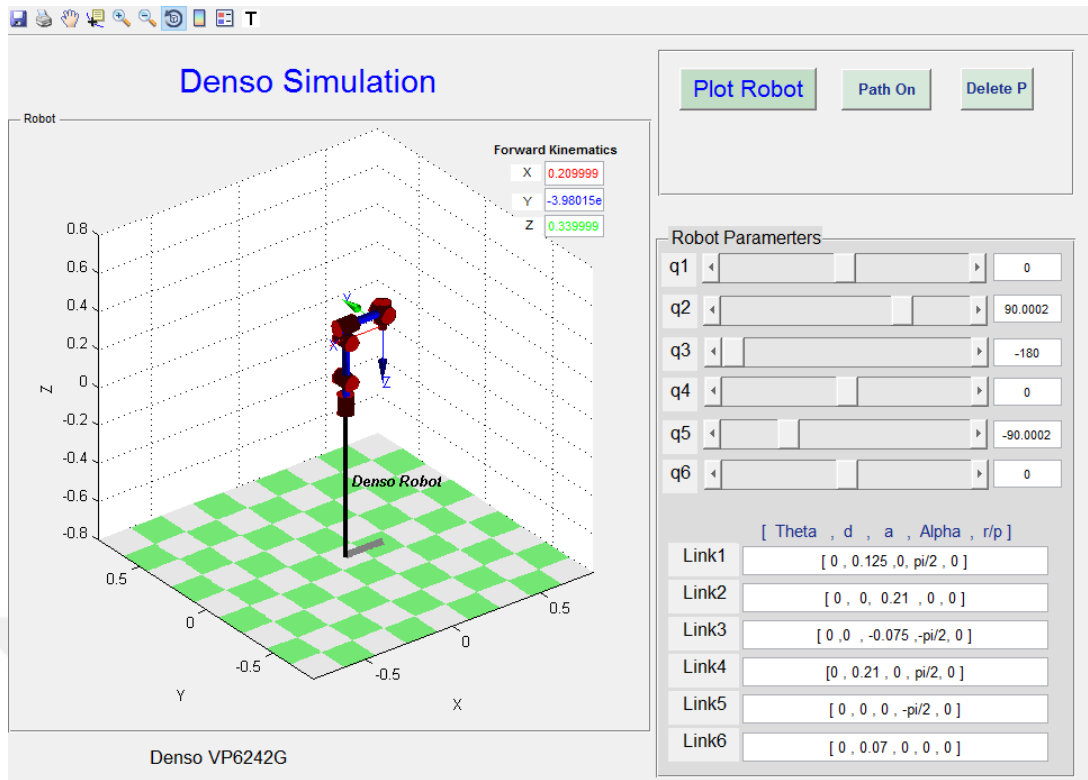


(a)

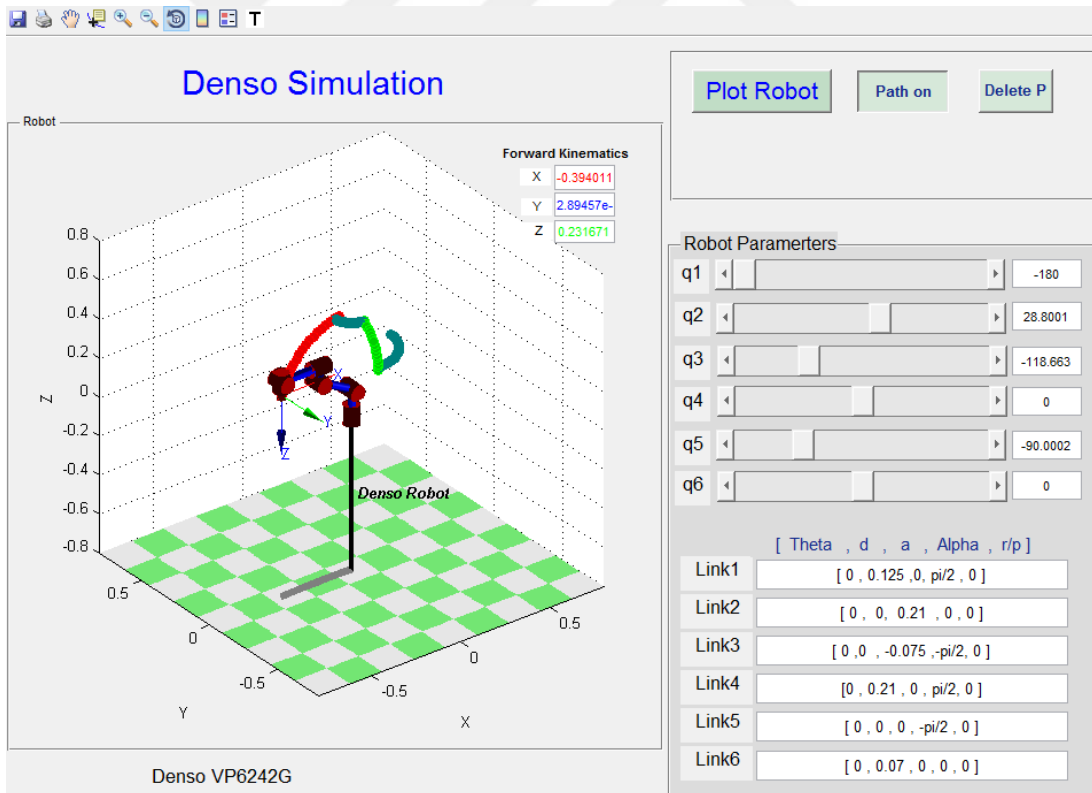


(b)

Figure 3.14 Designed GUI example.



(a)



(b)

Figure 3.15 Designed GUI example II.

When the model designed for Figure 3.14 is run,

- The first thing is to adjust the angles of the robot axes by sliders.
- The plot button is then pressed.
- By the way, robot configuration, general transformation matrix, robot hand position (X, Y, Z) & hand orientation (Roll, Pitch, Yaw) and Jacobian matrix are calculated and seen on the screen in real-time.

Figure 3.15 shows the designed off-line simulation model by MATLAB/GUIDE to create a serial link robot (Link 1-6) and change the joint angles (q_1, q_2, q_3, q_4, q_5 and q_6). DH parameters can directly be changed. Figure 3.15 (a) and Figure 3.15 (b) show the initial condition of the robot and the path generated with the given joint angles, respectively. The results are compared with the expressions obtained analytically. It is proved that the same results are obtained by Robotic Toolbox and analytical solution.

3.5.2 Offline Studies for the Inverse Kinematics

The angular displacements of the links are inputs to get a total transformation matrix in forward kinematics. Then the position and orientation of the end-effector are defined. Inverse kinematics analysis is vice-versa of forward kinematics analysis. A Simulink model including Simmechanics blocks is given in Figure 3.16. The desired position and orientation angles of the end-effector are selected. The total transformation matrix (T_{0_EE}) of the Denso robot is firstly obtained in this model by concatenating R (rotation matrix) and x (translation matrix). The required angular displacements of the links are calculated in Inverse Position Kinematics (IPK) function with the input (T_{0_EE}). Then they are fed into the joints of the Denso robot via Simmechanics blocks. So visual simulation of the system can be seen in real-time. Pure translation change in X, Y, Z coordinates, pure orientation change in roll, pitch, yaw angles, or change in both translation and orientation can be performed. Some trajectories with circular or quadratic shaped to be traced by the end-effector can be handled by adjusting (open/close) the manual switches located on the model.

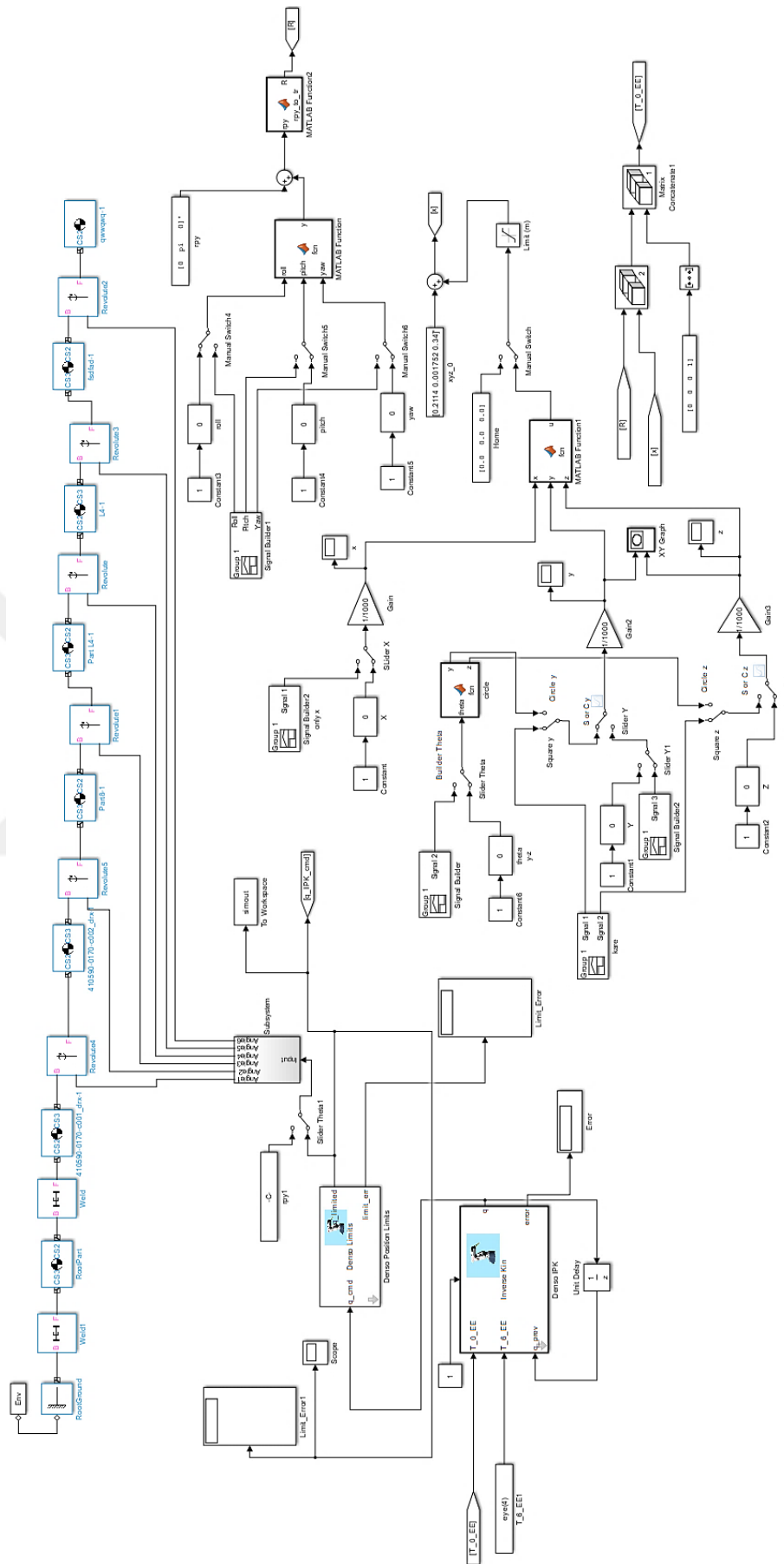
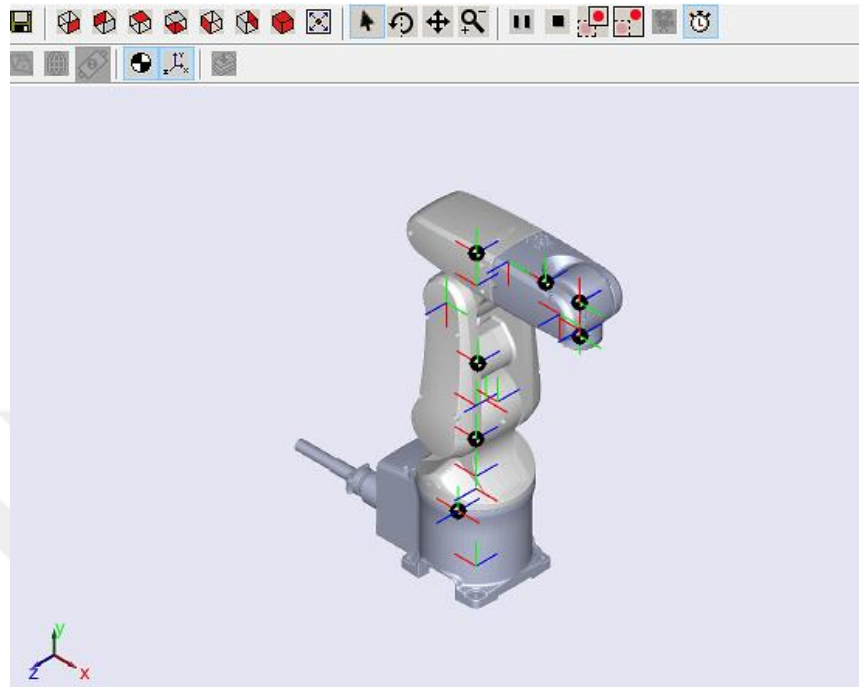
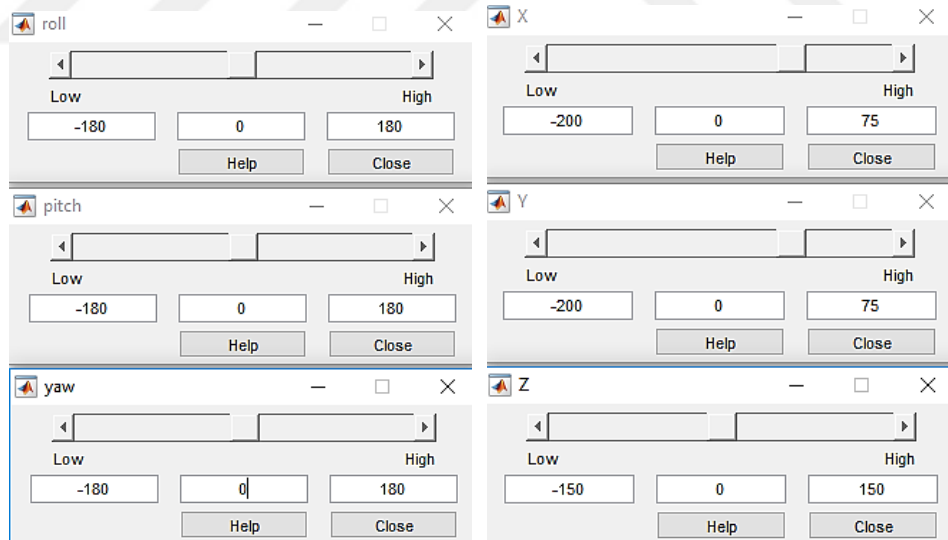


Figure 3.16 Simulink model for inverse kinematics analysis.

The Denso robot in home position is shown in Figure 3.17 (a, b and c). The slider values of the roll, pitch and yaw angles and X, Y, Z displacements in Cartesian coordinates are all zero.



(a)

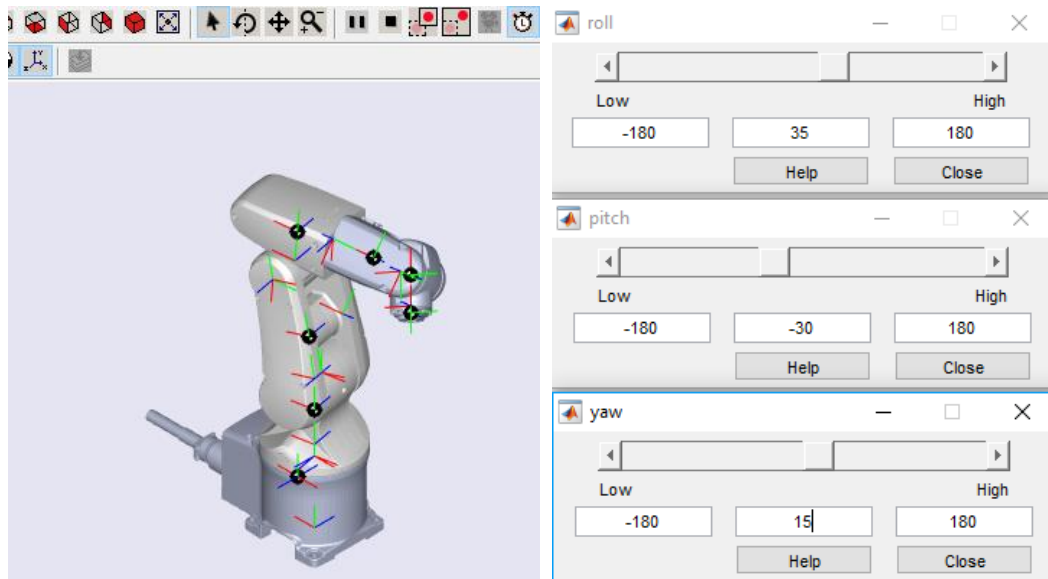


(b)

(c)

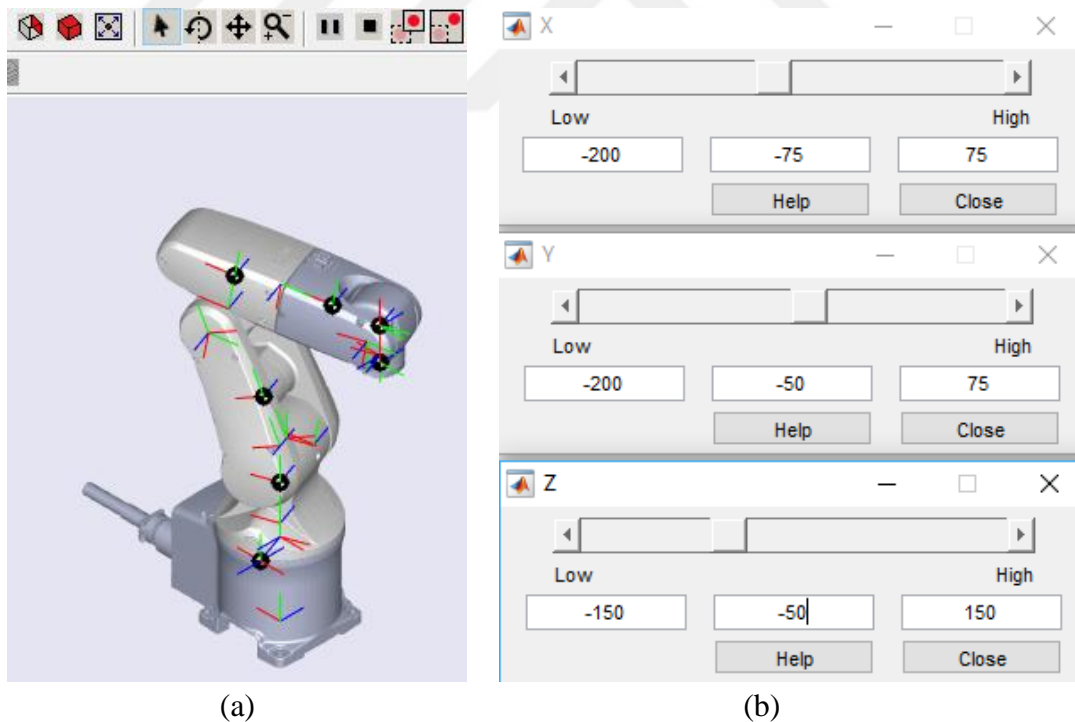
Fig. 3.17 Denso robot in home position.

The roll, pitch and yaw angles of the end effector can be changed while X, Y and Z displacements are stationary. While the position of the end-effector is stationary, the orientation of it alters simultaneously as shown in Figure 3.18 (a and b).



(a) (b)
Figure 3.18 The configuration of the Denso robot with pure orientation changes.

The reverse of the previous case can be operated. While the position of the end-effector changes, the orientation of it keeps stationary as illustrated in Figure 3.19 (a and b).



(a) (b)
Figure 3.19 The configuration of the Denso robot with pure position changes.

The orientation and position of the Denso robot can be changed at the same time. An example of this case is given in Figure 3.20 (a, b and c).

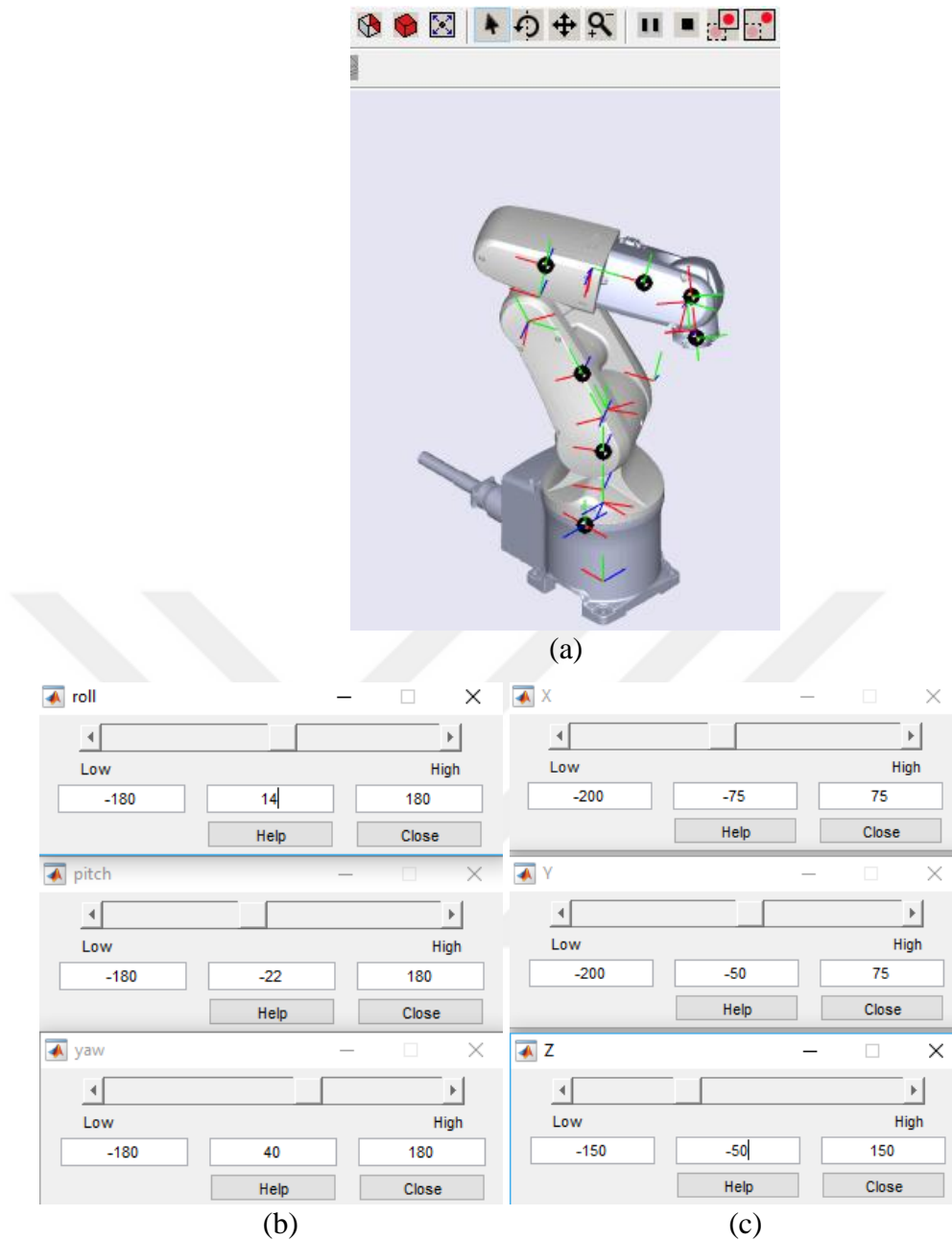


Figure 3.20 The configuration of the Denso robot with position and orientation changes.

The changes in positions and orientations of the end-effector of the Denso robot can be given one by one, point to point. The cases submitted in Figures (3.18-3.20) are point-to-point examples. The positions and orientations can be given with prescribed timing. Sinusoidal roll, pitch and yaw angles can be formed as shown in Figure 3.21. They are embedded in Figure 3.16. The angular displacements of the links of the Denso robot are calculated by IPK function are given in Figure 3.22. 3-D graphical display of the Denso robot can be seen during the analysis.

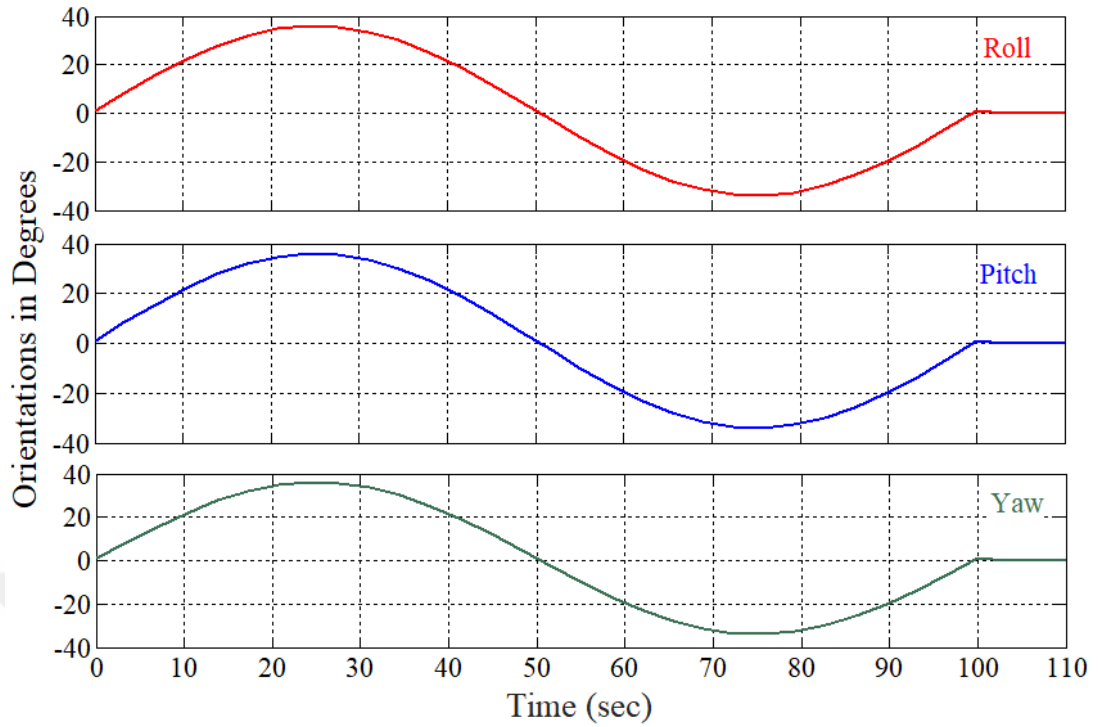


Figure 3.21 The orientation with prescribed timing.

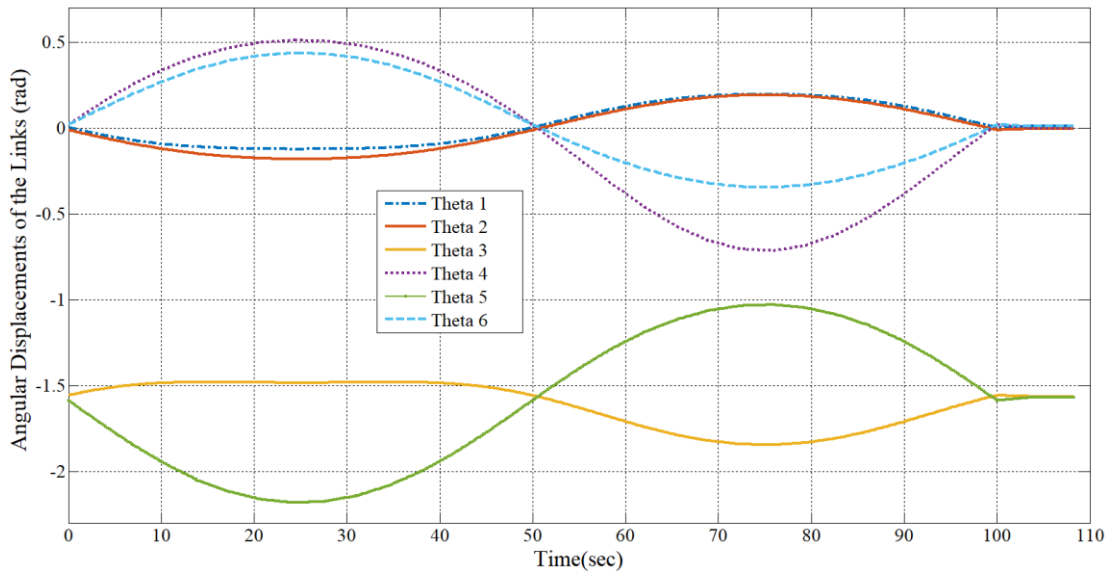


Figure 3.22 Angular displacements of the links for the orientation changes.

The end-effector of the Denso robot can trace some geometrical shapes with prescribed timing. 2D quadratic and circular shapes are given in Figure 3.23 (a, b) as examples embedded in Figure 3.16. Different geometrical shapes can be obtained.

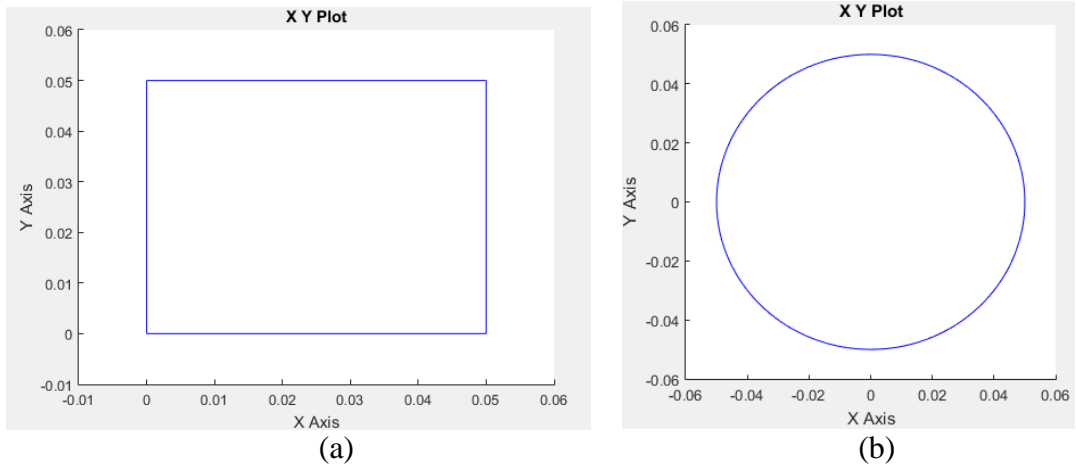


Figure 3.23 Geometrical shapes to be traced by the end-effector.

The angular displacements of the links for the quadratic and circular shapes are depicted in Figure 3.24 and Figure 3.25, respectively.

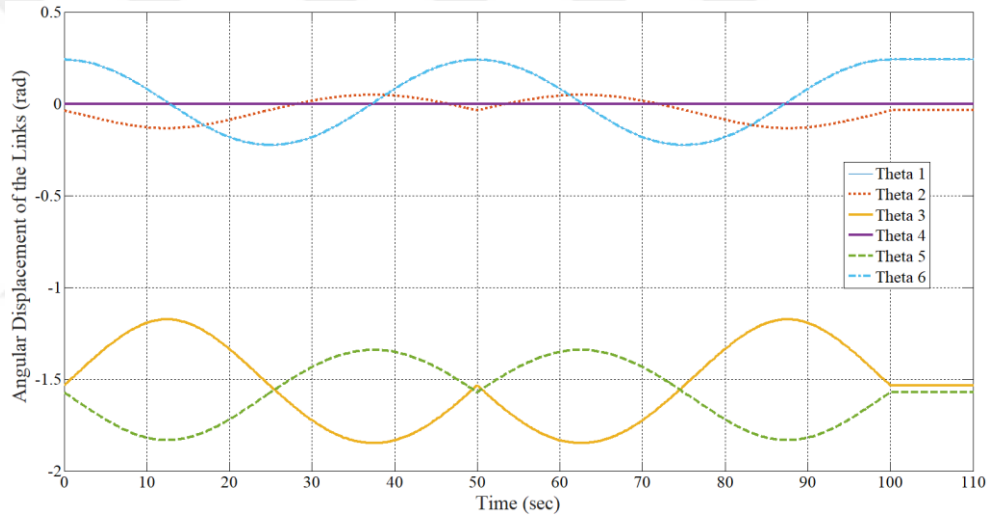


Figure 3.24 Angular displacements of the links - circular trajectory.

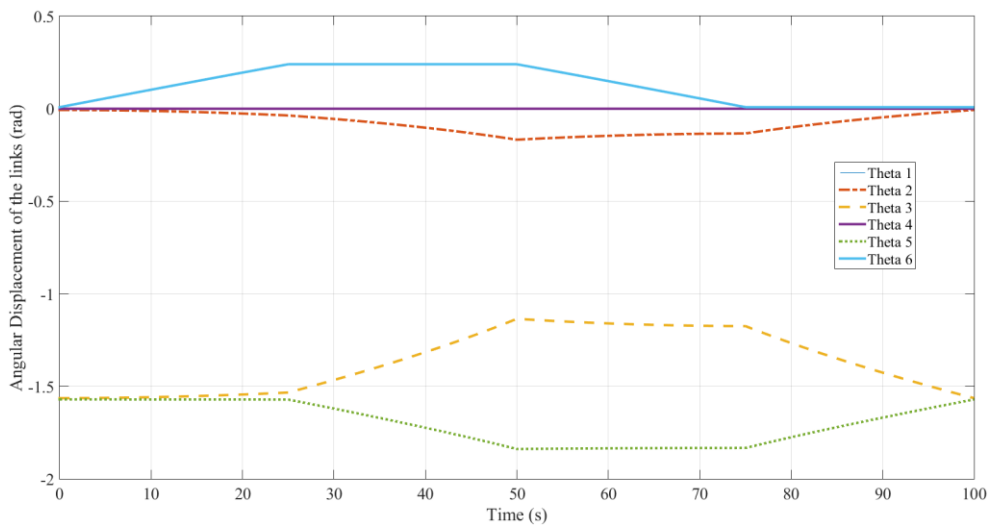


Figure 3.25 Angular displacements of the links - quadratic trajectory.

The animations while the end-effector of Denso robot is tracing the shapes shown in Figure 3.23 can be visualized in real-time. They are given in Figures 3.26 and Figure 3.27, respectively.

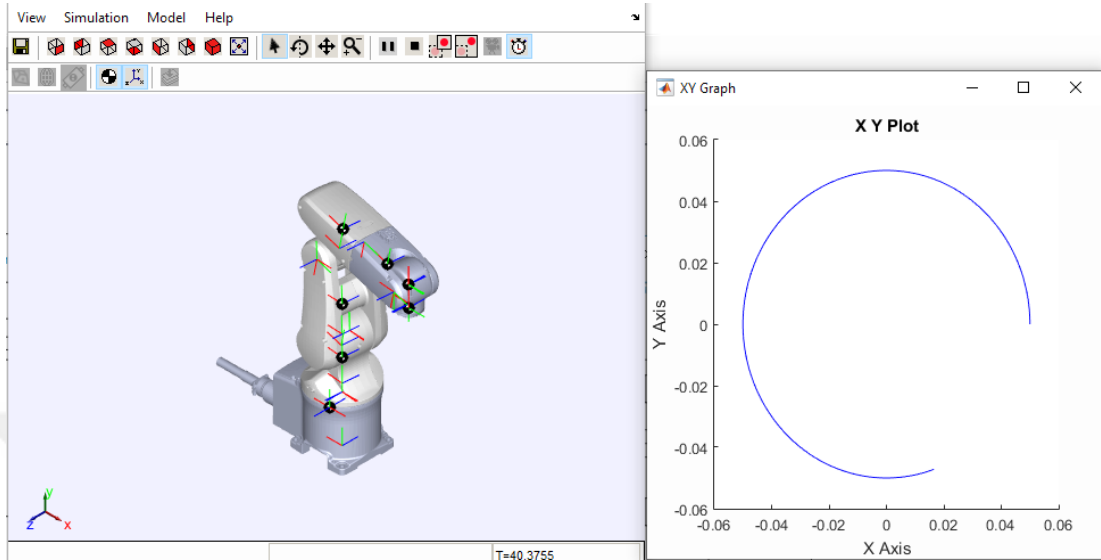


Figure 3.26 Robot in motion - circular trajectory.

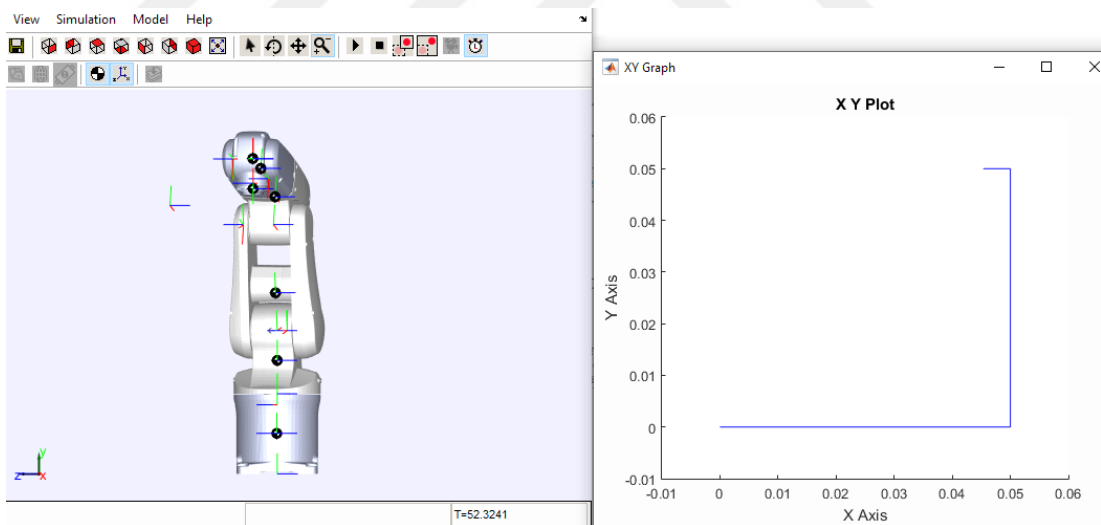


Figure 3.27 Robot in motion – quadratic trajectory.

CHAPTER IV

DESIGN OF A ROBOT-ASSISTED EXOSKELETON FOR WRIST AND FOREARM REHABILITATION

4.1 Wrist and Forearm Motions

A human uses the distal parts of his/her arm (i.e. wrist, forearm) in coordination with proximal parts (i.e. elbow, shoulder) in order to carry out movements required in daily life. Wrist and forearm motions are such as eating, writing, opening a door, driving an automobile and so on. The wrist joint has 2 DOF; Flexion/Extension (FE) and Radial-Ulnar deviation. Radial-Ulnar deviations can also be called as Adduction/Abduction (AA), respectively. Flexion is the bending of the wrist so that the palm approaches the anterior surface of the forearm. The Extension is the reverse of Flexion. Abduction (radial deviation) is the bending of the wrist towards the thumb side. The reverse of this motion is called Adduction (ulnar deviation). Pronation-Supination (PS) are the movements for the forearm. Pronation is applied to a hand such that palm turns backward or downward. Supination is the rotation of the forearm such that the palm of the hand faces anteriorly to the anatomic position (Omarkulov et al., 2016). These motions are given in Figure 4.1.

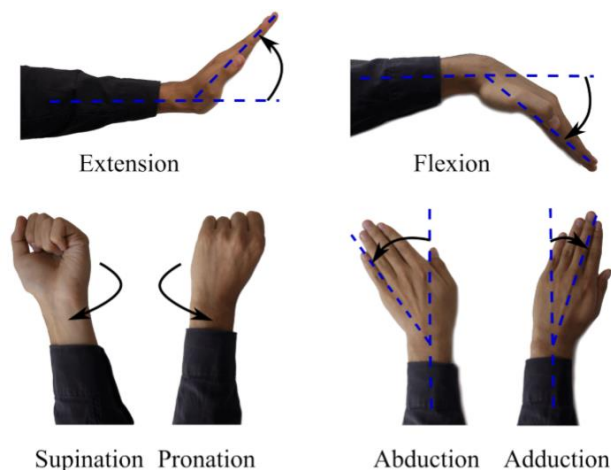


Figure 4.1 Degrees of Freedom of the wrist and forearm (Omarkulov et al., 2016).

The wrist motion is operated about an instantaneous center. Rotation axes of FE and AA can be assumed as fixed since the displacement of the centrode is insignificant. Actually, there is an offset of about 5 mm but compensating it is not so vital for the rehabilitation process (Gopura and Kiguchi, 2007).

4.2 Exoskeleton Design

The closest configuration resembling a human wrist and a rehabilitation robot can be employed by a 3 DOF system with three revolute joints. This configuration type enhances the functionality of devices providing rehabilitation services as it allows independence for specific motions of the wrist. RiceWrist (Gupta et al., 2008) and CRAMER (Spencer et al., 2008) use parallel mechanisms for wrist and forearm rehabilitation. RiceWrist-S (Pehlivan et al., 2012) is a 3 DOF exoskeleton system which is the developed version of RiceWrist (Gupta et al., 2008). A 3-axis gimbal called Wrist Gimbal (Martinez et al., 2013) offers flexibility to adjust rotation centres of the axes in order to match the wrist centre of the patient. A 3 DOF self-aligning exoskeleton given in (Beekhuis et al., 2013) compensates for the misalignment of the wrist and forearm. Parallelogram linkages are used for this purpose. Nu-Wrist (Omarkulov et al., 2016) is a novel self-aligning 3 DOF system allowing passive adaptation in the wrist joint.

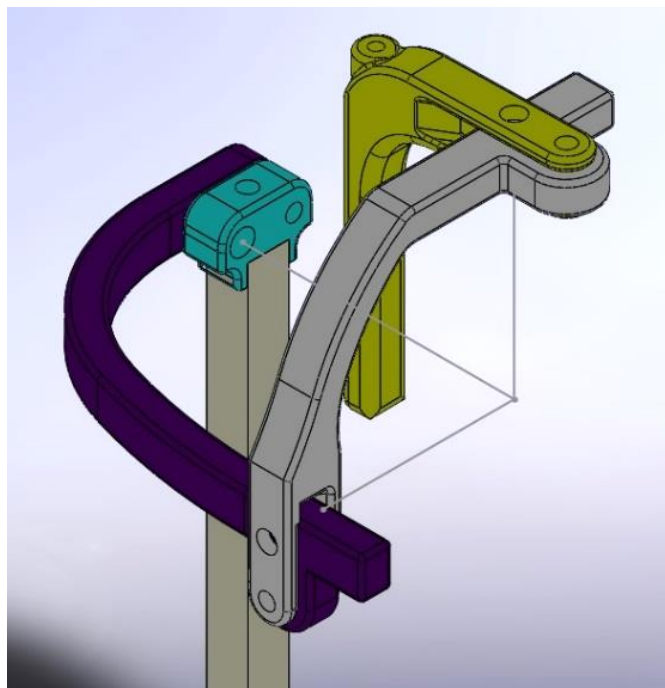


Figure 4.2 Designed exoskeleton.

An exoskeleton has been designed for the forearm Pronation-Supination motion, the wrist Flexion-Extension and Adduction-Abduction motions. It has 3 DOF which are all passive. The passive joints can be locked or unlocked manually in order to enable or restrict the motions. The holes near the axes of rotations are for locking or unlocking the links. The designed exoskeleton is illustrated in Figure 4.2. The axes of rotations are intersected in the wrist joint. The following design criteria must be achieved:

- (i) The exoskeleton must fit a human wrist in terms of the segmental lengths, the anatomical range of motion and the number of degrees of freedom (DOF). Anatomical range of motion of the wrist is 30° in Adduction, 20° in Abduction, 60° in Extension and 70° in Flexion. The acceptable limitations for Pronation-Supination (PS) of the forearm are 80° and 90° , respectively. (Schiele and Van Der Helm, 2006; Gopura and Kiguchi, 2007; Krebs et al., 2007).
- (ii) Mechanical stoppers are to be located in between the links for safety in order to prevent the exceeding of the range of motions. Stoppers are available for FE and AA movements. However, there is no stopper for PS motion. Due to the workable space limits of the robot, it is not possible to exceed the range of PS motion. The geometries of the links were designed by considering the discussed details and are shown limits in Figure 4.3 (a, b).

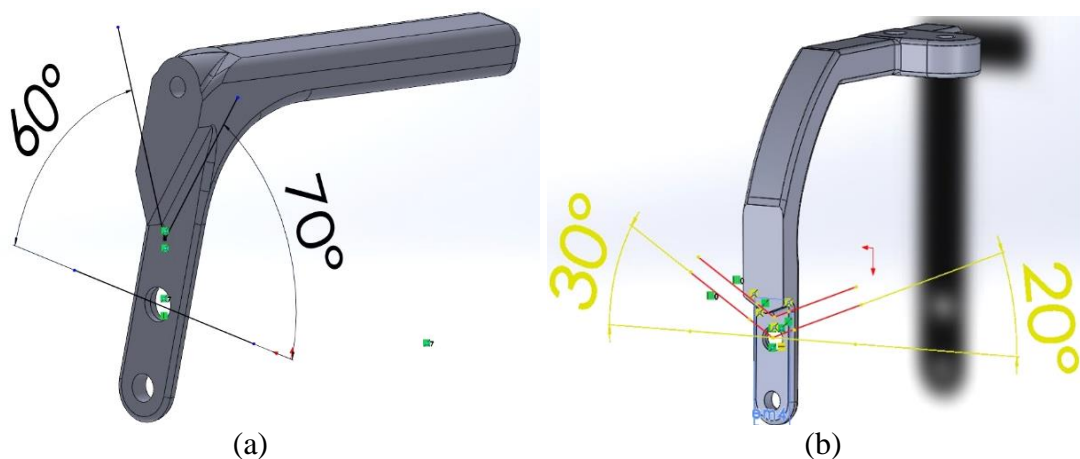
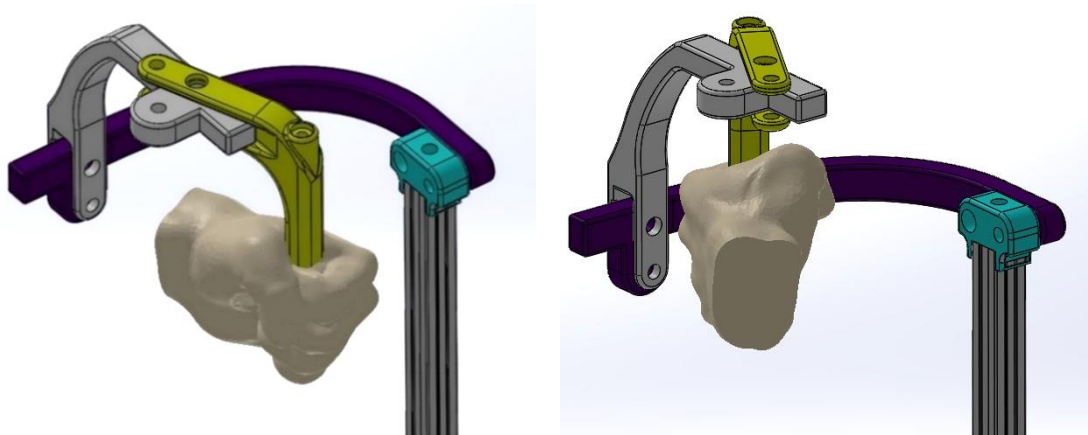


Figure 4.3 Mechanical limits of exoskeleton parts.

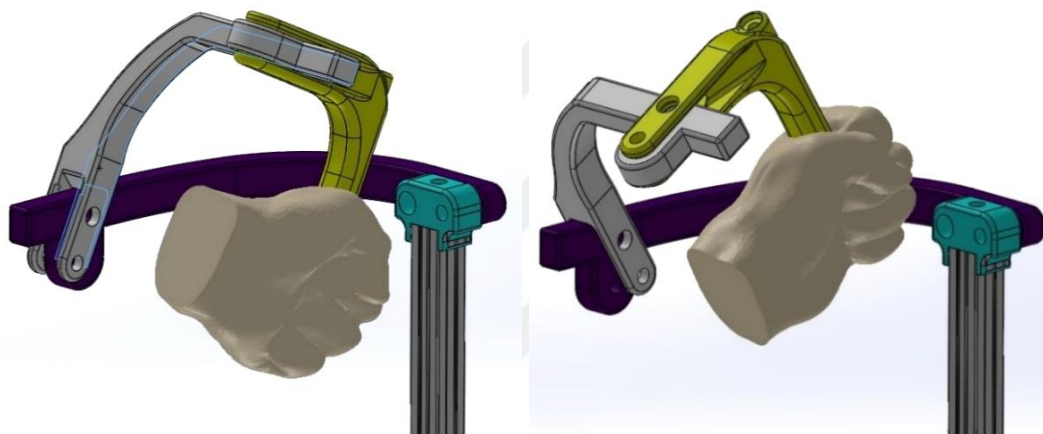
It is possible to illustrate the therapy motions with a virtual hand interface to ease visualization. FE motions are given in Figure 4.4 (a, b), respectively. AA and PS motions are given in Figures 4.5 (a, b) and Figure 4.6 (a, b), respectively.



(a)

(b)

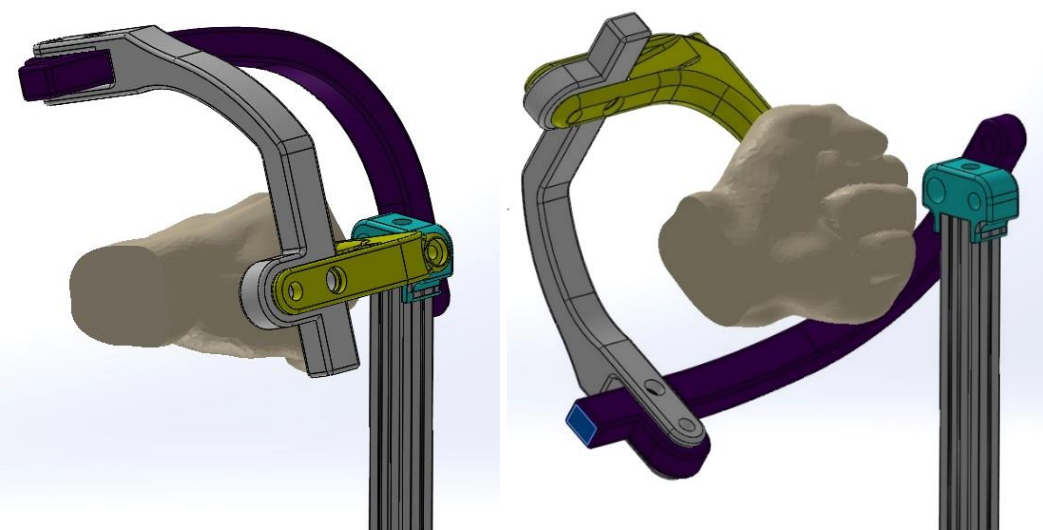
Figure 4.4 Virtual FE motions with exoskeleton.



(a)

(b)

Figure 4.5 Virtual AA motions with exoskeleton.



(a)

(b)

Figure 4.6 Virtual PS motions with exoskeleton.

The prototype has been made of ABS M-30 material by using 3D printing technology for experimental assessment. STRATASYS Fortus 450 MC, which is a very professional 3D printing device, has been used and the parts have been printed with % 100 infill density. Different views of the exoskeleton are illustrated in Figure 4.7 (a, b).

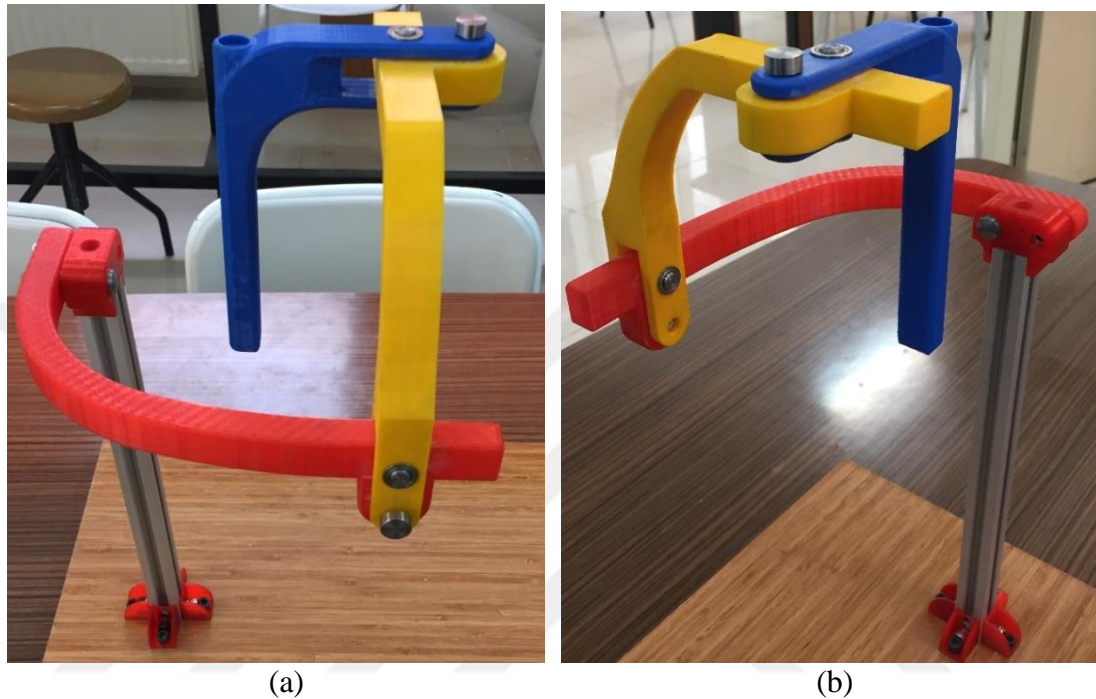


Figure 4.7 Manufactured exoskeleton.

The joints of exoskeletons are passive, so without any actuation on them (no motor). Denso robot will be used as a motion provider.

4.3 MTW Awinda (XSSENS)

The MTw™ is a miniature wireless inertial measurement unit. It includes 3D accelerometers, gyroscopes, magnetometers (3D compass) and a barometer (pressure sensor). Sampling, buffering, calibration and strap down integration of the inertial data are carried out by the embedded processor. It also performs the wireless network protocol for data transmission. The MTw Awinda development kit is equipped with a software called as MT Manager used to visualize and record the data. This simplifies the usage of the MTw and Awinda Master. The MTw supplies real-time 3D orientation for up to 20 wireless motion trackers in a network. Calibrated 3D linear acceleration, angular velocity, (earth) magnetic field and atmospheric pressure

data are provided at the same time. 3D drift-free orientation is serviced. MTw is a good unit in measuring the orientation of human body segments. A high accuracy time synchronization of the individual sensor is maintained. A micro USB is located in the front side of the MTw. LED is available on the top of the unit to indicate the device status (XSENS, 2018).

Being completely wireless expands the application area and increases the speed of attachment to people or objects. Application areas:

- Biomechanics
- Rehabilitation
- Sports and exercise science
- Virtual reality
- Animation
- Motion capture

The front and back views of the motion trackers and USB dongle are shown in Figure 4.8, respectively.



Figure 4.8 The motion tracker and USB dongle.

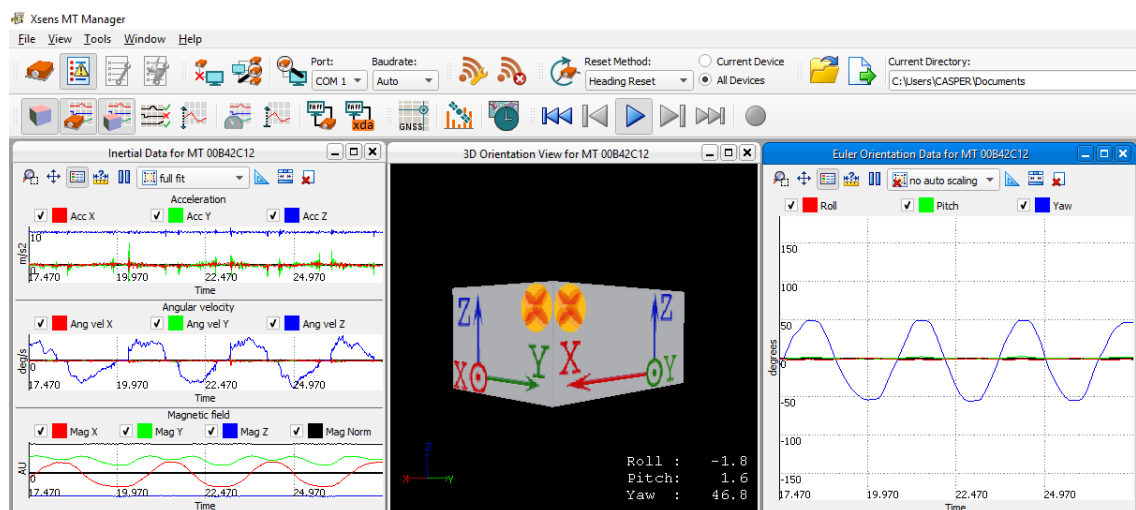


Figure 4.9 The Xsens MT Manager software.

The Awinda USB Dongle is in use by inserting it into the USB port of the PC. It provides communication between the motion tracker and software. Xsens MT Manager Software is given in Figure 4.9.

The motion tracker is located on the exoskeleton and the orientations of the exoskeleton were changed one by one, manually. The preliminary results are recorded for FE, AA and PS.

FE motions are given in Figure 4.10 (a, b), respectively.

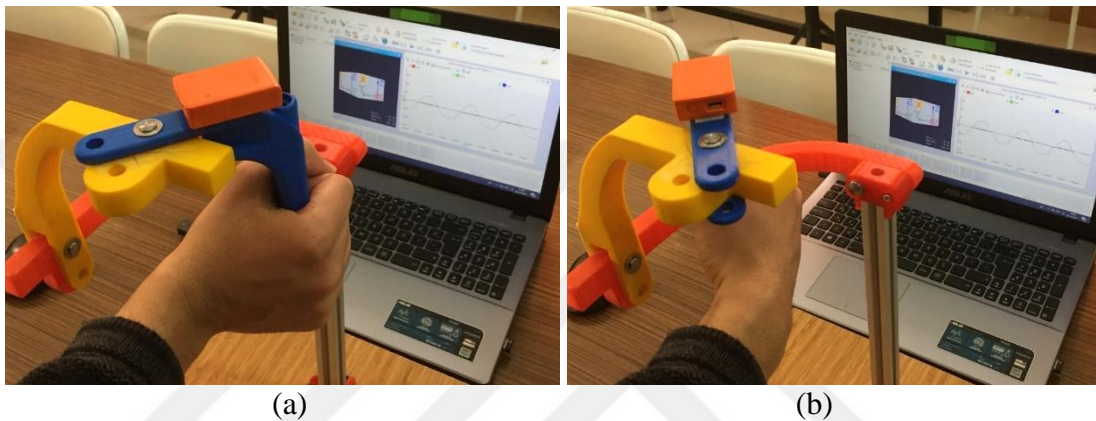


Figure 4.10 Manual FE motions with exoskeleton.

The experimental results of FE taken by the wireless sensor are shown in Figure 4.11.

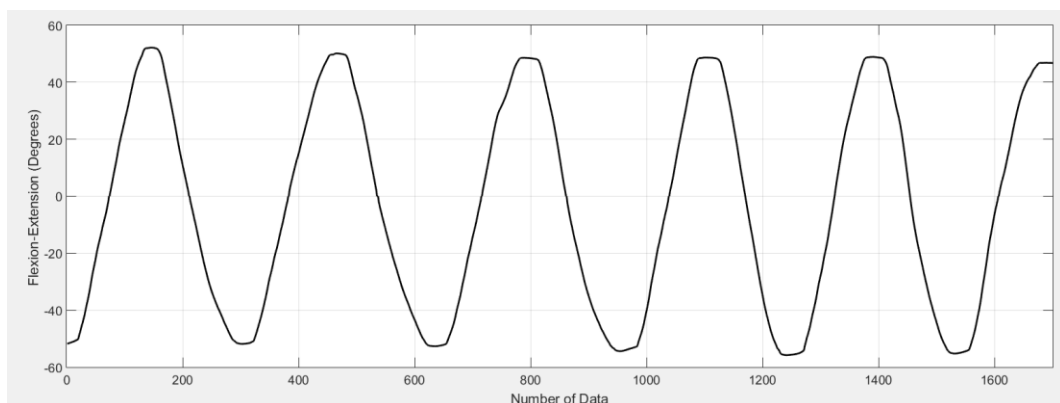


Figure 4.11 The Experimental results of FE measured by the wireless sensor.

AA motions are given in Figure 4.12 (a, b), respectively. The experimental results of AA taken by the wireless sensor are shown in Figure 4.13. PS motions are given in Figure 14 (a, b), respectively. The experimental results of PS taken by the wireless sensor are shown in Figure 4.15.

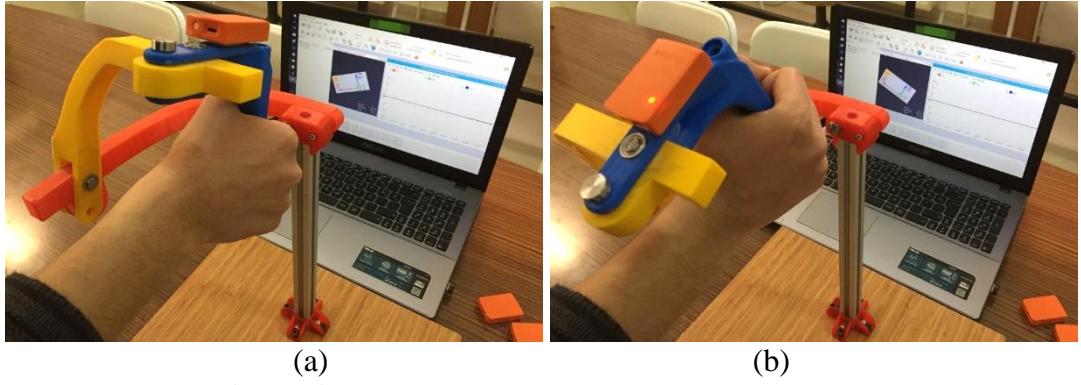


Figure 4.12 Manual AA motions with exoskeleton.

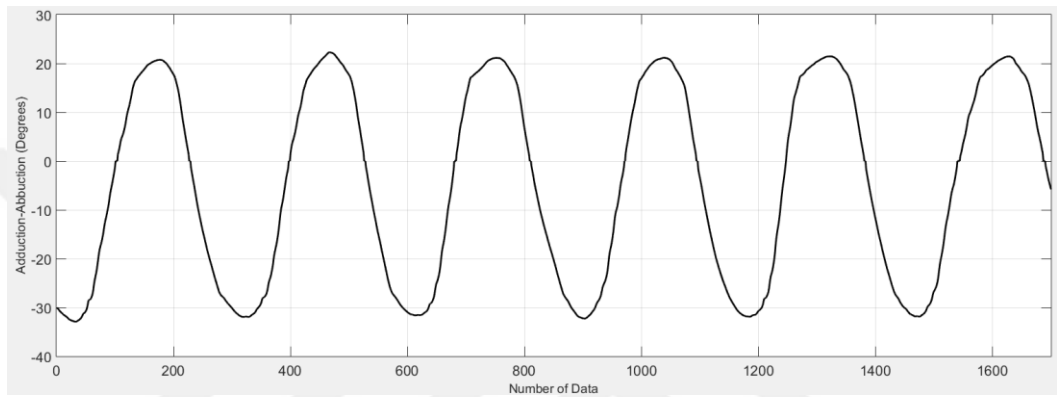


Figure 4.13 The experimental results of AA measured by the wireless sensor.

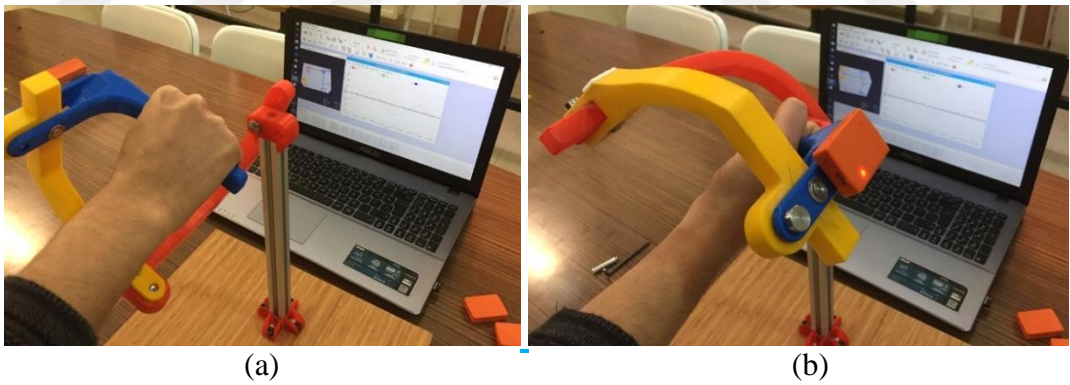


Figure 4.14 Manual PS motions with exoskeleton.

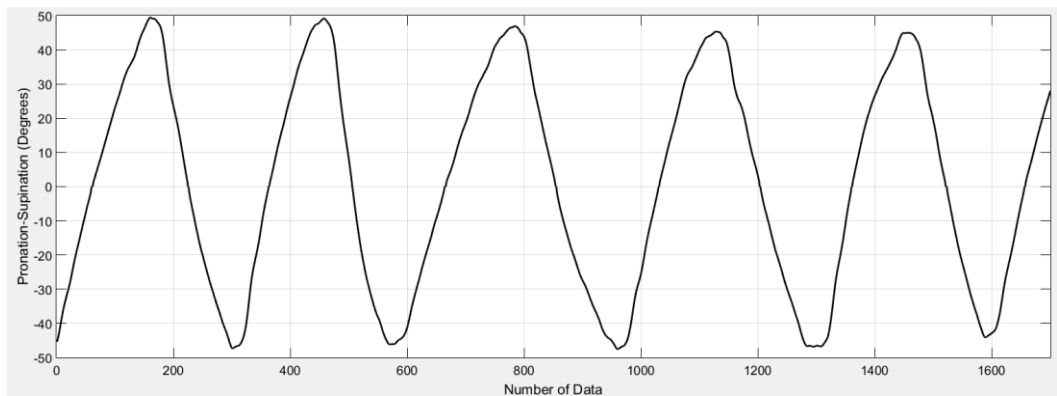


Figure 4.15 The experimental results of PS measured by the wireless sensor.

The experimental results measured by the sensor are not so accurate due to the fact that the exoskeleton is not driven by an automatic system. It is expected that they seem more accurate and repetitive when the Denso robot drives the exoskeleton.

4.4 Exoskeleton with Denso Robot

The joints of the exoskeleton are passive without any actuator on the exoskeleton. The Denso robot is used as a master motion provider. 3 specific motions are carried out one by one. While performing a specific motion, the other two axes on the exoskeleton may be locked for accurate motion. Gravity compensation is provided by the Denso robot. While 3 DOF of Denso robot are for keeping the wrist joint stationary, the other 3 DOF of the robot are for generating orientation change of the wrist joint for FE, PS and AA motions. The overall system is shown in Figure 4.16 (a, b).

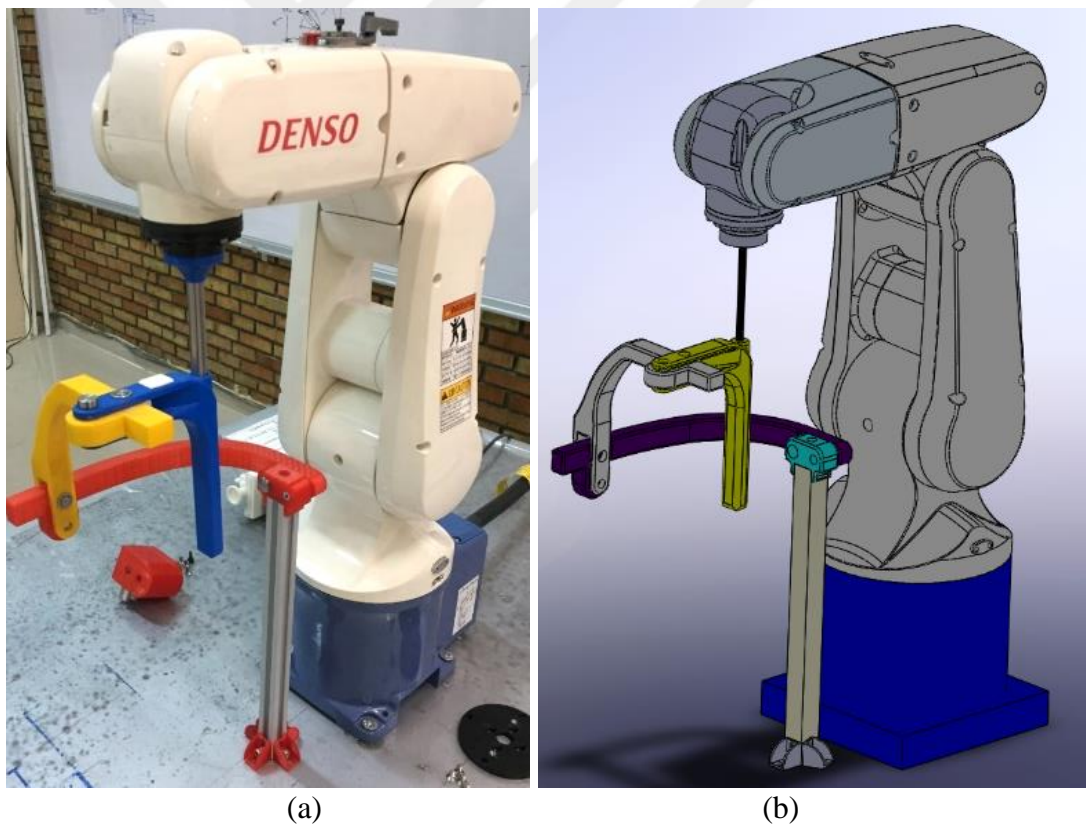


Figure 4.16 Exoskeleton driven by Denso robot.

The rotation axes of the exoskeleton are intersected with the wrist joint of a human as shown in Figure 4.2. Therefore, the position of the wrist joint is not changed during the motions. However, the orientations (roll, pitch and yaw) will be changed to perform the three rehabilitation motions.



(a)

(b)

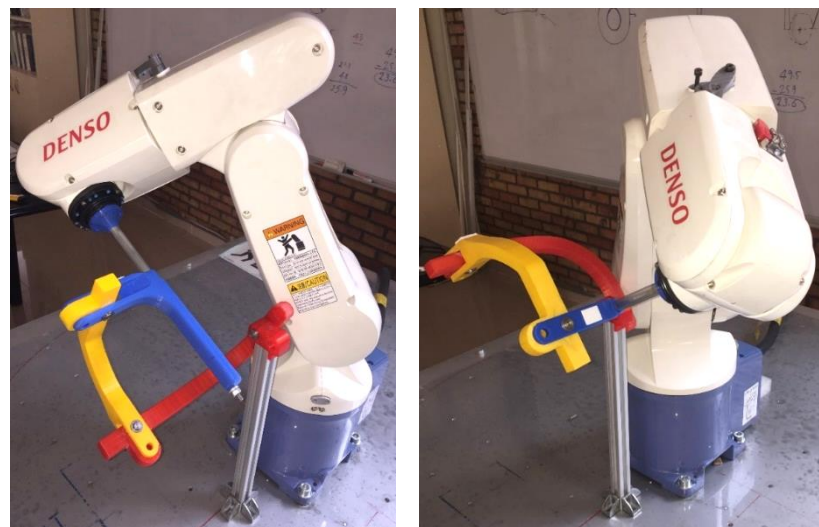
Figure 4.17 FE motion with Denso robot.



(a)

(b)

Figure 4.18 AA motion with Denso robot.



(a)

(b)

Figure 4.19 PS motion with Denso robot.

When the Denso robot and the exoskeleton are mounted to each other, the end-effector position of the robot is changed. The robot applies control for a remote centre of position. The new end-effector point is shifted to the human wrist from the sixth axis of the Robot.

- ✓ Robot operates PS motion by sending the trajectory data to Roll angle of the robot end-effector.
- ✓ Robot operates AA motion by sending the trajectory data to Pitch angle of the robot end-effector.
- ✓ Robot operates FE motion by sending the trajectory data to Yaw angle of the robot end-effector.

3x3 orientation matrix [R] of the transformation matrix given in Figure 3.10 is obtained in this way. The required modifications are performed on the Simulink model. The instantaneous configurations of the exoskeleton and Denso robot during 3 rehabilitation motions are depicted in Figure 4.17, 4.18 and 4.19, respectively.

FE and PS have been performed correctly. However, the fifth axis of the Denso robot have reached to limit position during Adduction period. The motion range of Adduction must be 20° . However, the approaching limit position in the fifth axis of the Denso robot could only let it be nearly 15° . There is no problem in Abduction part. Therefore, it is required not to bring the fifth axis of the Denso Robot to the limit angles. Adduction motion that Denso Robot have reached to the limit condition is given in Figure 4.20 (a, b) as the real system and a display from off-line programming, respectively.

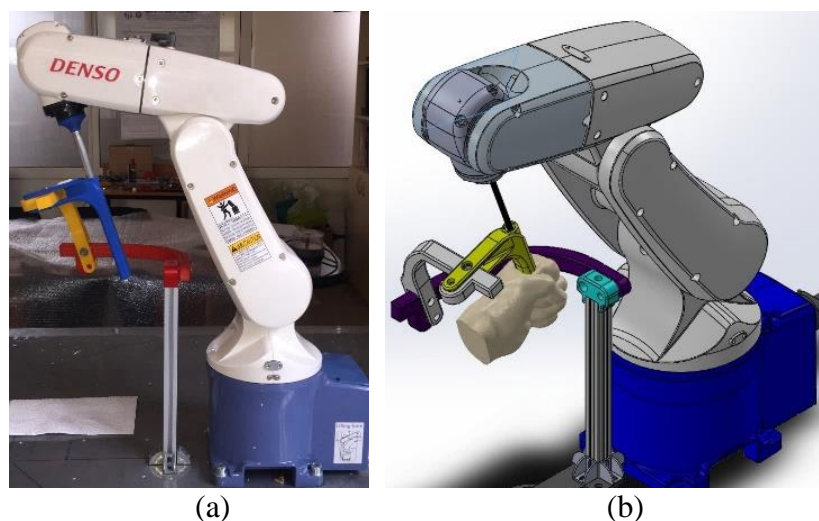


Figure 4.20 Limit condition of the fifth axis.

Therefore, a new solution was required in order to solve this problem. The key point of the problem is not to bring the fifth axes of the Denso Robot to the limit angles.

4.4.1 Solution Method I

A new apparatus in between the Denso robot and the exoskeleton has been designed. The main aim of this approach is to increase the motion limit of the fifth axis of the Denso robot. The home position of the Denso robot has been revised by changing the pitch angle orientation (about 22°) of the end-effector. This value is enough to discard the limit problem. Figure 4.21 (a, b) shows the new home position of the Denso robot and new apparatus with Denso robot & exoskeleton, respectively.

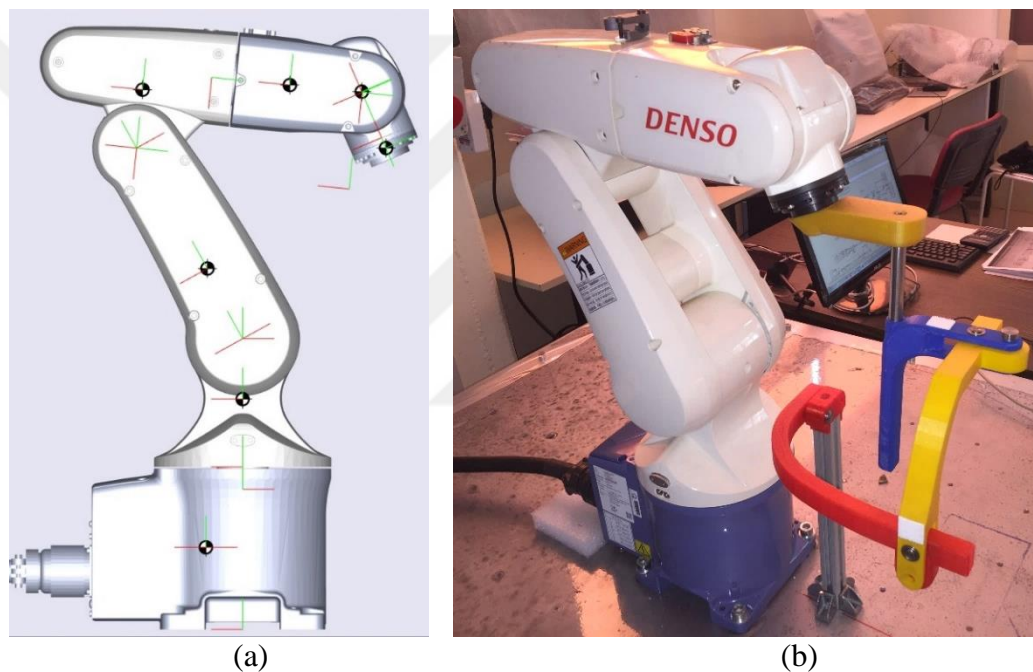


Figure 4.21 New home position and system with the designed apparatus.

The detailed drawing of the apparatus is shown in Figure 4.22. The geometry of the apparatus has been designed in such a way that the wrist joint position of the human is kept stationary and the exoskeleton stands at its original configuration like in Figure 4.16. The blue and red lines in Figure 4.23 show two configurations. The blue one shows the extension how to reach human wrist joint from the end-effector. The blue lines are virtual, the coordinates of them are used to define the new end-effector position and control the robot. The red one is for the natural position of the exoskeleton. Relative position of the blue and red lines define the geometry of the apparatus.

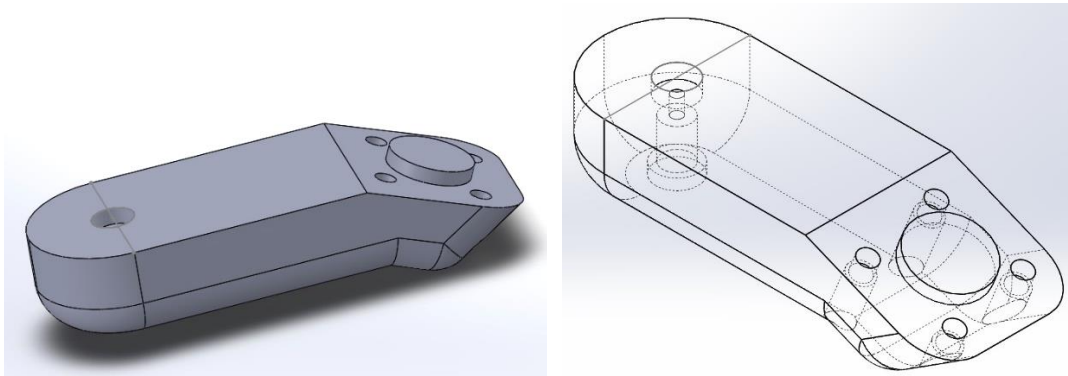


Figure 4.22 Details of the designed apparatus.

A rigid body (apparatus) is used to keep these configurations together. 2 coordinate frames are attached to the wrist joint representing blue and red lines. X, Y and Z are coordinates of the new end-effector of the Denso Robot. Rotations are performed about these axes. However, coordinates of the human wrist using exoskeleton are X', Y' and Z'. Being able to perform FE, AA and PS motions correctly depends on accurate motions in X', Y' and Z'.

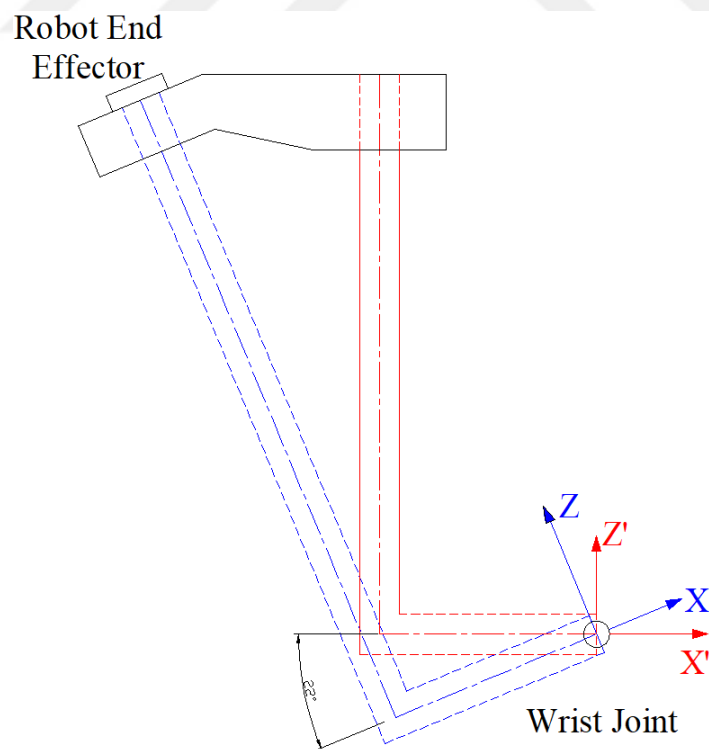


Figure 4.23 Coordinate frames of new end-effector and human wrist.

AA motion has been performed with the new design. It is obtained by changing the pitch angle about Y-axis. The pitch angle orientation change of the blue configuration about Y-axis also changes the pitch angle of the red configuration about Y' -axis. It is visible in Figure 4.24 (a) that Adduction motion which could not be achieved in previous design can be performed in the limits with the new apparatus. Abduction is also carried out in a good manner, shown in Figure 4.24 (b).

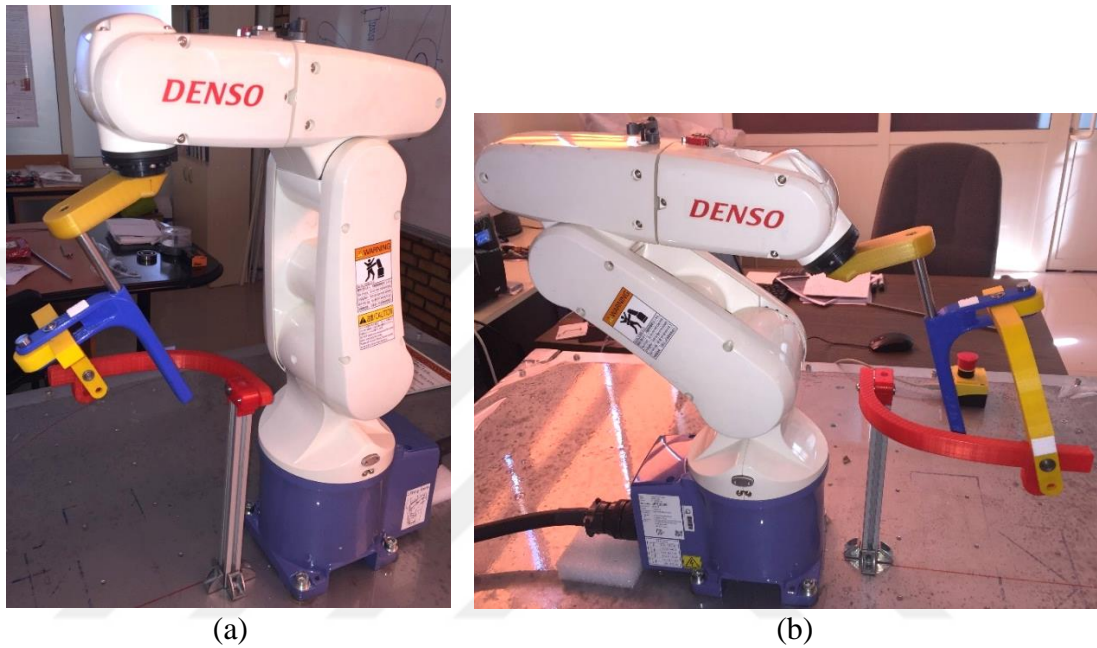


Figure 4.24 AA motion with apparatus.

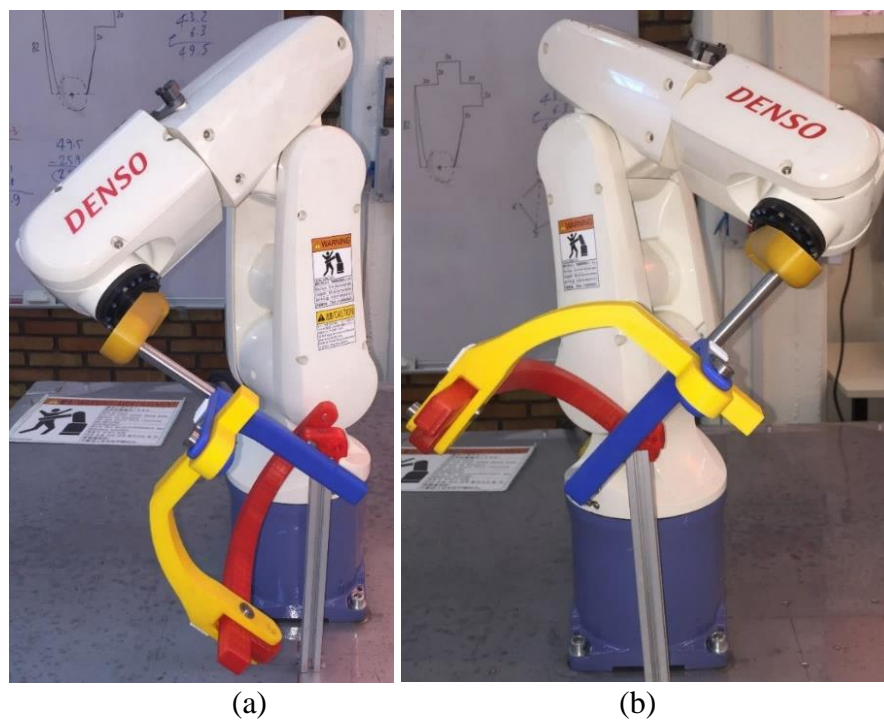


Figure 4.25 PS motion with apparatus.

PS Motion can also be performed accurately. It is obtained by changing the roll angle about X-axis. The roll angle orientation change of the blue configuration about X-axis also changes the roll angle of the red configuration about X'-axis. It is given in Figure 4.25 (a, b).

FE motion has been experienced by changing the yaw angle about Z-axis. However, changing the orientation of the yaw angle did not work in FE motion of the exoskeleton. The long part of the red configuration in Figure 4.23 must be perpendicular to the ground during the motion. It could not be achieved. Therefore, FE motion could not be performed. Making AA and PS motion with apparatus (like Figures 4.24, 4.25) and FE motion without apparatus (like Figure 4.17) is a solution. However, it is not practical since it takes time to get the system ready.

4.4.2 Solution Method II

Reaching the limit condition of the fifth axis of the Denso robot in AA motion has been mentioned as a problem. A way discarding this problem is to make AA motion in a different exoskeleton & Denso robot configuration. A new solution in which exoskeleton configuration can be changed practically has been found. The exoskeleton is used in two configurations shown in Figure 4.26 (a, b).

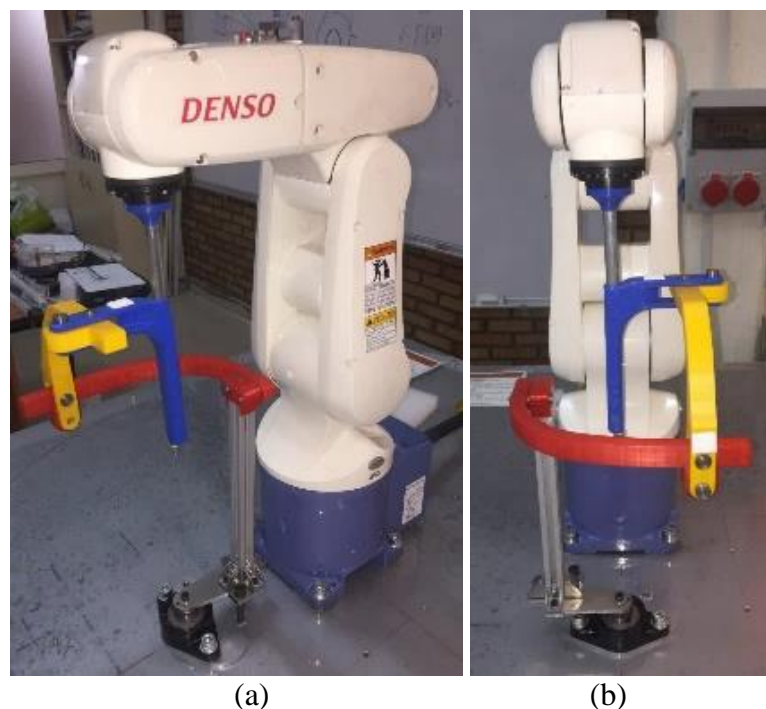
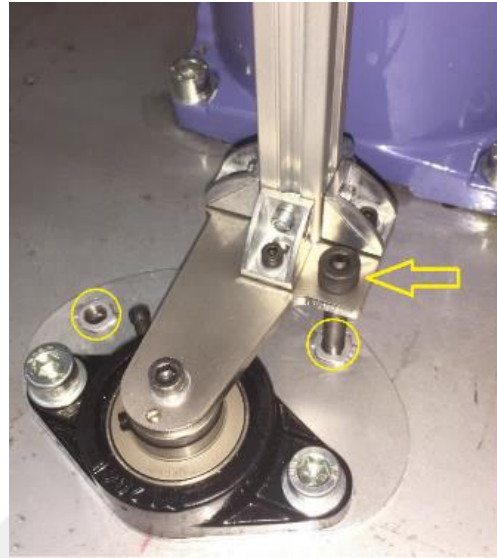


Figure 4.26. Configurations of exoskeleton & Denso robot.



(a)

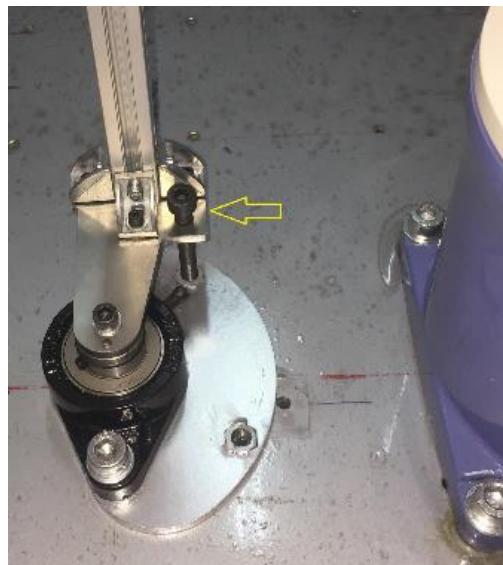


(b)

Figure 4.27 FE&PS configuration and rotatable system.



(a)



(b)

Figure 4.28 AA configuration and rotatable system.

Figure 4.26 (a) is for FE & PS Motion and Figure 4.26 (b) is for AA motion. This practical solution can be performed without loosening the screwed connections (shown with the red arrow in Figure 4.27(a)) between the tip of the robot and the

exoskeleton. The exoskeleton stays on a rotatable platform, which can be fixed to the ground in both configurations. Rotatable system and fixing the configurations with bolt are given in Figure 4.27 (b) and Figure 4.28 (b). The exoskeleton rotates on the bearing freely. The configurations given in Figure 4.27 (a) and Figure 4.28 (a) are shifted about 90° with respect to each other. Changing configuration is carried out by loosening the nut and the bolt shown with yellow arrows in Figure 4.27 (a, b), rotating the system and then tightening the nut and the bolt. The region where the patient holds the exoskeleton is considered to be the most critical place in terms of structural issues. This part is manufactured as being hollow. The rod that connects the robot with the exoskeleton is passed through this hollow part. The screw connection is then used at the bottom. Therefore, this part can be considered as strong as a metal rod.

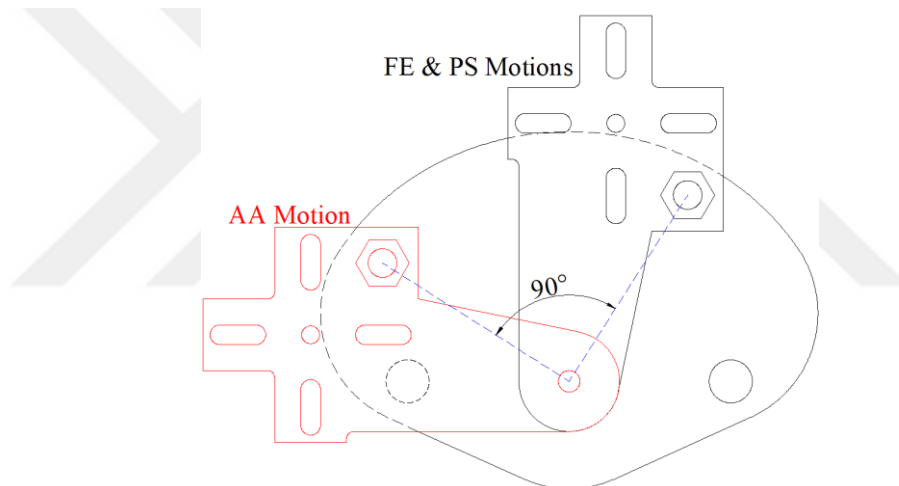


Figure 4.29 Two positions of the part carrying the exoskeleton.

Two nuts shown in the yellow circles in Figure 4.27 (b) are for fixing the desired configuration to the ground. The nuts are located on the part that is under the bearing. The positions of them are defined by considering the shifting angle, 90° shown in Figure 4.29.

Table 4.1 Positions of the wrist joint, xyz_0 (m)

Configuration	Value
FE&PS	[0.2774 0 0.138]
AA	[0.2114 0.066 0.138]

Human wrist positions are different in both configurations. The human wrist positions are given in Figure 4.30. Therefore, Simulink model shown in Figure 3.10

has been modified for each motion. Positions of the wrist joint in the global frame (xyz_0) are given in Table 4.1. The transformation matrices between the tip of the robot and wrist joint, $T_{6_EE_{FE-PS}}$ and $T_{6_EE_{AA}}$, are given in Eqs. (4.1, 4.2). AA motion in Configuration II is controlled by changing the roll angle of the end-effector.

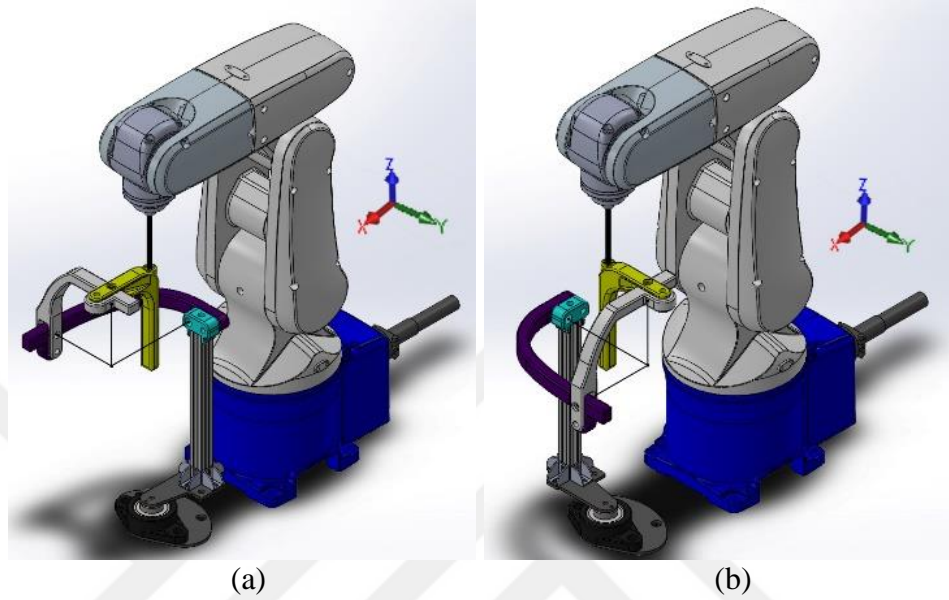


Figure 4.30 Human wrist positions.

$$T_{6_EE_{FE-PS}} = \begin{bmatrix} 1 & 0 & 0 & -0.066 \\ 0 & 1 & 0 & 0 \\ 0 & 0 & 1 & 0.202 \\ 0 & 0 & 0 & 1 \end{bmatrix} \quad (4.1)$$

$$T_{6_EE_{AA}} = \begin{bmatrix} 1 & 0 & 0 & 0 \\ 0 & 1 & 0 & 0.066 \\ 0 & 0 & 1 & 0.202 \\ 0 & 0 & 0 & 1 \end{bmatrix} \quad (4.2)$$

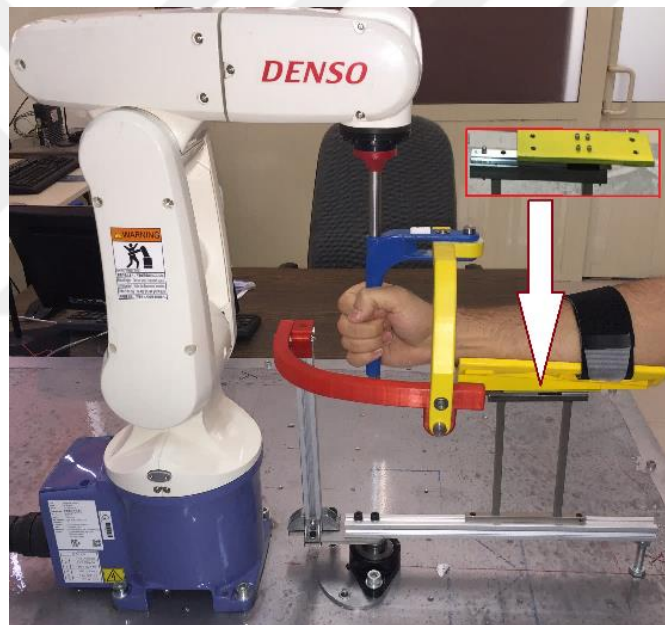
The overall system including a base for forearm for two configurations are given in Figure 4.31 (a, b). The base, which is a part between the forearm and the table, takes the main weight of the arm. The base with padding and straps is located on a linear slide rail. It is used to adjust the location of the wrist joint. Actually, there is a slight linear eccentricity between the bones corresponding to FE and AA (Gopura and Kiguchi, 2007; Schiele and Van der Helm, 2006; Omarkulov et al., 2016). This linear slide rail is a passive DOF to compensate for the misalignment during the exercise. Therefore, self-alignment is provided naturally during AA motion by changing the grasping level slightly and slide the base on the linear rail. It is shown in Figure 4.31 (c).



(a)



(b)



(c)

Figure 4.31 Overall system with base for forearm.

4.5 Trajectory Planning & Experimental Measurements

Trajectories are obtained for FE, AA and PS motions. There are three different velocity levels in each motion. They are performed as *slow*, *medium* and *fast* with periods of 70 s, 50 s and 35 s, respectively as given in Figure 4.32. A physiotherapist recommends these values. The amplitudes of the trajectories are defined as given in Section 4.2. The motion intervals are $\pm 70^\circ$ for PS, $+70^\circ$ and -60° for FE, $+30^\circ$ and -20° for AA motion.

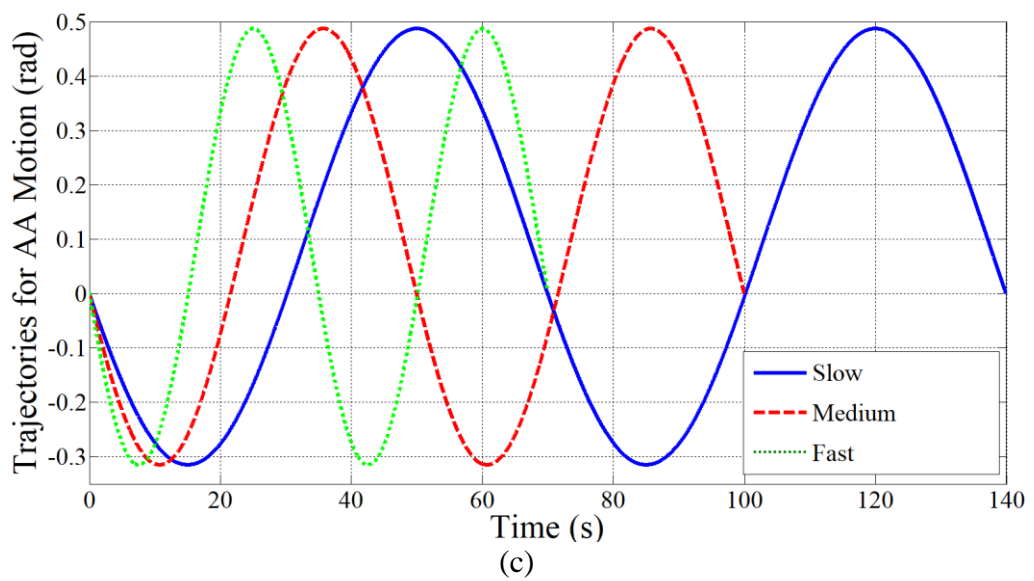
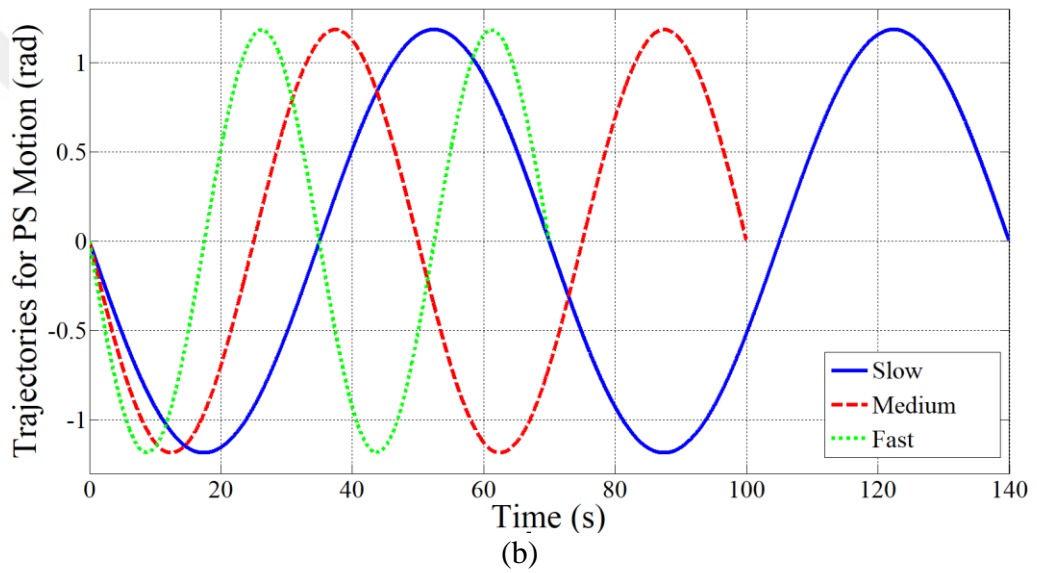
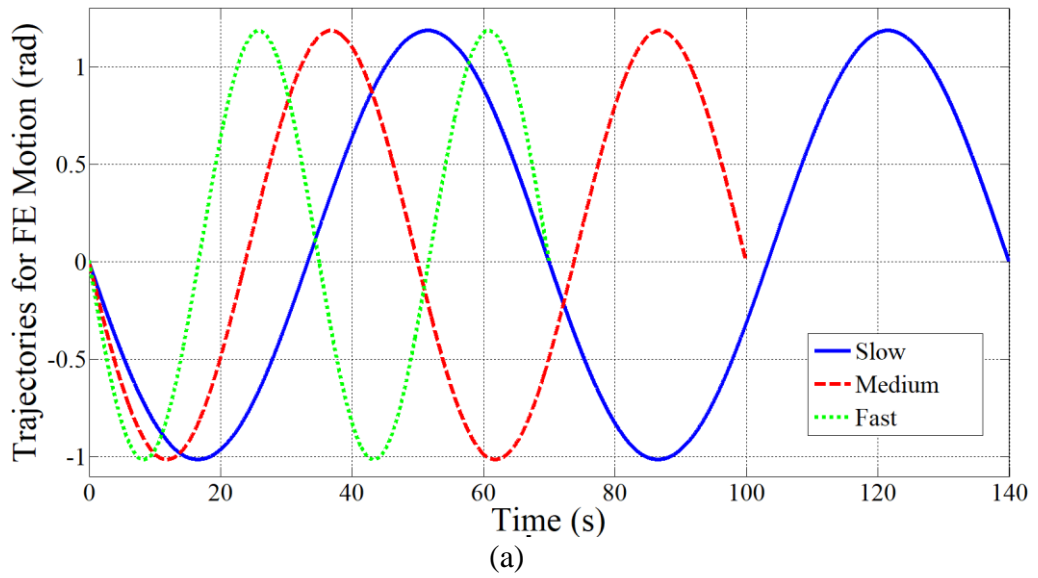


Figure 4.32 The trajectories with different velocity levels for PS, FE and AA motions.

The level of speed in rehabilitation is determined by the therapy the patient needs. The trajectories given in Figure 4.32 are embedded in the blocks in Figure 4.33. The desired motion (PS, FE, AA) with desired velocity (slow, medium, fast) is selected by manual switches given in Figure 4.33.

The model including FE and PS trajectories and Simmechanics[®] blocks of the exoskeleton is illustrated in Figure 4.33. The trajectories feed the orientation of the wrist point in terms of roll, pitch and yaw angles. They form the rotation matrix named [R]. The amplitudes of the trajectories may be changed for the patients having different levels of illnesses. Therefore, trajectory choices called *Limit* and *Safe* are also included. Simmechanics[®] blocks are also used to visualize the instantaneous configuration of the exoskeleton. The model for AA motion is very similar to Figure 4.33. The 3-dimensional graphical display of the exoskeleton can also be seen by using Simmechanics[®] blocks enriched with Solidworks[®] models. Three motion couples are given in Figure 4.34 (a, b and c).

The models developed are run and the 3 motions are obtained within anatomical ranges. Wireless motion tracker Mtw Awinda is assembled on the exoskeleton. The orientations of the exoskeleton are acquired on a wireless interface (XSENS). The angular orientation of the motion tracker and simultaneous configuration of the exoskeleton can be displayed in real time. PS, AA and FE motions with real human limb are given in Figure 4.35 (a, b), Figure 4.36 (a, b) and Figure 4.37 (a, b), respectively.

The recorded angular orientation data by Mtw Awinda for three velocity levels in PS, AA and FE motions are shown in Figure 4.35 (c), Figure 4.36 (c) and Figure 4.37 (c), respectively. Angular displacements characteristics of the robot links for PS, AA and FE motions are depicted in Figure 4.38 (a, b, c), respectively. Data from robot links are taken at medium velocity level during each motion.

Motion transmission from robot to exoskeleton is provided. The motors of the robot are strong enough to make the limbs trace the given trajectories. There are slight delay type errors in the measurements. They are sum of the error of Denso robot, bias error of the sensor, error from sensor location and error from the backlash in the joints of the exoskeleton.

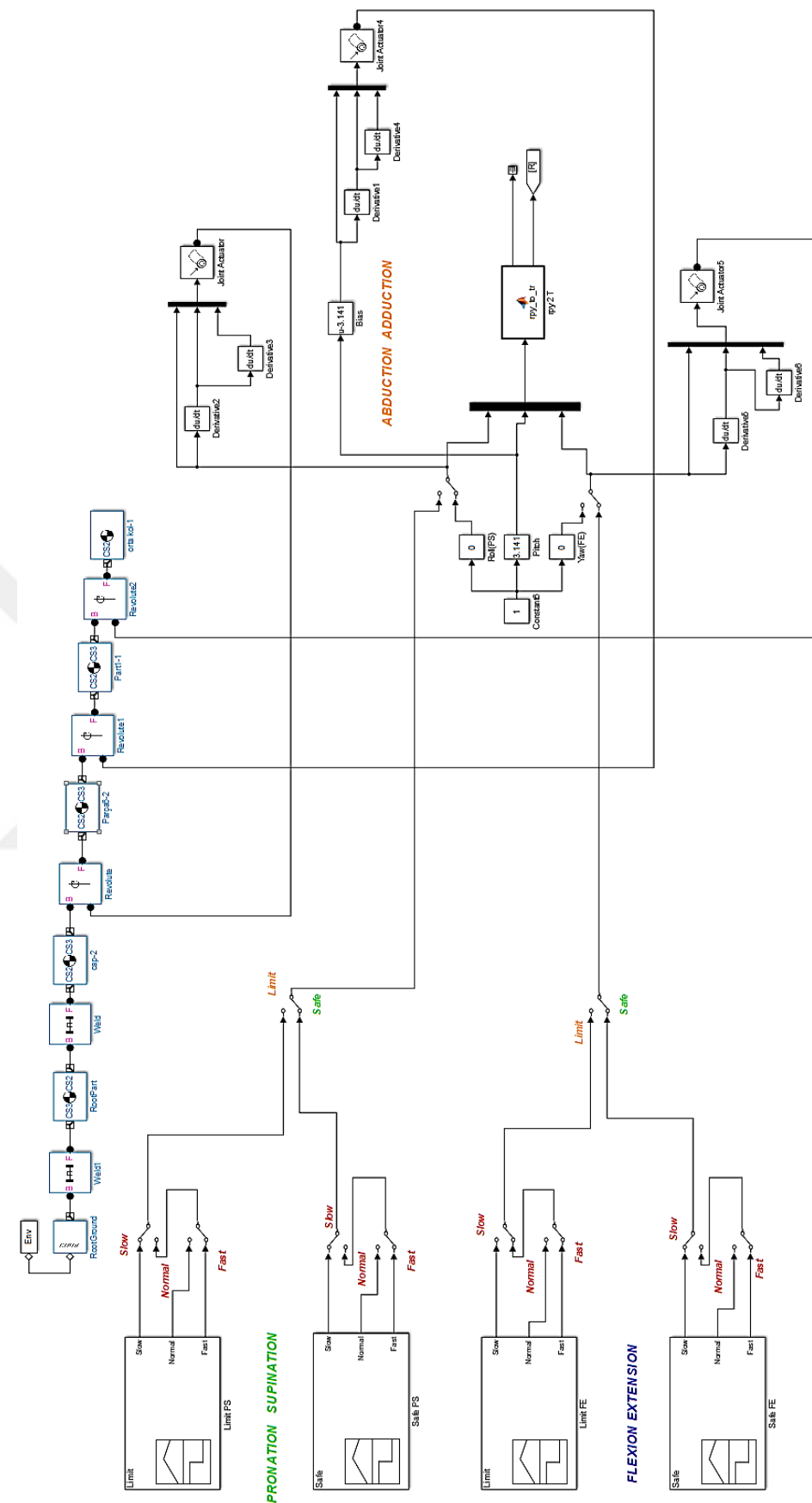
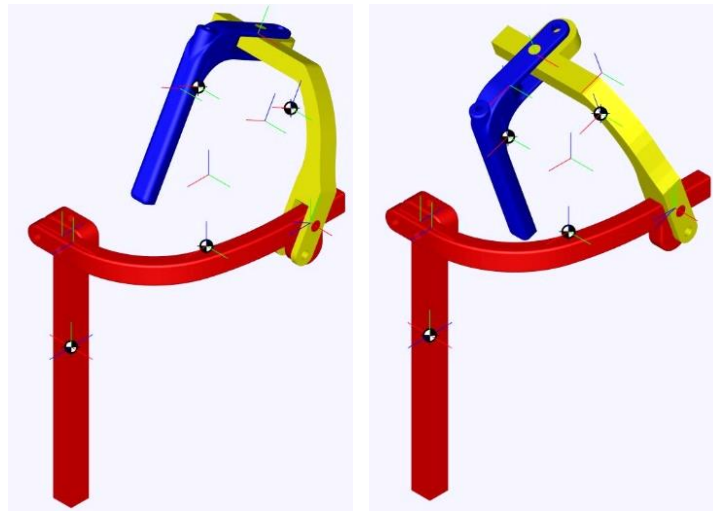
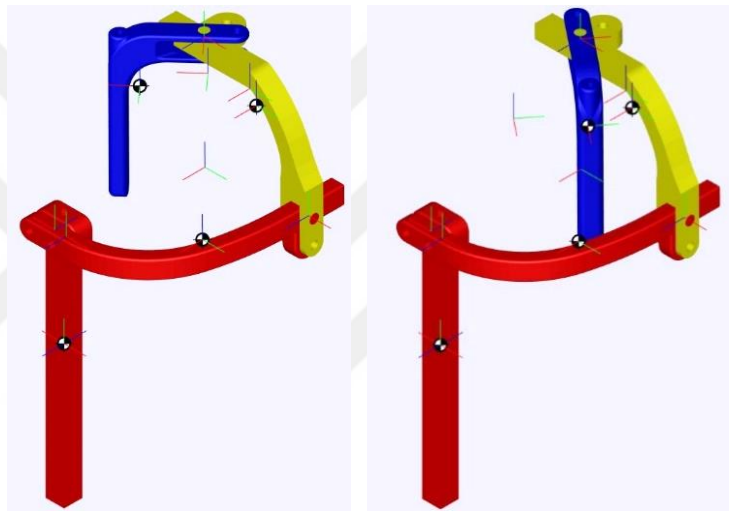


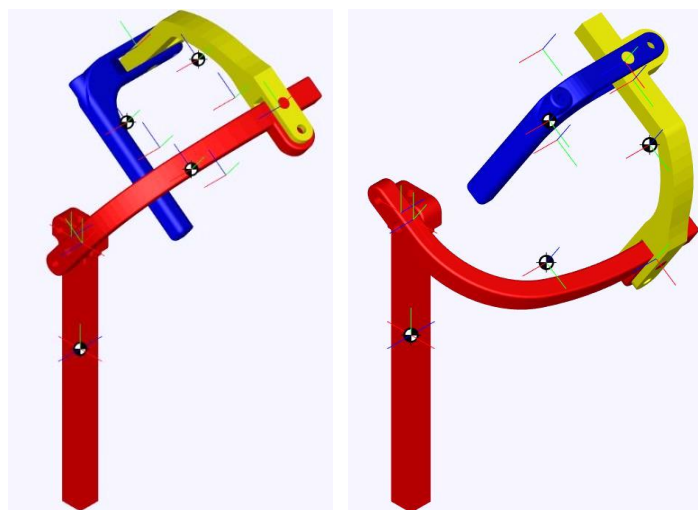
Figure 4.33 The trajectories and Simmechanics® blocks of the exoskeleton.



(a)

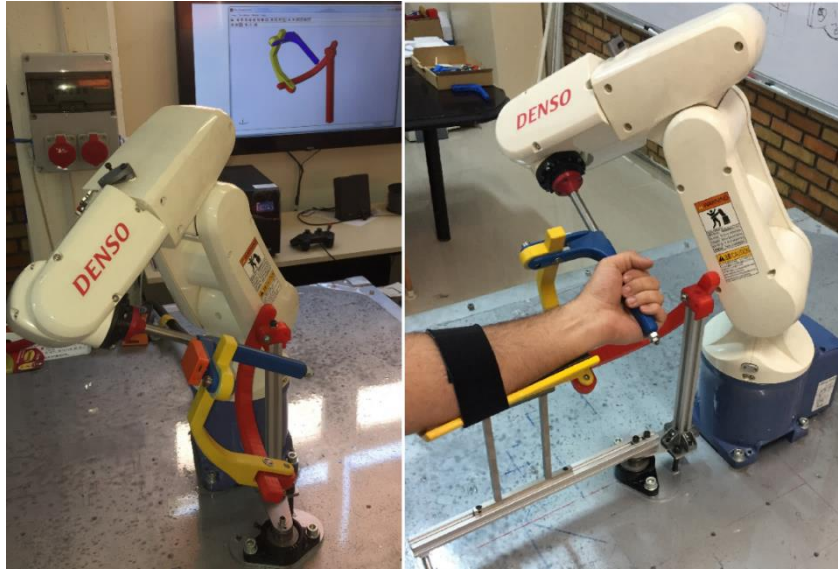


(b)



(c)

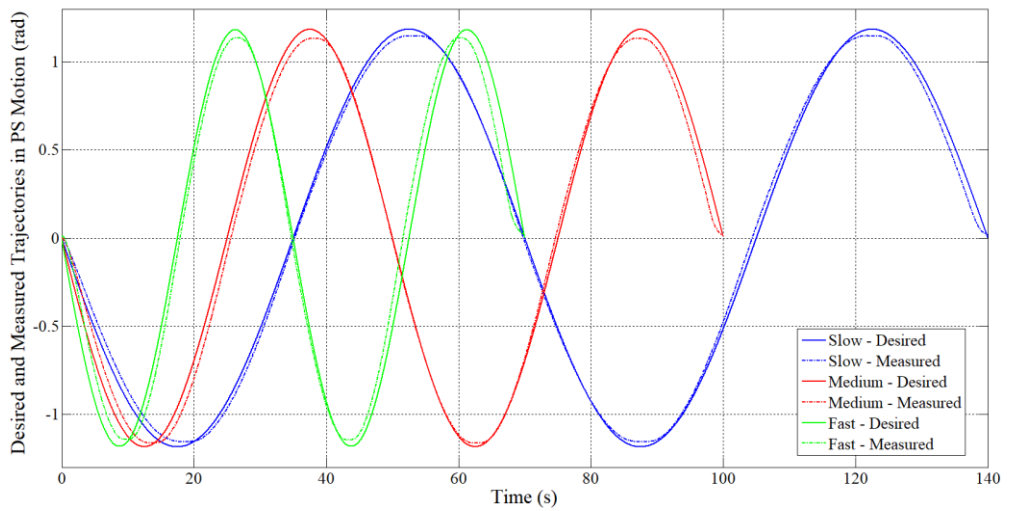
Figure 4.34 Graphical display of the exoskeleton.



(a)

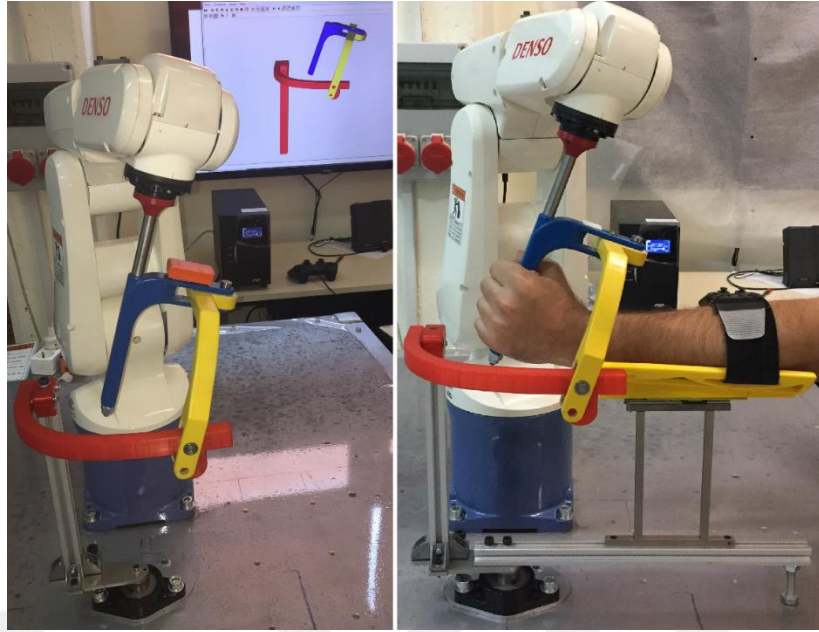


(b)

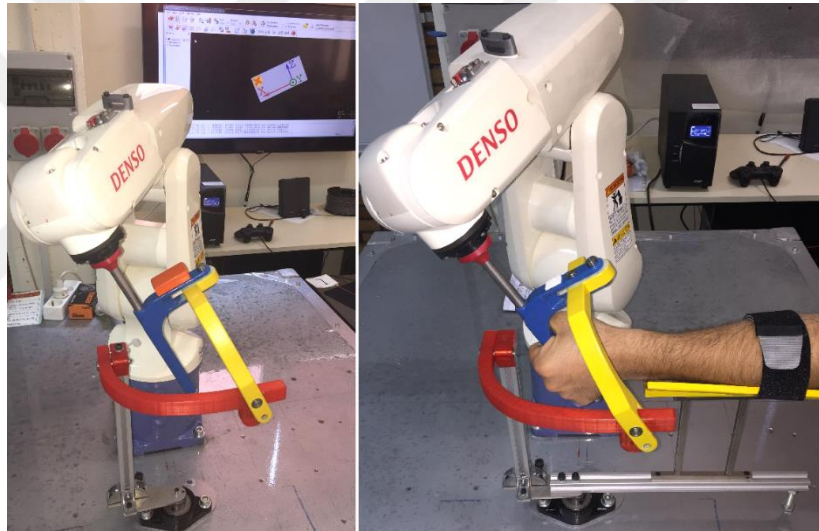


(c)

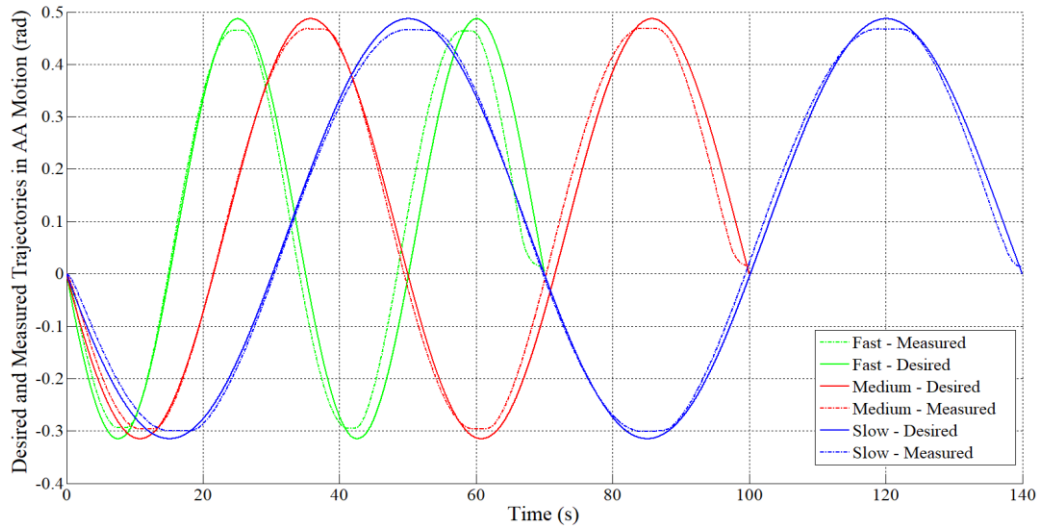
Figure 4.35 PS measurement with IMU



(a)

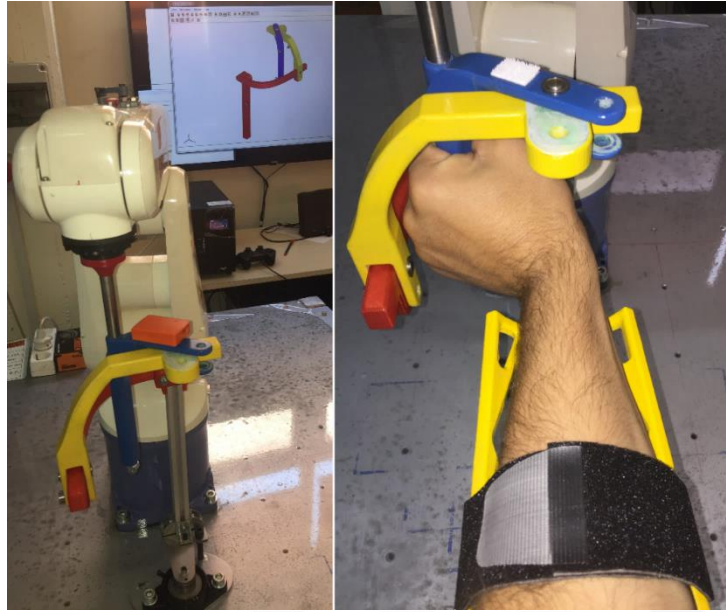


(b)

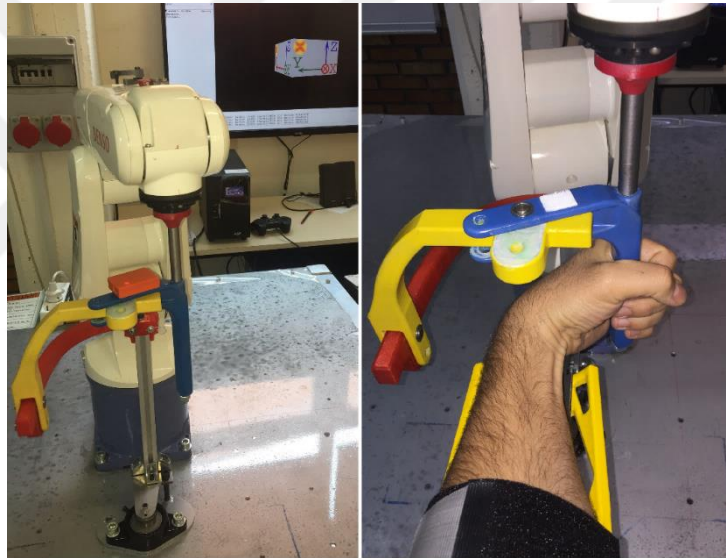


(c)

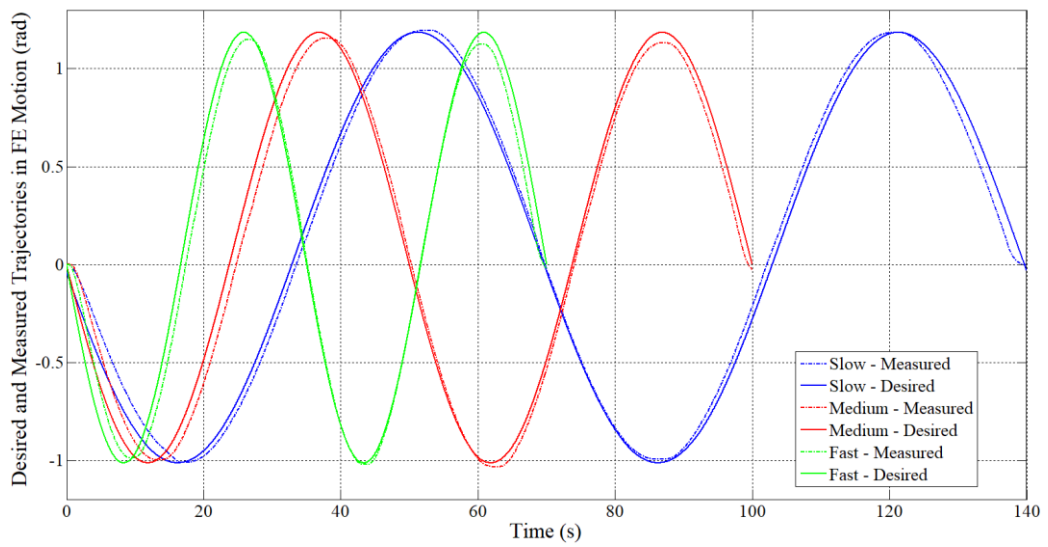
Figure 4.36 AA measurement with IMU



(a)



(b)



(c)

Figure 4.37 FE measurement with IMU

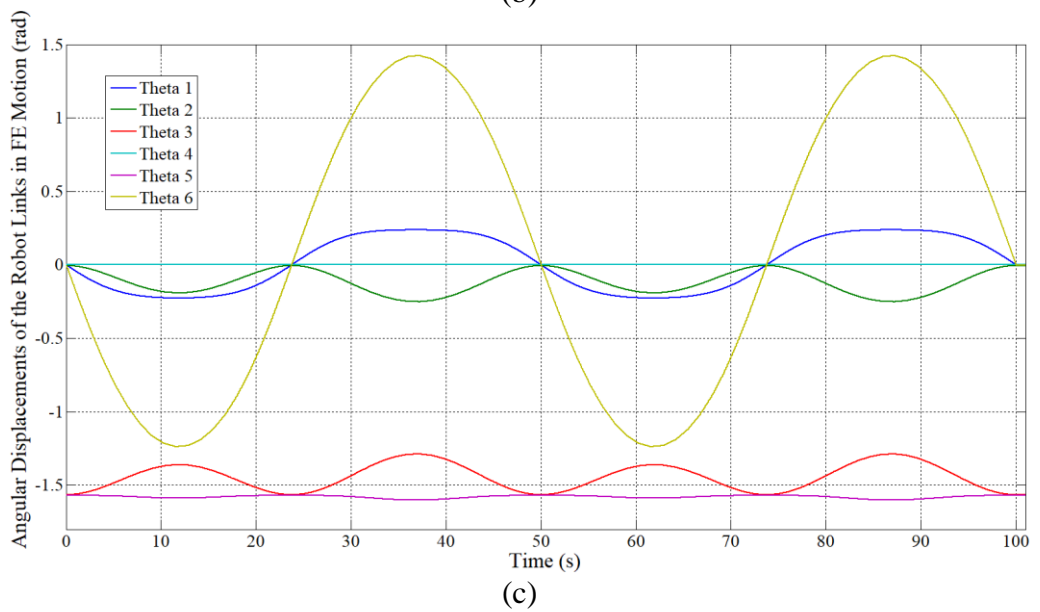
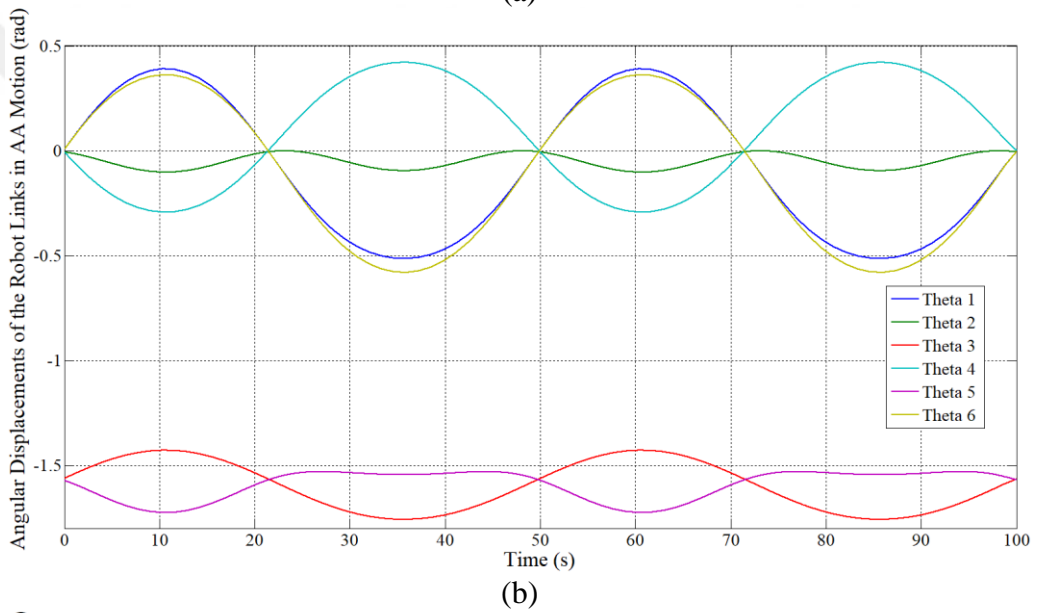
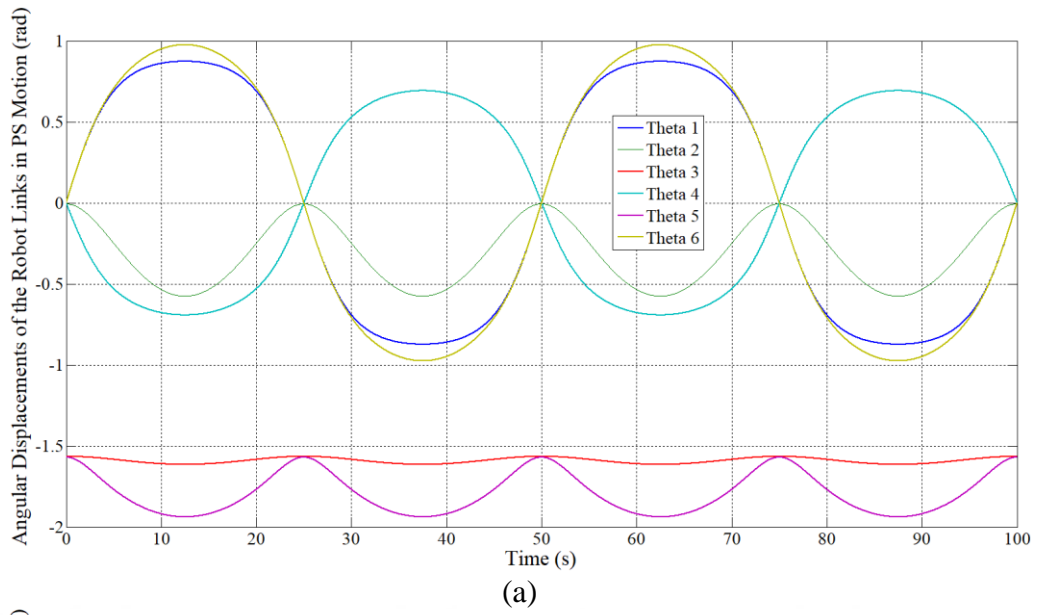


Figure 4.38 The angular displacements of the robot links.

4.6 FEM Analysis of the Exoskeleton

The exoskeletons are mechanisms having contact with the patients during rehabilitation and power assistance. Therefore, they must ensure some requirements like having adequate intensity and rigidity. There have already been published works investigating the structural issues of upper and lower limb exoskeletons (Ding et al., 2012; Guo et al., 2013; Yang et al., 2017).

3-D static structural Finite Element Analysis (FEA) of the exoskeleton has been carried out in ANSYS Workbench Static Structural Toolbox. The material model was assumed to be linearly elastic and isotropic, having mechanical properties of $E=2.413$ GPa (Modulus of Elasticity) and $\nu=0.35$ (Poisson's Ratio) of ABS-M30 material. Although exoskeleton assembly was free to rotate with the presence of rotational joints, it was assumed as fixed by defining all contacts between parts as bonded contact for preventing separation. The region where the exoskeleton is attached to the table and the surface of the inner hole of the handle were also assumed as fixed support. The maximum element size was defined as 5 mm and thus, the total number of elements is 27693 with 48728 nodes in all analyses. It was noticed that a finer mesh structure did not significantly affect the results. Torque was applied on the surface of the handle. Torque values required for activities of daily living (ADL) are given in Table 4.2 (Pehlivan et al., 2012).

Table 4.2 ADL Torques

Motion	Value (Nm)
PS	0.06
FE	0.35
AA	0.35

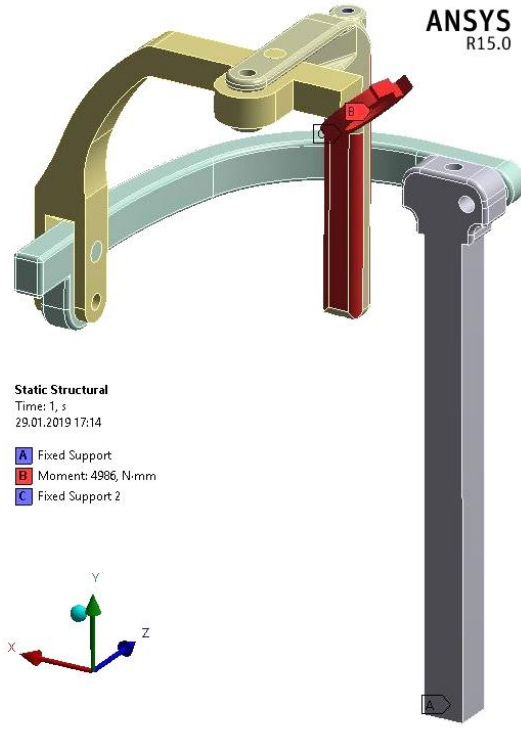
Torque values applied to the handle in the model are assigned as ten times bigger than the values given in Table 4.2. Increased torque values and assuming a free rotating part as fixed were done to make the model more complicated and to investigate the worst scenario. The mesh structure of exoskeleton, the boundary conditions, the equivalent stress and the total deformation are shown in Figure 4.39 (a, b, c, d), respectively.

ANSYS
R15.0



(a)

ANSYS
R15.0

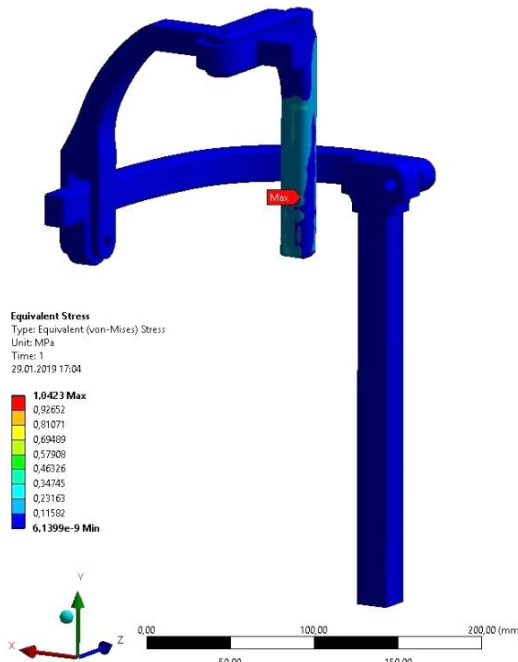


Static Structural

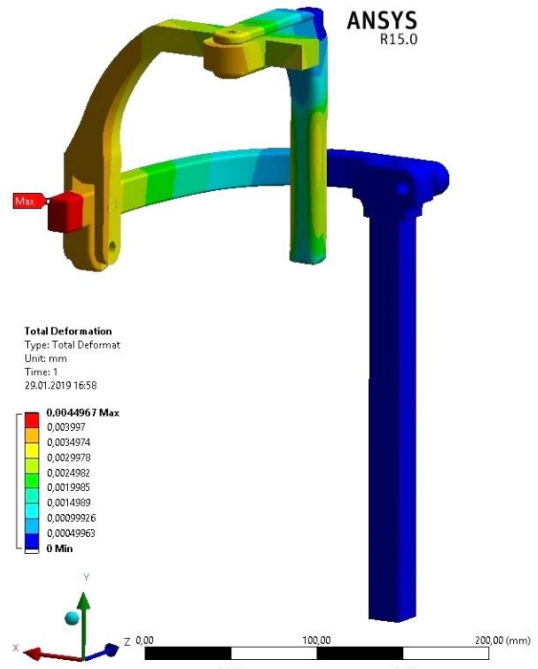
Time: 1, s
29.01.2019 17:14

- A Fixed Support
- B Moment: 4986, N-mm
- C Fixed Support 2

(b)



(c)



(d)

Figure 4.39 FEM analysis of the exoskeleton.

As seen in Figure 4.39, although increased torque values and fixing issues, maximum equivalent stress is 1.0423 MPa while approximately 26 MPa is required for yielding. It is also seen that total deformation is about 4 μm throughout exoskeleton. It is not a significant value.

As a second case, the exoskeleton is disconnected from the robot and used independently by cancelling the fixed support on the inner surface of the handle. When the same torque values are applied, the maximum equivalent stress of 7.5 MPa is observed throughout exoskeleton. Even in this case, it is well below the yield strength of the material. It is clear that the parts do not have any structural problems for the described activities. The equivalent stress and the total deformations are shown in Figure 4.40 (a, b), respectively.

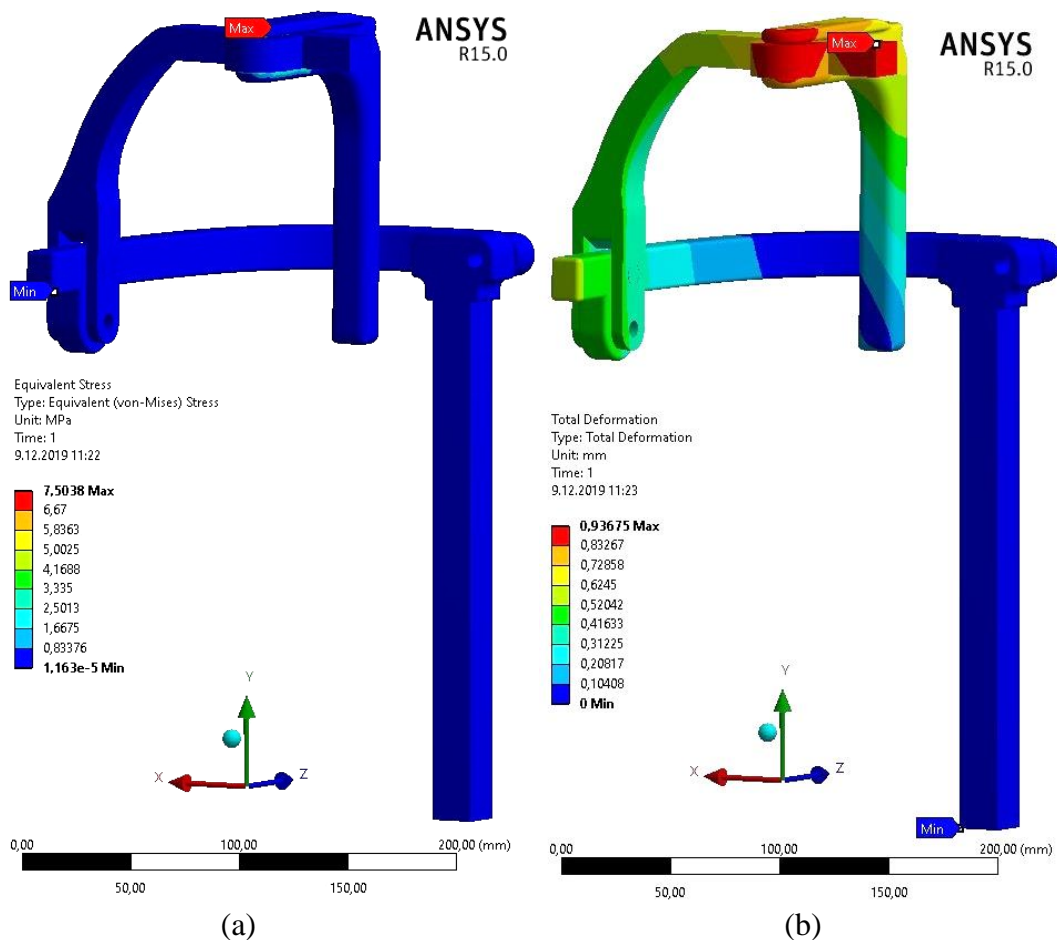


Figure 4.40 FEM analysis of the exoskeleton without robot.

CHAPTER V

CONCLUSIONS

This chapter gives a brief overview of the conclusions of the research described in this thesis. They are given in the order of kinematics analysis, off-line programming, robotic rehabilitation of the wrist and forearm and finally recommendations for the future works.

5.1 Conclusions of Kinematic Analysis and Off-line Programming

In this thesis, it is focused on determining the analytical solution of forward & inverse kinematics of the 6-axis Denso robot, which is available in the laboratory. The equations obtained are reported. Off-line programming (OLP) is a method required before the manipulation of the robots. The operations are visualized in many robotized processes like welding, cutting, even medical applications. These environments are graphical simulations of the real system. Off-line models are carried out including the forward and inverse kinematics of Denso VP-6242G. The Robotics Toolbox provides great simplicity in dealing with robot kinematics with the functions displayed on it. However, making calculations in a traditional way is important in order to control the robot and to form a background for further studies. Toolbox is then used to verify the results obtained by the analytical way. User interfaces are effective tools to show many works in a compact way. Therefore, GUIDE has been preferred in the forward kinematics analysis. The Robotic Toolbox has been embedded in GUIDE. It is possible to reach simultaneous transformation matrix, position & orientation of robot end-effector when DH parameters of the robots and then angular displacements of the motors are changed one by one. A Matlab-Simulink[®] model with SimMechanics[®] blocks for inverse kinematics tasks has been explained. The 3D model of the Denso robot designed by SolidWorks[®] has then been used for system visualization. Animations of the Denso robot have been obtained while performing the tasks given.

5.2 Conclusions of Robot-Assisted Exoskeleton for Rehabilitation

The contribution of this thesis is to provide an application of a serial-robot-driven passive exoskeleton for human wrist and forearm rehabilitation. Potential use of the proposed system is generating continuous passive motion for physiotherapy. The designed exoskeleton has been interfaced with a serial robot and adapted for upper-extremity rehabilitation. A study about an exoskeleton driven by a serial robot has not yet been explored in the literature. The investigation of kinematic parameters required for the proper use of the designed exoskeleton has been completed. 1 extra passive DOF is added under the base of the forearm in order to provide the self-alignment of limb–exoskeleton axes. Inverse kinematics analysis has been modified to perform the required exercises. The Remote Centre of Motion technique has been proposed for this application. The wrist joint has been taken as stationary. Thus, a fictitious wrist joint has been defined. Orientation changes in roll, pitch and yaw angles of the fictitious point have been applied and exercises in FE, PS and AA have been performed. Planned trajectories for FE, AA and PS motions are performed successively with three different velocity levels. The accuracy of the exercises is validated by the signals taken from the wireless motion tracker, MTw Awinda.

This study can be regarded as a design guide for the rehabilitation of other limbs. Using a printable exoskeleton offers flexibility to the users. The exoskeletons may also be designed for ankle, shoulder and/or elbow applications. They can be designed to be compatible with the robot and then manufactured by 3-D printing technology in an easy and cheap way. Therefore, a serial robot can be used as a master motion provider for different types of rehabilitation. The use of this technique is very feasible in limbs with a common rotation centre. For example, the human shoulder has 3 DOF, all of which rotate about a common rotation centre. Knee and ankle also have common rotation centres. Thus, using a serial robot and passive exoskeleton systems will be more practical instead of exoskeleton systems with motors on each axis. Adapting the inverse kinematics model is very easy for different types of rehabilitation.

If the exoskeleton mechanism is removed from the proposed system, it becomes an end-effector type device. The proposed system hybridized two systems in order to utilize the advantages and to avoid their disadvantages. The designed exoskeleton prevents the weight of the arm from being loaded directly to the robot. The robot

only applies the torque required for the corresponding pairs of exercises. When only one of the FE, AA, and PS movements is applied in the absence of an exoskeleton system, it is not possible to make the movement transmission correctly, because there is no restriction on the other two movement axes. The exoskeleton driven by robot precisely acts as a guide in the exercises. In addition, mechanical stoppers designed on the body of the exoskeleton by considering the anatomical structure will ensure that the damage to the patients will be minimized in case of an accident. The foregoing includes the advantages of the exoskeleton system for passive exercises.

5.3 Recommendations for the Future Studies

Active exercise is the topic of further study. The exoskeleton will also play an important role in active exercises. When the patient wants to apply any of the FE, AA, PS movements to the robot without the exoskeleton, it will be very difficult to only orientate around the movement axes of the limbs. Unwanted Cartesian movements will inevitably occur. Since there is no system to prevent Cartesian movements, only building the desired muscle group, which is the actual design goal of the exoskeleton systems, cannot be achieved.

It is contemplated to obtain direct input from the patient by means of a Force-Torque (FT) sensor to be placed between the exoskeleton and the robot. For active exercises, the position and placement of the FT sensor are very important. There are some problems when the sensor is mounted on the end-effector of the robot. Wrist and forearm exercises can be performed by applying torques in three different directions to the fictitious coordinate axis around the wrist point. In order for the robot to apply only rotational motion without displacement around the specified wrist point, the robot must receive only torque data, not force data from the FT sensor. A new design can be considered where the FT sensor is fixed to the ground. For these three movements, connecting the respective links of the exoskeleton system to the respective points of the FT sensor with flexible ropes may be a solution to generate only torque data. Thus, active exercises with different difficulty levels can be performed by torque to orientation control technique.

Due to the angular limit problems of the robot axes, the exoskeleton system had to be used in two different positions. Just changing the length of the metal rod between the

robot and the exoskeleton system with the trial and error method caused one of the motion pairs not to be performed. These reasons make the problem a geometric optimization problem. The design can be reconsidered with the objective functions and constraint equations to be determined.

The design of the exoskeleton has been made in accordance with the average limb sizes of adults. A design can be considered in which the exoskeleton link lengths can be changed manually for the subjects having different limb sizes.



REFERENCES

- Akdemir, N., Akkus, Y. (2006). Rehabilitation and Nursing, *Journal of Nursing College*. 82–91.
- Akdoğan, E., Aktan, M. E., Koru, A. T., Arslan, M. S., Atlıhan, M., Kuran, B. (2018). Hybrid Impedance Control of a Robot Manipulator for Wrist and Forearm Rehabilitation: Performance Analysis and Clinical Results, *Mechatronics*. **49**, 77–91.
- Almusawi, A. R. J., Dülger, L. C., Kapucu, S. (2016). A New Artificial Neural Network Approach in Solving Inverse Kinematics of Robotic Arm (Denso Vp6242), *Computational Intelligence and Neuroscience*.
- Amirabdollahian, F., Loureiro, R., Gradwell, E., Collin, C., Harwin, W., Johnson, G. (2007). Multivariate Analysis of the Fugl-Meyer Outcome Measures Assessing the Effectiveness of GENTLE/S Robot-Mediated Stroke Therapy, *J Neuroeng Rehabil*. **4(4)**.
- Angeles, J., Lopez-Cajun, C. (1988). Dexterity Index of Serial-Type Robotic Manipulators. ASME Trends and Developments in Mechanisms, *Machines and Robotics*. 79-84.
- Arnay, R., Aceituno J. H., Gonzalez E., Acosta L. (2017). Teaching Kinematics with Interactive Schematics and 3D Models, *Comput. Appl. Eng. Educ*. **25(3)**, 420–429.
- Ball, S. J., Brown, I. E., Scott, S. H. (2007). MEDARM: A Rehabilitation Robot with 5DOF at the Shoulder Complex, *IEEE/ASME International Conference on Advanced Intelligent Mechatronics*, 4–7 September, Zürich, 1-6.
- Ball, S. J. (2008). Novel Robotic Mechanisms for Upper - Limb Rehabilitation and Assessment, Ph.D. Thesis, Department of Electrical and Computer Engineering, Queen's University.
- Barkana, D. E., Ozkul, F. (2013). *A robot-assisted rehabilitation system – RehabRoby. Interdisciplinary mechatronics*. John Wiley & Sons, 145-162.

- Barreca, S., Wolf, S., Fasoli, S., Bohannon, R. (2003). Treatment Interventions for the Paretic Upper Limb of Stroke Survivors: A Critical Review, *Neurorehabil Neural Repair*. **17**(4), 220–226.
- Bayona, N. A., Bitensky, J., Salter, K., Teasell, R. (2005). The Role of Task Specific Training in Rehabilitation Therapies, *Top Stroke Rehabil*. **12**, 58-65.
- Beekhuis, J. H., Westerveld, A. J., Van der Kooij, H., Stienen, A. H. A. (2013). Design of a Self-Aligning 3-DOF Actuated Exoskeleton for Diagnosis and Training of Wrist and Forearm after Stroke, *IEEE 13th International Conference on Rehabilitation Robotics (ICORR)*, Seattle, WA, USA, 24–26 June.
- Bingul, Z., Koseeyaporn, P., Cook, G. E. (2002). Windows Based Robot Simulation Tools, *7th International Conference on Control, Automation, Robotics and Vision*, Singapore.
- Cao, Y., Lu, K., Li, X., Zang, Y. (2011). Accurate Numerical Methods for Computing 2D&3D Robot Workspace, *International Journal of Advanced Robotic Systems; INTECH*. **8**, 1-13.
- Chen, Y., Fan, J., Zhu, Y., Zhao, J., Cai, H. (2015). A Passively Safe Cable Driven Upper Limb Rehabilitation Exoskeleton, *Technol Health Care*. **23**, 197-202.
- Chiaverini, S., Egeland, O. (1990). A Solution to the Singularity Problem for Six-joint Manipulators, *Proc. IEEE for Robotics and Automation*. **1**, 644-649.
- Chinello, F., Scheggi, S., Mordibi, F., Prattichizzo, D. (2011). The KUKA Control Toolbox: Motion Control of KUKA Robot Manipulators with MATLAB, *IEEE Robot. Autom. Mag*. **18**, 69–79.
- Colizzi, L., Laneve, L., Savino, N., Martini, A., Potenza, A., Cirillo, P., Pignolo, L., Dolce, G. (2010). Aramis: A Virtua-Mechatronic Approach for Neuro-Rehabilitation Purposes, *Proceedings of the 10th IEEE International Conference on Information Technology and Applications in Biomedicine*. 3–5 November, Korfu.

- Colombo, R., Pisano, F., Mazzone, A., Delconte, C., Micera, S., Carrozza, M. C., Dario, P., Minuco, G. (2007). Design Strategies to Improve Patient Motivation during Robot-Aided Rehabilitation, *J Neuroeng Rehabil.* **4**(3).
- Constantin, D., Lupoae, M., Baciuc, C., Buliga, D. (2015). Forward Kinematic Analysis of an Industrial Robot, *Proceedings of the International Conference on Mechanical Engineering (ME 2015)*. 90-95.
- Corke, P. I. (1996). A Robotics Toolbox for MATLAB, *IEEE Robot. Autom. Mag.* **3**, 24–32.
- Corke, P. (2011). *Robotics, vision and control. Fundamental algorithms in Matlab®*. Springer.
- Coote, S., Murphy, B., Harwin, W., Stokes, E. (2008). The Effect of the GENTLE/s Robot-Mediated Therapy System on Arm Function after Stroke, *Clin Rehabil.* **22**, 395-405.
- Craig, J. J. (2005). *Introduction to robotics mechanics and control*. Pearson, Prentice-Hall.
- Cui, X., Chen, W., Jin, X., Agrawal, S. K. (2017). Design of a 7-DOF Cable-Driven Arm Exoskeleton (CAREX-7) and a Controller for Dexterous Motion Training or Assistance, *IEEE/ASME Transactions on Mechatronics.* **22**, 161-172.
- Cakir, M., Butun, E. (2007). An Educational Tool for 6-DOF Industrial Robots with Quaternion Algebra, *Comput. Appl. Eng. Educ.* **15**, 143–154.
- Das, H., Bao, X., Bar-Cohen, Y., Bonitz, R., Lindemann, R., Maimone, M., Nesnas, I., Voorhees, C. (1999). Robot Manipulator Technologies for Planetary Exploration, *Proceedings of the Smart Structures and Integrated Systems Symposium*. Newport Beach CA, March 1–5.
- Deneve, A., Moughamir, S., Afilal, L., Zaytoon, J. (2008). Control System Design of a 3-DOF Upper Limbs Rehabilitation Robot, *Computer Methods and Programs in Biomedicine*, **89**, 202 - 214.

Denso Robotics: www.denso.com/, 20.11.2018.

Ding, B., Qian, J., Shen, L., Zhang, Y. (2012). Finite Element Analysis and Optimized Design of Exoskeleton for Lower Extremity Rehabilitation Training, *Proceedings of the 2012 IEEE International Conference on Robotics and Biomimetics*, 1397-1402.

Denavit, J., Hartenberg, R. S. (1955). A Kinematic Notation for Lowerpair Mechanisms based on Matrices, *J. Appl. Mech.* **1**, 215–221.

Dobkin, B. H. (2004). Strategies for Stroke Rehabilitation, *Lancet Neurol.* **3**, 528-536.

Donnan, G. A., Fisher, M., Macleod, M., Davis, S. M. (2008). Stroke, *The Lancet.* **371**, 1612–1623.

Duka, A. V. (2014). Neural Network based Inverse Kinematics Solution for Trajectory Tracking of a Robotic Arm, *Procedia Technology.* **12**, 20-27.

Duleba, I., Opalka, M. (2013). A Comparison of Jacobian-based Methods of Inverse Kinematics for Serial Robot Manipulators, *International Journal of Applied Mathematics and Computer Science.* **23(2)**, 373–382.

Duret, C., Grosmaire, A. G., Krebs, H. I. (2019). Robot-Assisted Therapy in Upper Extremity Hemiparesis: Overview of an Evidence-Based Approach, *Front. Neurol.* **10**, 412.

Fitle, K. D., Pehlivan, A. U., Malley, M. K. O. (2015). A Robotic Exoskeleton for Rehabilitation and Assessment of the Upper Limb following Incomplete Spinal Cord Injury, *Robotics and Automation.* 4960-4966.

Flanders, M., Kavanagh, R. C. (2015). Build-A-Robot: Using Virtual Reality to Visualize the Denavit–Hartenberg Parameters, *Comput. Appl. Eng. Educ.* **23(6)**, 846-853.

Frisoli, A., Salsedo, F., Bergamasco, M., Rossi, B., Carboncini, C. M. (2009). A Force Feedback Exoskeleton for Upper-Limb Rehabilitation in Virtual Reality, *Appl Bionics Biomech.* **6**, 115-126.

Funda, J., Taylor, R. H., Paul, R. P. (1990). On Homogeneous Transforms, Quaternions, and Computational Efficiency, *IEEE Trans. Robot. Automation.* **6**, 382-388.

Garrido, J., Yu, W., Li, X. (2016). Modular Design and Control of an Upper Limb Exoskeleton, *J Mech Sci Technol.* **30**, 2265-2271.

Gil, A., Reinoso, O., Marin, J. M., Paya, L., Ruiz, J. (2015). Development and Deployment of a New Robotics Toolbox for Education, *Comput. Appl. Eng. Educ.* **23(3)**, 443–454.

González-Palacios, M. A., González-Barbosa, E. A., Aguilera-Cortés, L. A. (2013). SnAM: A Simulation Software on Serial Manipulators, *Eng. Comput.* **29(1)**, 87–94.

Gopura, R., Kiguchi, K. (2007). Development of an Exoskeleton Robot for Human Wrist and Forearm Motion Assist, *International Conference on Industrial and Information Systems*, Penadeniya, Sri Lanka, 9–11 August.

Gopura, R., Kiguchi, K. (2008). A Human Forearm and Wrist Motion Assist Exoskeleton Robot with EMG-based Fuzzy-Neuro Control, *Proc. 2nd IEEE RAS & EMBS International Conference on Biomedical Robotics and Biomechatronics (BioRob)*. Scottsdale, AZ, 550–555.

GUIDE Creating Graphical User Interfaces:
www.mathworks.com/help/matlab/creating_guis/about-the-simple-guide-gui-example.html/, 20.11.2018.

Guo, S., Zhang, F., Wei, W., Guo, J., Ge, W. (2013). Development of Force Analysis based Exoskeleton for the Upper Limb Rehabilitation System, *ICME International Conference on Complex Engineering China.* 285-289.

Gupta, A., O'Malley, M. (2006). Design of a Haptic Arm Exoskeleton for Training and Rehabilitation, *IEEE ASME TransMechatronics*. **11(3)**, 280.

Gupta, A., O'Malley, M. K., Patoglu, V., Burgar, C. (2008). Design, Control and Performance of Ricewrist: A Force Feedback Wrist Exoskeleton for Rehabilitation and Training, *Int. J. Rob. Res.* **27**, 233–251.

Hasegawa, Y., Mikami, Y., Watanabe, K., Sankai, Y. (2008). Five-Fingered Assistive Hand with Mechanical Compliance of Human Finger, *IEEE Int. Conf. Robotics and Automation (ICRA)*. Pasadena, CA, 718–724.

Hesse, S., Schulte-Tigges, G., Konrad, M., Bardeleben, A., Werner, C. (2003). Robot-Assisted Arm Trainer for the Passive and Active Practice of Bilateral Forearm and Wrist Movements in Hemiparetic Subjects, *Arch Phys Med Rehabil.* **84(6)**, 915–920.

Higuma, T., Kiguchi, K., Arata, J. (2018). Low-Profile Two-Degree-of-Freedom Wrist Exoskeleton Device Using Multiple Spring Blades, *IEEE Robotics and Automation Letters*. **3(1)**, 305-311.

Hill, B., Tesar, D. (1996). Rapid Analysis Manipulator Program (RAMP) as a Design Tool for Serial Revolute Robot, *Proceedings of the IEEE International Conference on Robotics and Automation*. **4**, 2896–2901.

Hu, X. L., Tong, K. Y., Song, R., Zheng, X. J., Lui, K. H., Leung, W. W. F., Ng, S., Au-Yeung, S. S. Y. (2009). Quantitative Evaluation of Motor Functional Recovery Process in Chronic Stroke Patients during Robot-Assisted Wrist Training, *J Electromyogr Kinesiol.* **19(4)**, 639–650.

Jackson, A. E., Holt, R. J., Culmer, P. R., Makower, S. G., Levesley, M. C., Richardson, R. C., Cozend, J. A., Williams, M. M., Bhakta, B. B. (2007). Dual Robot System for Upper Limb Rehabilitation after Stroke: The Design Process, *Proceedings of the Institution of Mechanical Engineers, Part C: Journal of Mechanical Engineering Science*. **221(7)**, 845–857.

- John, M. R. S., Thomas, N., Sivakumar, V. P. R. (2016). Design and Development of Cable Driven Upper Limb Exoskeleton for Arm Rehabilitation, *International Journal of Scientific & Engineering Research*. **7**, 1432-1440.
- Kang, H. B., Wang, J. H. (2015). Adaptive Robust Control of 5 DOF Upper-Limb Exoskeleton Robot, *Int J Control, Automation and Systems*. **13**, 733-741.
- Khor, K. X., Chin, P. J. H., Yeong, C. F., Su, E. L. M., Narayanan, A. L. T., Abdul Rahman, H., Khan, Q. I. (2017). Portable and Reconfigurable Wrist Robot Improves Hand Function for Post-Stroke Subjects, *IEEE Transactions on Neural Systems and Rehabilitation Engineering*. **25**, 1864-1873.
- Kiguchi, K., Iwami, K., Yasuda, M., Watanabe, K., Fukuda, T. (2003). An Exoskeletal Robot for Human Shoulder Joint Motion Assist, *Mechatronics, IEEE/ASME Transactions*. **8**, 125–135.
- Kikuchi, T., Xinghao, H., Fukushima, K., Oda, K., Furusho, J., Inoue, A. (2007). Quasi-3-DOF Rehabilitation System for Upper Limbs: Its Force-Feedback Mechanism and Software for Rehabilitation, *In Proc. IEEE 10th International Conference on Rehabilitation Robotics (ICORR)*. Noordwijk, Netherlands, 24–27.
- Kim, H., Miller, L. M., Fedulow, I., Simkins, M., Abrams, G. M., Byl, N., Rosen, J. (2013). Kinematic Data Analysis for Post-Stroke Patients Following Bilateral Versus Unilateral Rehabilitation with an Upper Limb Wearable Robotic System, *IEEE Transactions on Neural Systems and Rehabilitation Engineering*. **21(2)**, 153-164.
- Kim, B., Deshpande, A. D. (2017). An Upper-Body Rehabilitation Exoskeleton Harmony with an Anatomical Shoulder Mechanism: Design, Modeling, Control, and Performance Evaluation, *The International Journal of Robotics Research*. **36(4)**, 414-435.
- Köker, R. (2013). A Genetic Algorithm Approach to a Neural-Network-based Inverse Kinematics Solution of Robotic Manipulators based on Error Minimization, *Information Sciences*. **222**, 528-543.

Krebs, H. I., Hogan, N., Aisen, M. L., Volpe, B. T. (1998). Robot-Aided Neurorehabilitation, *IEEE Trans Rehabil Eng.* **6**, 75–87.

Krebs, H. I., Ferraro, M., Buerger, S. P., Newbery, M. J., Makiyama, A., Sandmann, M., Lynch, D., Volpe, B. T., Hogan, N. (2004). Rehabilitation Robotics: Pilot Trial of a Spatial Extension for MIT-Manus, *Journal of NeuroEngineering and Rehabilitation.* **1(5)**.

Krebs, H. I., Volpe, B. T., Williams, D., Celestino, J., Charles, S. K., Lynch, D., Hogan, N. (2007). Robot-Aided Neurorehabilitation: A Robot for Wrist Rehabilitation, *IEEE Trans Neural Syst Rehabil Eng.* **15(3)**, 327–335.

Kung, P. C., Ju, M. S., Lin, C. C. K. (2007). Design of a Forearm Rehabilitation Robot. *Proc. IEEE 10th International Conference on Rehabilitation Robotics ICORR*. Noordwijk, Netherlands, 228–233.

Kucuk, S., Bingul, Z. (2004). The Inverse Kinematics Solutions of Industrial Robot Manipulators, *IEEE Conference on Mechatronics.* 274-279.

Küçük, S., Bingül, Z. (2005). An Off-Line Simulation Package for Robotics Education and Industrial Purposes, *11th IEEE International Conference on Methods and Models in Automation and Robotics*. Poland.

Kucuk, S., Bingul, Z. (2006). Comparative Study of Performance Indices for Fundamental Robot Manipulators, *IEEE Conference on Mechatronics.* 274-279, Turkey, June, Istanbul.

Küçük, S., Bingül, Z. (2009). An Off-Line Robot Simulation Toolbox, *Comput. Appl. Eng. Educ.* **18**, 41–52.

Kwakkel, G., Kollen, B. J., Krebs, H. I. (2007). Effects of Robot-Assisted Therapy on Upper Limb Recovery after Stroke: A Systematic Review, *Neurorehab Neural Repair.* **22**, 111-121.

Liu, Y., Wang, D., Sun, J., Chang, L., Ma, C., Ge, Y., Gao, L. (2015). Geometric Approach for Inverse Kinematics Analysis of 6-DOF Serial Robot, *IEEE*

International Conference on Information and Automation. 852-855.

Liu, L., Shi, Y. Y., Xie, L. (2016). A Novel Multi-DOF Exoskeleton Robot for Upper Limb Rehabilitation, *Journal of Mechanics in Medicine and Biology*. **16**, 1640023.

Lo, H. S., Xie, S. Q. (2012). Exoskeleton Robots for Upper-limb Rehabilitation: State of the Art and Future Prospects, *Medical Engineering & Physics*. **34**, 261-268.

Loureiro, R., Amirabdollahian, F., Topping M., Driessen B., Harwin W. (2003). Upper Limb Mediated Stroke Therapy – GENTLE/s Approach, *Autonomous Robots*. **15**, 35–51.

Lum, P. S., Burgar, C. G., Shor, P. C., Majmundar, M., Van der Loo, M. (2002). Robotassisted Movement Training Compared with Conventional Therapy Techniques for the Rehabilitation of Upper-Limb Motor Function after Stroke, *Archives of Physical Medical and Rehabilitation*. **83**, 952-959.

Lum, P. S., Burgar, C. G., van der Loos, M., Shor, P. C., Majmundar, M. (2006). MIME Robotic Device for Upper-Limb Neurorehabilitation in Subacute Stroke Subjects: A Follow-up Study, *J Rehabil Res Dev*. **43**, 631-642.

Maciejasz, P., Eschweiler, J., Gerlach-Hahn, K., Jansen-Troy, A., Leonhardt, S. (2014). A Survey on Robotic Devices for Upper Limb Rehabilitation, *Journal of Neuroengineering and Rehabilitation*. **11(3)**.

Malin, G. (2015). 6-REXOS: Upper Limb Exoskeleton Robot with Improved pHRI, *Int J Advanced Robot Systems*.

Manocha, D., Canny, J. F. (1994). Efficient Inverse Kinematics for General 6R Manipulators, *IEEE Transactions on Robotics and Automation*. **10(5)**, 648-657.

Marchal-Crespo, L., Reinkensmeyer, D. J. (2009). Review of Control Strategies for Robotic Movement Training after Neurologic Injury, *J. Neuroeng Rehabil*. **6(20)**.

Martinez, J., Ng, P., Lu, S., Campagna, M., Celik, O. (2013). Design of Wrist Gimbal: A Forearm and Wrist Exoskeleton for Stroke Rehabilitation, *IEEE 13th*

International Conference on Rehabilitation Robotics (ICORR). Seattle, WA, USA, 24–26 June.

Mao, Y., Agrawal, S. K. (2012). Design of a Cable-Driven Arm Exoskeleton (CAREX) for Neural Rehabilitation, *IEEE Trans. on Robotics*. **28(4)**, 922-931.

Masiero, S., Celia, A., Armani, M., Rosati, G. (2006). A Novel Robot Device in Rehabilitation of Post-Stroke Hemiplegic Upper Limbs, *Aging Clinical and Experimental Research*. **18**, 531-535.

Mehrholz, J., Platz, T., Kugler, J., Pohl, M. (2008). Electromechanical and Robot-Assisted Arm Training for Improving Arm Function and Activities of Daily Living after Stroke, *Cochrane database of systematic reviews*. **4**.

Mehta, J. A., Bain, G. I. (2004). Elbow Dislocations in Adults and Children, *Clin Sports Med*. **23**, 609-627.

Mitsi, S., Bouzakis, K. D., Mansour, G., Sagris, D., Maliaris, G. (2004). Off-Line Programming of an Industrial Robot for Manufacturing, *Int. J. Adv. Manuf. Technol*. **26(3)**, 262–267.

Mushage, B. O., Chedjou, J. C., Kyamakya, K. (2017). Fuzzy Neural Network and Observer-based Fault-Tolerant Adaptive Nonlinear Control of Uncertain 5-DOF Upper-Limb Exoskeleton Robot for Passive Rehabilitation, *Nonlinear Dynamics*. **87**, 2021-2037.

Nayar, H.D. (2002). Robotect: Serial-Link Manipulator Design Software for Modeling, Visualization and Performance Analysis, *7th International Conference on Control, Automation, Robotics and Vision*. Singapore.

Nef, T., Mihelj, M., Riener, R. (2007). ARMin: A Robot for Patient-Cooperative Arm Therapy, *Medical & Biological Engineering & Computing*. **45**, 887-900.

Nef, T., Guidali, M., Riener, R. (2009). ARMin III—Arm Therapy Exoskeleton with an Ergonomic Shoulder Actuation, *Applied Bionics and Biomechanics*. **6**, 127-142.

- Nethery, J. F., Spong, M. W. (1994). Robotica: A Mathematica Package for Robot Analysis, *IEEE Robot. Autom. Mag.* **1**, 113–120.
- Neto, P., Mendes, N. (2013). Direct Off-Line Robot Programming via a Common CAD Package, *Robot. Auton. Syst.* **61**, 896–910.
- Niku, S. B. (2001). *Introduction to robotics: Analysis, systems, applications*. Prentice Hall.
- Nubiola, A., Bonev, I. A. (2014). Geometric Approach to Solving the Inverse Displacement Problem of Calibrated Decoupled 6R Serial Robots, *Transactions of the Canadian Society for Mechanical Engineering.* **38**, 31-44.
- Oblak, J., Cikajlo, I., Matjacic, Z. (2009). Universal Haptic Drive: A Robot for Arm and Wrist Rehabilitation, *IEEE Trans Neural Syst Rehabil Eng.*
- Oda, K., Isozumi, S., Ohyama, Y., Tamida, K., Kikuchi, T., Furusho, J. (2009). Development of Isokinetic and Iso-Contractile Exercise Machine MEM-MRB using MR Brake, *In Proc. IEEE Int. Conf. on Rehabilitation Robotics (ICORR)*. Kyoto, Japan, 6–11.
- Omarkulov, N., Telegenov, K., Zeinullin, M., Tursynbek, I. (2016). Preliminary Mechanical Design of Nu-Wrist: A 3 DOF Self-Aligning Wrist Rehabilitation Robot, *6th IEEE International Conference on Biomedical Robotics and Biomechanics (BioRob)*. Singapore, 26–29 June.
- Ozakyol, H., Karaman, C., Bingul, Z. (2019). Advanced Robotics Analysis Toolbox for Kinematic and Dynamic Design and Analysis of High-DOF Redundant Serial Manipulators, *Comput Appl Eng Educ.* 1–24.
- Ozkul, F., Barkana, D. E. (2013). Upper-Extremity Rehabilitation Robot RehabRoby: Methodology, Design, Usability and Validation, *International Journal of Advanced Robotic Systems.* **10(12)**, 1-13.
- Qiao, S., Liao, Q., Wei, S., Su, H. (2010). Inverse Kinematic Analysis of the General 6R Serial Manipulators based on Double Quaternions, *Mechanism and Machine*

Theory. **45**, 193-199.

Quanser: www.quanser.com/, 20.11.2018.

Pehlivan, A. U., Lee, S., O'Malley, M. K. (2012). Mechanical Design of RiceWrist-S: A Forearm-Wrist Exoskeleton for Stroke and Spinal Cord Injury Rehabilitation, *The Fourth IEEE RAS/EMBS International Conference on Biomedical Robotics and Biomechatronics*.

Perry, J. C., Rosen, J., Burns, S. (2007). Upper-Limb Powered Exoskeleton Design, *IEEE/ASME Transactions on Mechatronics*. **12**, 408-417.

Platz, T. (2003). Evidence-based Arm Rehabilitation - A Systematic Review of the Literature, *Nervenarzt*. **74(10)**, 841-849.

Prange, G. B., Jannink, M. J., Groothuis-Oudshoorn, C. G. (2006). Systematic Review of the Effect of Robot-Aided Therapy on Recovery of the Hemiparetic Arm after Stroke, *J Rehabil Res Dev*. **43**, 171-184.

Proietti, T., Crocher, V., Roby-Brami, A., Jarrasse, N. (2016). Upper-Limb Robotic Exoskeletons for Neurorehabilitation: A Review on Control Strategies, *IEEE Reviews in Biomedical Engineering*. **9**, 4-14.

Rahman, M. H., Saad, M., Kenne, J. P., Archambault, P. S. (2010). Modeling and Development of an Exoskeleton Robot for Rehabilitation of Wrist Movements, *IEEE/ASME International Conference on Advanced Intelligent Mechatronics (AIM 2010)*.

Rahman, M., Ouimet, T. K., Saad, M., Kenne, J. P., Archambault, P. (2010). Development and Control of a Wearable Robot for Rehabilitation of Elbow and Shoulder Joint Movements, *IECON 2010-36th Annual Conference on IEEE Industrial Electronics Society (IEEE)*. 1506-1511.

Rahman, M., Ouimet, T. K., Saad, M., Kenne, J. P., Archambault, P. (2012). Development and Control of a Robotic Exoskeleton for Shoulder, Elbow and Forearm Movement Assistance, *Applied Bionics and Biomechanics*. **9**, 275-292.

- Rahman, M. H., Saad, M., Kenné, J. M., Archambault, P. S. (2013). Control of an Exoskeleton Robot Arm with Sliding Mode Exponential Reaching Law, *International Journal of Control, Automation, and Systems*. **11**, 92-104.
- Rahman, M. H., Rahman, M. J., Cristobal, O. L., Saad, M., Kenné, J. P., Archambault, P. S. (2015). Development of a Whole Arm Wearable Robotic Exoskeleton for Rehabilitation and to Assist Upper Limb Movements, *Robotica*. **33**, 19-39.
- Reinkensmeyer, D. J., Takahashi, C. D., Timozyk W. K., Reinkensmeyer, A. N., Khan, L. E. (2001). Design of Robot Assistance for Arm Movement Therapy Following Stroke, *Advanced Robotics*. **14(7)**, 625–637.
- Riener, R. (2007). Robot-Aided Rehabilitation of Neural Function in the Upper Extremities, *Acta Neurochir Suppl*. **97(1)**, 465–471.
- Rocon, E., Belda-Lois, J. M., Ruiz, A. F., Manto, M., Moreno, J. C., Pons, J. L. (2007). Design and Validation of a Rehabilitation Robotic Exoskeleton for Tremor Assessment and Suppression, *IEEE Trans. Neural Syst. Rehabil. Eng.* **15(3)**, 367–378.
- Rosati, G., Gallina, P., Masiero, S. (2007). Design, Implementation and Clinical Tests of a Wire-based Robot for Neurorehabilitation, *IEEE Trans. Neural Syst. Rehabil. Eng.* **15(4)**, 560–569.
- Sanchez, R. J., Wolbrecht, E., Smith, R., Liu, J., Rao, S., Cramer, S., Rahman, T., Bobrow, J. E., Reinkensmeyer, D. J. (2005). A Pneumatic Robot for Re-Training Arm Movement After Stroke: Rationale and Mechanical Design, *Proceedings of IEEE 9th International Conference on Rehabilitation Robotics*. 28 June – 1 July, 500–504.
- Sasaki, D., Noritsugu, T., Takaiwa, M. (2004). Development of Active Support Splint Driven by Pneumatic Soft Actuator (ASSIST), *Proc. IEEE International Conference on Robotics and Automation (ICRA)*. Barcelona.

- Schiele, A., van der Helm, F. C. T. (2006). Kinematic Design to Improve Ergonomics in Humanmachine Interaction, *IEEE Trans. Neural Syst. Rehabil. Eng.* **14(4)**, 456–469.
- Schoone, M., van Os, P., Campagne, A. (2007). Robot-Mediated Active Rehabilitation (ACRE) A User Trial, *Proc. IEEE 10th International Conference on Rehabilitation Robotics (ICORR)*. Noordwijk, Netherlands, 477–481.
- Shah, S. V., Nandihal, P. V., Saha, S. K. (2012). Recursive Dynamics Simulator (ReDySim): A Multibody Dynamics Solver, *Theor. Appl. Mech. Lett.* **2**, 6.
- Sivan, M., Gallagher, J., Makower, S., Keeling, D., Bhakta, B., O'Connor, R. J., Levesley, M. (2014). Home-Based Computer Assisted Arm Rehabilitation (hCAAR) Robotic Device for Upper Limb Exercise after Stroke: Results of a Feasibility Study in Home Setting, *Journal of NeuroEngineering and Rehabilitation*. **11**, 163.
- Song, R., Tong, K. Y., Hu, X. L., Zheng, X. J. (2007). Myoelectrically Controlled Robotic System that Provide Voluntary Mechanical Help for Persons after Stroke, *Proc. IEEE 10th International Conference on Rehabilitation Robotics (ICORR)*. Noordwijk, Netherlands, 246–249.
- Sugar, T. G., Jiping, H., Koeneman, E. J., Koeneman, J. B., Herman, R. (2007). Design and Control of RUPERT: A Device for Robotic Upper Extremity Repetitive Therapy, *IEEE Transactions on Neural Systems and Rehabilitation Engineering*. **15**, 336-346.
- Spencer, S. J., Klein, J., Minakata, K., Le, V., Bobrow, J. E., Reinkensmeyer, D. J. (2008). A Low Cost Parallel Robot and Trajectory Optimization Method for Wrist and Forearm Rehabilitation using theWii, *Proc. 2nd IEEE RAS & EMBS International Conference on Biomedical Robotics and Biomechatronics (BioRob)*. Scottsdale, AZ, 869–874.
- Stienen, A. H. A., McPherson, J. G., Schouten, A. C., Dewald, J. P. A. (2011). The ACT-4D: A Novel Rehabilitation Robot for the Quantification of Upper Limb Motor

Impairments Following Brain Injury, *IEEE International Conference on Rehabilitation Robotics Rehab Week*. Zurich, 29 June – 1 July, 1-6.

Sukal, T. M., Ellis, M. D., Dewald, J. P. A. (2005). Dynamic Characterization of Upper Limb Discoordination Following Hemiparetic Stroke, *Proceedings of the IEEE 9th International Conference on Rehabilitation Robotics*. 28 June – 1 July, Chicago, 519-521.

Takaiwa, M., Noritsugu, T. (2005). Development of Wrist Rehabilitation Equipment Using Pneumatic Parallel Manipulator, *Proc. IEEE International Conference on Robotics and Automation (ICRA)*. Barcelona, Spain, 2302–2307.

Tao, H., Minghong, W. (2017). Research on the Simulation of Robotic Motion based on Matlab, *Int. J. Res. Eng. Sci. (IJRES)*. **5(9)**, 1–6.

Toth, A., Fazekas, G., Arz, G., Jurak, M., Horvath, M. (2005). Passive Robotic Movement Therapy of the Spastic Hemiparetic Arm with REHAROB: Report of the First Clinical Test and the Follow-up System Improvement, *Proc. 9th International Conference on Rehabilitation Robotics (ICORR)*. Chicago, IL, 127–130.

Turnell, D. J., Turnell, Q. V., Fatima, M. D. E. (2001). SimBot—A Simulation Tool for Autonomous Robots, *IEEE International Conference on Systems Man, and Cybernetics*. **5**, 2986–2990.

Vollmann, K. (2002). A New Approach to Robot Simulation Tools with Parametric Components, *IEEE International Conference on Industrial Technology*. **2**, 881–885.

Xiao, F., Gao, Y., Wang, Y., Zhu, Y., Zhao, J. (2017). Design of a Wearable Cable Driven Upper Limb Exoskeleton based on Epicyclic Gear Trains Structure, *Technology and Health Care Preprint (Preprint)*. 1-9.

XSENS: www.xsens.com/, 20.11.2018.

Wang, J., Li, Y. (2010). Hybrid Impedance Control of a 3 - DOF Robotic Arm used for Rehabilitation Treatment, *6th Annual IEEE Conference on Automation Science and Engineering*, Toronto, 21 - 24 August, 768-773.

Yang, K., Jiang, Q. F., Wang, X. L., Xia, X., Ma, X. (2017). Mechanism Design and Static Analysis of Exoskeleton Robot for Rehabilitation of Lower Limb, *2nd International Conference on Mechatronics and Information Technology (ICMIT 2017)*. 278-283.

Yeong, C. F., Calderon, A. M., Gassert, R., Burdet, E. (2009). ReachMAN: A Personal Robot to Train Reaching and Manipulation, *IEEE/RSJ International Conference on Intelligent Robots and Systems*. 10 – 15 October, St. Louis, 4080-4085.

Yeong, C. F., Karen, B., Calderon, A. M., Burdet, E., Playford, E. D. (2010). ReachMAN to Help Sub-Acute Patients Training Reaching and Manipulation, *IEEE Conference on Robotics, Automation and Mechatronics*. 28 – 30 June, Singapore, 90-95.

Zariffa, J., Kapadia, N., Kramer, J. L. K., Taylor, P., Alizadeh-Meghbrazi, M., Zivanovic, V. (2012). Feasibility and Efficacy of Upper Limb Robotic Rehabilitation in a Subacute Cervical Spinal Cord Injury Population, *Spinal Cord*. **50**, 220–226.

Zhang, K., Chen, X., Liu, F., Tang, H., Wang, J., Wen, W. (2018). System Framework of Robotics in Upper Limb Rehabilitation on Poststroke Motor Recovery, *Behavioural Neurology*.

Zlajpah, L. (2000). Integrated Environment for Modelling, Simulation and Control Design for Robotic Manipulators, *3rd MATHMOD, IMACS Symposium on Mathematical Modelling*. Vienna, Austria, 761–764

CURRICULUM VITAE

PERSONAL INFORMATION

Name, Surname: Mehmet Erkan KÜTÜK
Nationality: Republic of Turkey
Date and Place of Birth: 03.08.1986 / Ankara
Phone: +(90) 342 3172534
Fax: +(90) 342 3601104
E-mail: mekutuk@gantep.edu.tr
erkan0ktk @gmail.com

EDUCATIONAL INFORMATION

M.Sc. Gaziantep University, Department of Mechanical Eng., 2013
(3.92/4.00).
B.Sc. Gaziantep University, Department of Mechanical Eng., 2010
(3.15/4.00).

WORK EXPERIENCE

2011-Present Gaziantep University, Department of Mechanical Eng. Res. Asst.
2010-2011 Kuruman Industrial Cooling Systems/Gaziantep Engineer

PUBLICATIONS

Journal Articles

[1] Kütük, M. E., Dülger, L. C., Daş, M. T. (2019). Design of a Robot-Assisted Exoskeleton for Passive Wrist and Forearm Rehabilitation, *Mechanical Sciences*, **10**, 107-118.

- [2] Kütük, M. E., Artan, M., Dülger, L. C. (2019). Hybrid Seven-Bar Press Mechanism: Link Optimization and Kinetostatic Analysis, *Tehnički Glasnik*, **12(3)**, 181-187.
- [3] Kütük, M. E., Dülger, L. C. (2016). A Hybrid Press System: Motion Design and Inverse Kinematics Issues, *Engineering Science and Technology, an International Journal*, **19(2)**, 846-856.
- [4] Kütük, M. E., Dülger, L. C. (2016). Dynamic Modeling, Simulation and Control of a Hybrid Driven Press Mechanism, *International Journal of Mechanics*, **10**, 288-293.
- [5] Kütük, M. E., Halıcioğlu, R., Dülger, L. C. (2015). Kinematics and Simulation of a Hybrid Mechanism: Matlab/Simmechanics, *Journal of Physics: Conference Series*, **574**.
- [6] Dülger, L. C., Erdoğan H., Kütük, M. E. (2014). Matlab's GA and Optimization Toolbox: A Fourbar Mechanism Application, *IJISAE*, **2(1)**, 10-15.
- [7] Kütük, M. E., Dülger, L. C. (2012). Hibrid Makine Sistemleri: Yapılanmalar ve Analizi Üzerine Bir Araştırma, *Electronic Journal of Machine Technologies*, **9(1)**, 61-72.

Book Chapters

- [1] Kütük, M. E., Dülger, L. C., Daş, M. T. (2020). A Simulation Tool for Kinematics Analysis of a Serial Robot, *Lecture Notes on Mechanical Engineering, Advances in Design, Simulation and Manufacturing II (Springer)*, 593-601.
- [2] Kütük, M. E., Daş, M. T., Dülger, L. C. (2019). An Exoskeleton Design Robotic Assisted Rehabilitation: Wrist & Forearm, *Advances in Mechanism and Machine Science (Springer)*, 155-164.

Conference Papers

- [1] Kütük, M. E., Almusawi A. J. R., Dülger L. C., Daş M. T., Kapucu S. (2019). Tıpta Robotik Uygulamalar: Torakoskopi Ve Rehabilitasyon Durum Çalışmaları, *UMTS 2019 (ISTE)*, 314-320. (Full-text, National).
- [2] Kütük, M. E., Dülger, L. C., Daş, M. T. (2019). A Simulation Tool for Kinematics Analysis of a Serial Robot, *DSMIE 2019 (Lutsk)*. (Published as a book chapter, International)
- [3] Kütük, M. E., Daş, M. T., Dülger, L. C. (2019). An Exoskeleton Design Robotic Assisted Rehabilitation: Wrist & Forearm, *IFTOMM 15th World Congress (Krakow)*. (Published as a book chapter, International)
- [4] Kütük, M. E., Dülger, L. C., Daş, M. T. (2018). Robotik Destekli Bilek ve Ön Kol Rehabilitasyonu Üzerine Bir Ön Çalışma, *TOK 2018 (Kayseri)*, 259-264. (Full text, National).
- [5] Kütük, M. E., Daş, M. T., Dülger, L. C. (2018). An Off-line Programming for a 6-DOF Serial Robot (Denso VP 6242G), *4th International Conference on Engineering and Natural Science (Kiev)*, 483. (Abstract, International).
- [6] Kütük, M.E., Olguner, S., Dulger, L.C., Bozdana, A.T. (2018). Design and Implementation of Motion Scenarios for Deep Drawing Process on a Servo Press, *The 7th International Conference on Power, Energy and Mechanical Engineering (Barcelona)*, 25. (Abstract, International).
- [7] Kütük, M.E., Keklikçioğlu, E., Dulger, L.C. (2018). EMG ve IMU Sinyalleri: Bilek Rehabilitasyonunda Kullanılması, *TIPTEKNO 2018 (Gazimagosa)*, 19-22. (Full text, IEEE Xplore, National).
- [8] Kütük, M. E., Daş, M. T., Dülger, L. C. (2017). The Preliminary Design of a Passive Exoskeleton Used in Upper Extremity Rehabilitation, *3rd International Conference on Engineering and Natural Science (Budapest)*, 423. (Abstract, International).

- [9] Kütük, M. E., Daş, M. T., Dülger, L. C. (2017). Adapting an Industrial Robot to Upper Extremity Rehabilitation, *4th International Conference on Computational and Experimental Science and Engineering (Antalya)*, 419. (Abstract, International).
- [10] Kütük, M. E., Daş, M. T., Dülger, L. C. (2017). Forward and Inverse Kinematics Analysis of Denso Robot, *AzciFTOMM 2nd International Symposium of Mechanism and Machine Science (Baku)*, 71-78. (Full text, International).
- [11] Kütük, M. E., Daş, M. T., Dülger, L. C. (2017). Motion Teaching for Upper Extremity Rehabilitation: Haptic Assisted Robot, *4th International Conference on Computational and Experimental Science and Engineering (Antalya)*, 420. (Abstract, International).
- [12] Kütük, M. E., Daş, M. T., Dülger, L. C. (2017). Üst Ekstremitte Rehabilitasyon Robotunun Kinematik Analizi ve Yörünge Planlaması, *IDEFIS 2017 (Kırıkkale)*, 388-394. (Full text, National).
- [13] Kütük, M. E., Dülger, L. C., Daş, M. T. (2016). Haptik Rehabilitasyon Uygulamaları, *Tiptekno 2016 (Antalya)*, 293-296. (Full text, IEEE Xplore, National).
- [14] Kütük, M. E., Dülger, L. C. (2016). Optimization with Genetic Algorithm (GA) and Simulated Annealing (SA): Application to Planar Mechanisms, *3rd International Conference on Computational and Experimental Science and Engineering (Antalya)*, 363. (Abstract, International).
- [15] Kütük, M. E., Dülger, L. C. (2015). Hibrid Sürücülü Bir Pres Mekanizmasının Dinamik Modellemesi ve Benzetimi, *UMTS 2015 (TrISToMM, IFTOMM affiliated) (İzmir)*, 950. (Full text, National).
- [16] Kütük, M. E., Dülger, L. C. (2013). Hibrid Pres Yapılanması: Hareket Tasarımı-Kinematik Analizi, *UMTS 2013 (Erzurum)*. (Full text, National).

PROJECTS

- [1] Sanayi Bakanlığı (SAN-TEZ) PROJESİ: 01422.STZ.2012-I. (01.10.2012-01.04.2015). Servo ve Hibrid Preslerin Tasarımı, Uygulanması ve Denetimi: Karşılaştırmalı Çalışma. (Position: Project Student).

[2] Gaziantep University, BAP, Project Number: MF.DT.17.03. (12.10.2017-12.08.2018). Robotik Destekli Bilek ve Ön Kol Rehabilitasyonu. (Position: Researcher).

AWARDS

[1] 3rd Rank in Bachelor Graduation (2010), Mechanical Engineering Department, Gaziantep University.

[2] MSc. Thesis Award (2013), Graduate School Of Natural & Applied Sciences, Gaziantep University.

[3] Young Delegates Grant by IFTOMM (2016), Summer School on Mechanism Design for Applications, MDA 2016 (*Palermo*).

[4] Tübitak-Bideb 2224-A (2019), Support Program for Participation in International Scientific Activities.